Physical layer network coding based communication systems in frequency selective channels

Alaa H Ahmed

Newcastle University

Newcastle upon Tyne, UK.

A thesis submitted for the degree of

Doctor of Philosophy

June 2017

To my loving family

Seek knowledge from cradle to grave .

-Muhammed

Knowledge is better than money, because knowledge keeps thee while you're guarding money. Money fades with spending, while knowledge can be gained through teaching.

-Imam Ali

Acknowledgements

I like to express my thanks to everyone who helped me in this adventure in one way or another, starting with my first supervisor Dr. Charalampos Tsimenidis for his continued guidance and support throughout this journey. His office door was always open whenever I had a question or needed advice and I feel forever in his debt. I would also like to thank my second supervisor, Mr. Jeffrey Neasham for his valuable contribution in the completion of this work. I offer my regards to current and former staff at Newcastle university especially Prof. Bayan Sharif, Prof. Said Boussakta, Dr Stephane Le Goff, Professor Gui Tian and all the other talented staff for the helpful tips and valuable information.

I would also like to thank my colleagues for their help and the wonderful time we spent together. A special thanks to Dr. Sangar Qader for his valuable help in the early days of my study. I also like to mention my dear friend Mr. Hasan M. Kadhim who without his help I wouldn't have come to the UK. I want to apologise for all my other colleagues not mentioned by name but rest assured you will all be in my heart.

I like to thank all my family members especially my father, my wife and my wonderful children for being such a great help and for tolerating me throughout the days of my study.

Finally, I would like thank my sponsor the Iraqi Government, Ministry of Higher Education for all the help, funding and support that I needed to study in the UK.

Abstract

The demand for wireless communications is growing every day which requires more speed and bandwidth. In two way relay networks (TWRN), physical layer network coding (PLNC) was proposed to double the bandwidth. A TWRN is a system where two end users exchange data through a middle node called the relay. The two signals are allowed to be physically added before being broadcasted back to the end users. This system can work smoothly in flat fading channels, but can not be applied straightforward in frequency selective channels. In a multipath multi-tap FIR channel, the inter-symbol interference (ISI) spreads through several symbols. In this case, the symbols at the relay are not just an addition of the sent symbols but also some of the previous symbols from both sides. This not only causes a traditional PLNC to fail but also a simple one equalizer system will not solve the problem. Three main methods have been proposed by other researchers. The OFDM based PLNC is the simplest in terms of implementation and complexity but suffers from the disadvantages of the OFDM like cyclic prefix overhead and frequency offset. The main disadvantage, however is the relatively low BER performance because it is restricted to linear equalizers in the PLNC system. Another approach is pre-filtering or pre-equalization. This method also has some disadvantages like complexity, sensitivity to channel variation and the need of a feedback channel for both end nodes. Finally, the maximum likelihood sequence detector was also proposed but is restricted to BPSK modulation and exponentially rising complexity are major drawbacks. The philosophy in this work is to avoid these disadvantages by using a time domain based system. The DFE is the equalizer of choice here because it provides a non-trivial BER performance improvement with very little increase in complexity. In this thesis, the problem of frequency selective channels in PLNC systems can be solved by properly adjusting the design of the system including the DFE. The other option is to redesign the equalizer to meet that goal. An AF DFE

system is proposed in this work that provides very low complexity especially at the relay with little sensitivity to channel changes. A multi-antenna DNF DFE system is also proposed here with an improved performance. Finally, a new equalizer is designed for very low complexity and cost DNF approach with little sacrifice of BER performance. Matlab was used for the simulations with Monte Carlo method to verify the findings of this work through finding the BER performance of each system. This thesis opens the door for future improvement on the PLNC system. More research needs to be done like testing the proposed systems in real practical implementation and also the effect of adding channel coding to these systems.

Contents

List of Figures

List of Tables

Nomenclature

Acronyms

$3G$ Third Generation

$4G$ Fourth Generation

AF Amplify and Forward

AOA Angle Of Arrival

$AWGN$ Additive White Gaussian Noise

BER Bit Error Rate

$BPSK$ Binary Phase Shift Keying

CCI Co-Channel Interference

$CDMA$ Code Division Multiple Access

CFO Carrier Frequency Offset

CP Cyclic Prefix

$CPFSK$ Continuous Phase Frequency Shift Keying

CR Cognitive Radio

DFE Decision Feedback Equalizer

DMT Discrete Multi-Tone

DNF De-Noise and Forward

DOA Direction Of Arrival

$E2E$ End To End

EPA Extended Pedestrian channel A

FDE Frequency Domain Equalization

FIR Finite Impulse Response

IIR Infinite Impulse Response

ISI Intersymbol Interference

ITU International Telecommunication Union

$LDPC$ Low Density Parity Check

LOS Line Of Sight

$MIMO$ Multiple Input Multiple Output

ML Maximum Likelihood

MLD Maximum Likelihood Detector

$MLDF$ Maximum Likelihood Decision Feedback

$MLJD$ Maximum Likelihood Joint Detector

$MLSE$ Maximum Likelihood Sequence Estimation

$MMSE$ Minimum Mean Square Error

$NLMS$ Normalised Least Mean Square

$NSDOA$ Null Steering based on the Direction Of Arrival

$NSEP$ Null Steering by Element Position

$NSWC$ Null Steering by real Weight Control

OC Optimum Combining

$OFDM$ Orthogonal Frequency Division Multiplexing

PAM Pulse Amplitude Modulation

$PAPR$ Peak to Average Power Ratio

$PLNC$ Physical Layer Network Coding

QAM Quadrature Amplitude Modulation

$QPSK$ Quadrature Phase Shift Keying

RLS Recursive Least Square

RRC square-Root Raised Cosine

$SC-FDE$ Single Carrier Frequency Domain Equalization

$SINR$ Signal to Interference plus Noise Ratio

SNR Signal to Noise Ratio

SVD Singular Value Decomposition

TDE Time Domain Equalization

$TDMA$ Time Division Multiple Access

$TWRN$ Two Way Relay Network

$WCDMA$ Wideband Code Division Multiple Access

$WLAN$ Wireless Local Area Network

XOR Exclusive OR

ZFE Zero Forcing Equalizer

Chapter 1

Introduction

1.1 Background

Wireless communications plays an important role in our everyday life. From one look to our mobile phones we can appreciate the power of and liberty that it provides compared wired landline phones. The applications of wireless communications doesnt stop there as it ranges from satellite television, radio and wireless networks to the more simple indoor applications like wireless keyboards and headsets. Wireless communications are based on the simple idea of using the available medium like air or water as a channel depending on the application. The signal is transmitted using one or more antennas in the form of an electromagnetic wave that travels freely in the mentioned channel leaving both transmitter and receiver free to move in the meanwhile.

The main improvements in the area of wireless communications amongst other things, include cost effective design and spectral efficiency that leads to higher communication speed. To meet both these needs, physical layer network coding (PLNC) was proposed in two way relay networks (TWRN). In these systems, two end users or end nodes exchange packages of data via an intermediate node called the relay node. In traditional TWRN, data packets are exchanged in four time slots to avoid overlap while in PLNC this overlap is turned from a disadvantage to an advantage. PLNC is still a hot topic and a relatively new area for research.

This research is concentrated at solving some of its problems or improving the existing solutions to those problems. The main advantages of PLNC systems are spectral efficiency and simple design. Simple design comes from the fact that both end node transceivers are identical from an electronics point of view as they share the same bandwidth and operate in a similar manner. The spectral efficiency is double that of the traditional TWRN systems as only two time slots are required for packet exchange between end nodes compared to four time slots in traditional TWRN.

1.2 Objectives

The broad goal in this thesis is to make the implementation of a PLNC system possible in frequency selective environments or to introduce improved schemes over some existing ones.

There are two basic methods of performing a PLNC system, namely amplify and forward scheme (AF) and de-noise and forward scheme (DNF). In both these cases, new

methods are suggested here with either improved performance, cost effectiveness or relaxed implementation conditions and assumptions.

Performance improvement especially in the AF scheme is due to the use of a non-linear time domain equalizer, namely the decision feedback equalizer (DFE). For the DNF scheme, a multi antenna relay is proposed with improved performance over the AF scheme. Also, a new type of equalizers is derived that depends on a one shot maximum likelihood estimator and a feedback filter referred to in this thesis as the maximum likelihood decision feedback equalizer (MLDF). This equalizer requires less computation and therefore is faster than the DFE and more cost effective. Another important feature of the MLDF is the absence of the delay compared to linear and DFE equalizers. This can be an importamt factor in some cases. Finally, the MLDF is used in both AF and DNF PLNC systems to reduce the cost and complexity with asymptotic performance to that of the DFE.

In brief, the following points summarise the contributions of the work

1. Design of an AF PLNC system in frequency selective channels using DFE equalizers with the proper design equations for the DFEs.

2. A multi antenna relay system that uses optimum combining and two DFEs for a successful DNF PLNC system.

3. Design equations for a low complexity MLDF equalizer.

4. A low complexity AF PLNC system using the MLDF equalizer.

5. Single antenna DNF PLNC system using a special MLDF design with theoretical performance analysis when ideal MLDF is used.

6. Low complexity DNF PLNC with multiple antennas using the MLDF equalizer and optimum combining method.

1.3 Limitations and Assumptions

In this section, some of the general limitations and assumptions are discussed in brief. Other assumptions may apply to different chapters in this work and will be discussed there in detail.

1.3.1 Channel Modelling and Estimation

It is not uncommon for a communication channel to have more than one obstacle or object that reflects the transmitted signal to the receiver. This results in receiving multiple copies of the original signal with different delays or propagation times and with different attenuations. If this is the case then the channel is called a multipath fading channel.

Before the channel can be modelled, the model type and the estimation method have to be chosen. In this work, only multi-tap FIR or the tapped delay line model is considered. Previous work has been done requiring this model to be fixed for several transmission packets, yet in this work, a more realistic assumption is made that requires the model to be fixed for the duration of only one packet.

Many channel estimation techniques exist that offer high accuracy when the channel is fixed for the duration of one packet transmission. These methods impose an overhead on the packets in the form of estimation symbols. This overhead is essential to any kind of channel estimation and is usually small compared to the packet size. In this work, the timing diagrams are simplified by not showing this small overhead. For simplicity and without loss of generality, the channel estimation is assumed to be perfect, yet in some cases, the effect of imperfect estimation is studied here. This error is not due to the imperfection of the estimation process but rather due to the variation in the channel when the passing time is greater than that of a single packet.

1.3.2 Synchronization

Ideally, packets from two senders or end nodes are expected to reach the middle node or relay at the same time in the PLNC scheme. This is not the case in practice. A similar kind of mismatch is present in other coherent communication systems. In OFDM systems for example, there are different ways to deal with this problem like feedback loops or other methods that use the properties of OFDM systems and other information like the position of training symbols or pilots in addition to information about the cyclic prefix [1]. These treatments are necessary in such systems to tackle the arising problems like carrier frequency offset and some of these algorithms are iterative in nature. In time domain PLNC systems, researchers have been assuming ideal synchronization. Even without any synchronization we still get a higher capacity than direct networking without PLNC [2]. For practical implementation, a relay or router trigger protocol was proposed by Katti et al [3]. In this protocol the router sends a signal to both end nodes to trigger the uplink

transmission phase. The required protocol depends on the environment used. In cellular networks for example, strict scheduling protocols already exist like time division multiple access (TDMA) and code division multiple access (CDMA). Synchronization of 3 node systems studied in fields such as wireless networks [4] and in OFDM [5]. This 3 node synchronization scheme can be extended to general N node synchronization by dividing them into groups of 3 nodes [6]. Some attempts have been made to mitigate the synchronization error effect on PLNC systems like by Lu and S. Liew [7] and reduction with fractional delay in[8]. In this thesis, perfect synchronization is assumed for simplicity and due to its small effect as mentioned above.

1.3.3 Pre-filtering vs Direct Filtering

Pre-filtering is mentioned here in the context of pre-equalization. The basic goal of pre-equalization is to reduce the signal distortion that occurs due to channel impairments by placing the filter in the transmitter side. This type of design has some advantages and relocates the required resources from the transmitter to the receiver. By doing this, the system avoids noise amplification which would occur if the equalizer was to be placed at the receiver. When the channel has a spectral null (or a small value), the receiver side equalizer will compensate for that gain loss by amplifying that part of the spectrum. As a result, the noise will be also amplified which will impact the performance of the system. This does not occur when the equalizer is at the transmitter side.

Pre-filtering can be implemented in different ways. A simple design for this idea is to estimate the channel at the receiver side. The channel estimation is then passed to the transmitter side through a feedback channel. Finally, the transmitter uses the channel coefficients to design the pre-equalizer or pre-filter which in most cases will be a linear FIR filter. The implication of such a design is that the channel will need to be constant or slightly changed during this cycle. Another disadvantage of this design is that a feedback channel is required. Other pre-filtering strategies also exist which do not involve complete equalization of the signal but share the previously mentioned disadvantages.

Normal equalization, on the other hand, does not require the channel to be constant for the whole uplink-downlink cycle and does not require a feedback channel. Moreover, direct equalization can have enhanced performance through using non-linear methods and therefore lead to simpler system designs.

For these reasons, the direct equalization is the method of choice in this work.

1.3.4 Time Domain vs Frequency Domain Equalization

The best representative system for frequency domain equalization is the well known orthogonal frequency division multiplexing (OFDM) system. In this system, the signal is divided into frequency sub-bands and the frequency domain equalizer FDE will compensate for the gain loss in each sub-band separately assuming that the channel will become flat fading in every sub-band. In frequency selective channels, this is not always true. Consider a channel with one frequency null. In this case, the frequency will be sharply changing in the sub-bands adjacent to that null and this will result in a performance degradation. Even if this was not the case, then there will always be at least one error symbol corresponding to that null.

Another FDE system is the single carrier with frequency domain equalization (SC-FDE). The SC-FDE was proposed to solve some of the problems related to OFDM like sensitivity to non-linearities of the power amplifiers, high peak to average power ratio (PAPR) and carrier frequency offset (CFO). The SC-FDE nevertheless, uses a frequency domain equalization technique and therefore has the same problem with sever frequency selective channels as the OFDM system. For this reason, the frequency domain methods will have limited performance.

Another way to look into this issue is to consider the fact that FDE methods are limited to linear equalization, while time domain equalization TDE can be non-linear. This is because non-linear techniques require a feedback signal coming out of a decision device and as such devices map the symbols to the closest constellation point in the time domain, then the signal must be first converted back to the time domain. It is well known that non-linear equalizers outperform their linear counterparts. Therefore, we can conclude that non-linear TDE filters are better suited to applications with frequency selective channels than linear FDE devices.

1.4 Digital Bandpass Transmission

Consider a signal $S_b(t)$ with baseband properties. Such signals are usually modulated with a carrier frequency f_c. Regardless of the modulation technique that is used, the signal can be represented by an equivalent complex valued function when f_c is greater than the original signal bandwidth. Let $S(t)$ be the modulated passband signal. Then $S(t)$ can be written as $S(t) = Re\{S_b(t)e^{j2\pi f_c t}\}$, where $Re\{\}$ represents the real part operator. The

complex representation of the signal can be defined as

$$S_b(t) = S_{br}(t) + jS_{bi}(t), \tag{1.1}$$

where $S_{br}(t) = R_e\{S_b(t)\}$ and $S_{bi}(t) = Im\{S_b(t)\}$ and $Im\{\}$ is the imaginary part operator.

The passband signal can therefore be written as

$$S(t) = S_{br}(t)\cos(2\pi f_c t) - S_{bi}(t)\sin(2\pi f_c t). \tag{1.2}$$

Representing the signal in complex notation as in equation (1.1) is important in studying communication systems. From a theoretical point of view, this representation simplifies the analysis because the absence of the carrier frequency simplifies the equation. Also, the simulation at the symbol level requires much less time than when it is done in the sampling frequency level. From a practical point of view, this complex representation makes it much easy to design and improve new signal processing methods. For these reasons, this equivalent complex representation will be used throughout this work.

1.5 Publications Arising From This Research

1. **A. H. Ahmed**, C. C. Tsimenidis, J. A. Neasham and B. S. Sharif, "DFE for frequency selective PNC channels using AF," *IEEE 11th International Conference on Wireless and Mobile Computing, Networking and Communications (WiMob)*, vol. 2015, doi: 10.1109/WiMOB.2015.7348048.

2. **A. H. Ahmed**, C. C. Tsimenidis and J. A. Neasham, "PLNC using a multichannel DFE receiver at the relay for shallow-water acoustic communications," *submitted to 4th IEEE UACE Conf., Skiathos Island, Greece*.

3. **A. H. Ahmed**, C. C. Tsimenidis and J. A. Neasham, "Maximum Likelihood Decision Feedback Equalizer for Fast Implementation of PLNC Systems," *submitted to IET comms. and under review*.

1.6 Thesis Outline

The thesis is organized as follows:

Chapter 2 presents the network strategies used in two way relay networks (TWRN) and their evolution to PLNC. The chapter briefly describes the methods used within PLNC like amplify and forward and de-noise and forward techniques. Some fading channels are also described with emphasis on the tapped delay line modeling of frequency selective channels. The choice of receiver side equalization over pre-equalization is justified along with the specific type of equalizer, namely the DFE.

Chapter 3 Presents a detailed description of the design equation used in the DFE. The chapter presents a novel AF scheme that enables the use of PLNC in frequency selective environments while relaxing some of the major conditions required by the pre-equalization methods. The design equations for the new DFE method are derived and simulation results are presented showing the robustness of the method compared to the pre-equalization method when channel change occur between successive data packets.

In Chapter 4, a novel DNF PLNC is proposed with the aid of an antenna array at the relay node. The choice of combining scheme is justified and the number of required antennas specified. The superiority of the method is showcased through the simulated BER performance.

Chapter 5, presents another interesting alternative to the problem of incompatibility of the PLNC system with frequency selective channels. A novel type of equalizer is introduced which has very low complexity in design and implementation and does not result in a delayed signal. The design is inspired by the DFE and the single symbol maximum likelihood detector. Simulation results show the performance of the new method in different scenarios including single and multiple relay antennas. Theoretical BER performance of the new equalizer is derived and shown to match the simulated BER.

Chapter 6 concludes the thesis and suggests possible future work.

Chapter 2

PLNC in Frequency Selective Channels

2.1 Introduction

In recent years, Physical Layer Network Coding (PLNC) has attracted significant amount of research work due to its ability to save transmission bandwidth, which is one of the most valuable resources in communication systems. One of the aims of this chapter is to explore the principles of this relatively new technique and explain why the direct implementation of it in frequency selective channels is not possible. This in turn will help the reader to understand and appreciate the findings in this research. The other goal is to introduce the DFE equalizer and justify its use. High speed transmission of information suffers inevitably from intersymbol interference (ISI) induced by multipath propagation over frequency selective channels. Equalization methods are used to handle this problem. Equalization techniques have diversified over time, yet little enhancements are gained over the DFE equalizer with more complex techniques at the cost of very high computational complexity. For example the complexity grows exponentially with the data packet length in the trellis based equalization technique amongst other factors [9]. This computational complexity is one of the determining factors of the relay nodes especially in low power wireless communication systems. On the other hand, simple linear equalization methods have significantly lower performance while only using one filter instead of two in the DFE case and hence the pick of the optimal DFE equalizer becomes both logical and practical. S. Zhang et al were the first to propose the concept of physical layer network coding in 2006 [6]. The basic structure of a PLNC system consists of two transceivers or end nodes which are the actual users of the system and a relay in between called the relay node. The relay not only acts as power booster but also controls the data flow between the end users and determines the type of scheme that is used for this exchange. This operation is half duplex but the data is exchanged in both directions. The constraint of half duplex is introduced to the system for simplicity and can be extended to full duplex. When the two signals from both end nodes are transmitted as electromagnetic waves, they will added or superimposed naturally without intervention. This can be considered as a type of network coding operation [10].

2.2 TWRN without Network Coding

Much attention has been given recently to wireless networks with relay nodes playing a key part in the communication process. A relay is placed in the midway between two users

or end nodes basically as a booster to extend the coverage distance of a wireless network. This setup is called a two way relay network (TWRN). PLNC systems are studied in the context of TWRN. This is done for simplicity as it can be extended to more complex network configurations. For example, a single relay can be used as an intermediary that controls data exchange between more than one pair of end nodes. In this case the end nodes are sharing one relay. Another example is the case of a line of relays that are connected in succession to extend the coverage distance of the network even further. In both these examples, the network can be broken down to groups of three nodes each consisting of two end nodes and a relay. In other words, the TWRN is considered as a building block for more complex networks. In this three node configuration, interference is avoided by using time division. Let U_1 and U_2 be denote users 1 and 2 respectively.

Figure (2.1) shows the four time slots required for one cycle of transmission in a TWRN.

Two time slots are allocated to data transfer from U_1 to U_2 via the relay (R), then the

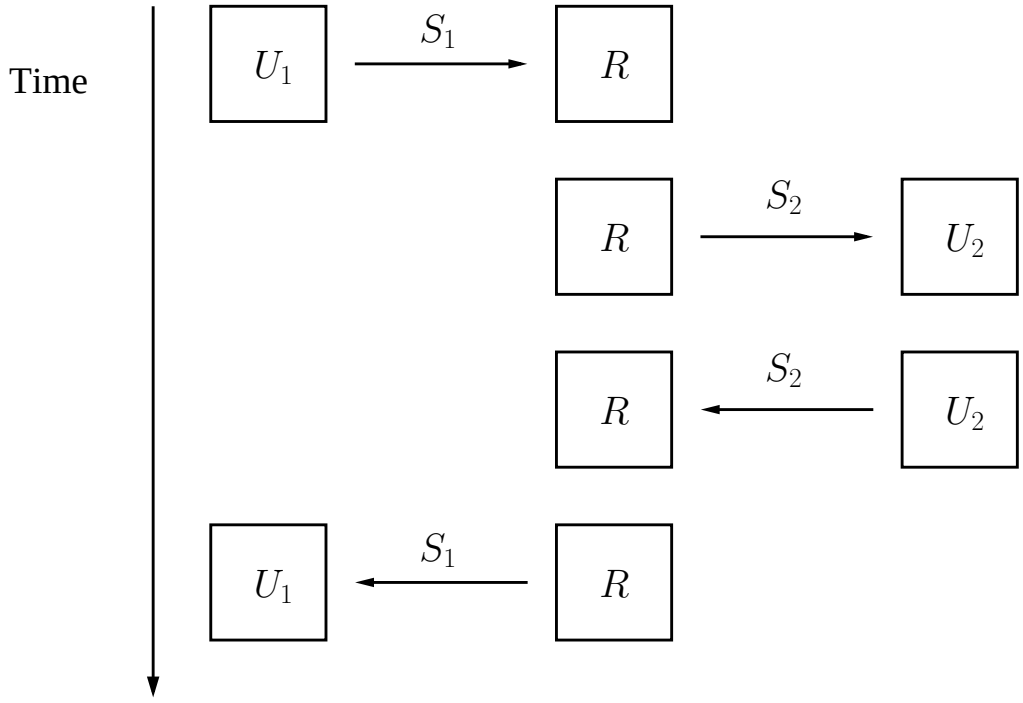

Figure 2.1: TWRN without network coding

other two slots are used for transmission from U_2 to R and then to U_1.

2.3 TWRN with Standard Network Coding

The emergence of computer network applications raised the problem of information flow in the network layer. The network layer is where routing and forwarding are executed amongst other things like addressing and packet sequencing. Ahlswede et al.[10] dealt with the problem of information flow and started the work on network coding. A further algebraic approach to network coding can be found in [11]. This work was applied to linear network codes in [12, 13] and to wireless communications [14, 15].

Network coding refers to the fact that network nodes can perform additional operations or coding instead of just passing on data. In the TWRN at hand, this operation is the binary addition or bitwise XOR. Figure (2.2) shows how the data packets are exchanged.

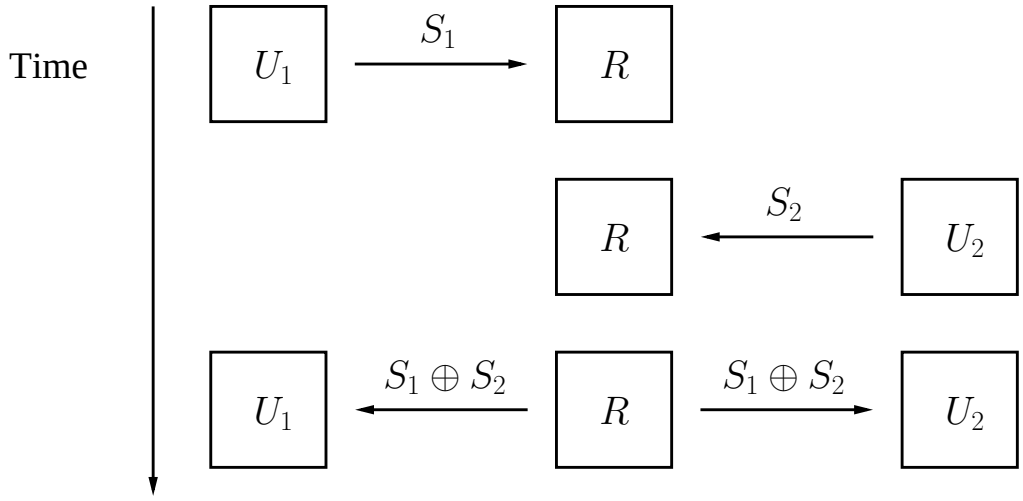

Figure 2.2: TWRN with standard network coding.

Both end users transmit their data packets S_1 and S_2 in two consecutive time slots then the relay performs network coding in the form of bitwise addition. Finally the coded data is broadcasted back to the end nodes. The broadcasted packet S_3 will be $S_3 = S_1 \oplus S_2$. Where $\oplus$ denotes the bitwise addition operation. At node U_1 the desired signal S_2 can be extracted from S_3 by performing the same bitwise operation between the received packet and the known sent packet S1 as follows

$$S_3 \oplus S_1 = (S_1 \oplus S_2) \oplus S_1 = S_2. \tag{2.1}$$

The same can be done at node U_2 with the stored packet S_2. This direct network coding is a good alternative to the conventional four time slot scheme in a TWRN as it offers a throughput improvement of 33% due to the fact that it only uses three time slots to

complete its transmission.

2.4 PLNC

In PLNC, the coding or addition operation is done in the physical layer and this is why this term is used here. In computer network theory, the system is divided into layers which is a conceptual framework that helps the study and understanding of complex communication systems. This framework is also referred to as open system interconnection and the word node itself is borrowed from network theory. The network layer is where routing and forwarding is executed amongst other things like addressing and packet sequencing. Instead of the traditional coding being done in the network layer, the addition occurs without any effort in the physical layer. In standard network coding, the two data packets are sent in two separate time slots. By doing this the designers not only avoid interference, but also resolve some synchronization issues like potential symbol timing mismatch. Later research showed that this interference not only can be a good thing but also that the synchronization problem can theoretically be solved and practical implementation of this system is possible [3, 16, 17, 18, 19, 20, 21, 22, 23, 2]. This practical implementation also includes the field of optical communications [24]. Figure (2.3) shows the timing diagram of a PLNC system in which both end nodes transmit their data packets at the same time slot. In the second time slot the combined or coded signals are broadcasted back to the end nodes. Transmitting and receiving in this way saves 100% bandwidth over the traditional TWRN scheme without coding.

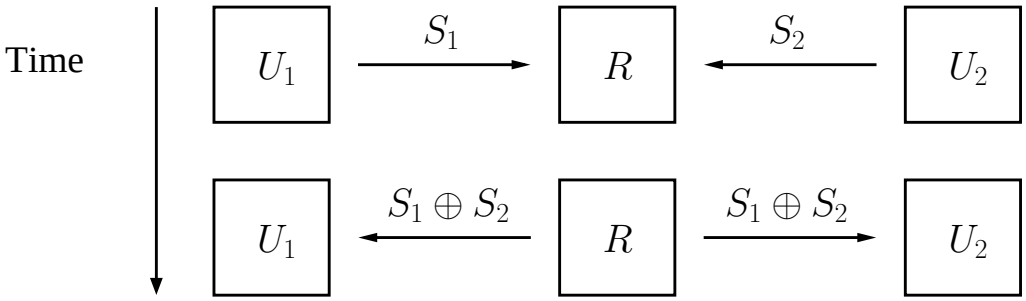

Figure 2.3: TWRN with physical layer network coding.

Consider the simple case of a PLNC system without noise and with equal unity gain for both packets. Although this gain can be set to unity through using power control, yet this is not necessary, especially when these gains are close. Also assuming perfect

synchronization we can study how the coding process is completed after the symbols have been added physically. It should be noted that the received symbols at the relay are not a bitwise XOR even under the previous assumptions and an additional mapping is required to calculate the bitwise XOR of the two signals. To understand how this mapping works, consider the time period of a single symbol. If the sent symbols from end nodes 1 and 2 are $S_1(t)$ and $S_1(t)$ respectively then the received signal in one symbol period will be

$$y = S_1 + S_2. \tag{2.2}$$

For QPSK modulation, these symbols can be represented in complex form as $S_1 = S_1^I + jS_1^Q$ and $S_2 = S_2^I + jS_2^Q$ where the superscripts I and Q represent the in-phase and quadrature components respectively. If we neglect the effect of noise then the received signal can be written as

$$\begin{aligned} y &= (S_1^I + jS_1^Q) + (S_2^I + jS_2^Q) \\ &= (S_1^I + S_2^I) + j(S_1^Q + S_2^Q), \end{aligned} \tag{2.3}$$

where $S_i^I \in \{-1, 1\}$, $S_i^Q \in \{-1, 1\}$ and $i \in \{1, 2\}$. The binary data bit 0 is represented by a value of 1 while the binary bit 1 is represented by -1. This holds true for both the in-phase and quadrature components S_i^I and S_i^Q. This assignment makes the direct multiplication of these components $S_i^I S_j^I$ equivalent to bitwise XOR of their binary counterparts.

Up to this point, the receiver only has two available values namely the in-phase and quadrature components which are

$$\begin{aligned} y^I &= S_1^I + S_2^I, \\ y^Q &= S_1^Q + S_2^Q. \end{aligned} \tag{2.4}$$

This means that the receiver has four unknown variables with only two equations. As the relay only needs to broadcast the bitwise XOR of the in-phase components $S_1^I \oplus S_2^I$ and the XOR of the quadrature components $S_1^Q \oplus S_2^Q$, then the mapping can be made using y^I to find $S_1^I \oplus S_2^I$ and similarly $S_1^Q \oplus S_2^Q$ is found from y^Q. The mapping table for the in-phase components is constructed by finding all the possible combinations of S_1^I and S_2^I, finding the arithmetic addition of the two and then matching the result to the XOR of these two components as shown in table (2.1).

In this table, the first row can be interpreted as follows, S_1^I and S_2^I are both 1 which

Table 2.1: Symbol mapping table for the PLNC in-phase components at the relay.

First symbol S_1^I	Second symbol S_2^I	Received symbol $S_1^I + S_2^I$	Mapped symbol $S_1^I S_2^I$
1	1	2	1
1	-1	0	-1
-1	1	0	-1
-1	-1	-2	1

comes from an original logic 0 bit. The arithmetic addition is therefore 2 and this happens directly in the physical layer. Then this value is corrected or mapped to logic 0 because $0 \oplus 0 = 0$ which is represented by a value of 1 that appears in the end of the first row. The rest of the table is completed in a similar way. This mapping is only necessary in PLNC systems. For example, in the standard TWRN with network coding, the first two time slots are used from transmitting the two data symbols that will be available in the form of bits after demodulation. An XOR operation is then done in the network layer and no further mapping is required. In the previous case, the noise was neglected and the symbols at the relay were assumed to be correct. Practically this is not the case and with AWGN introduced to the arriving signals, errors will occur. The BER of an ideal PLNC system in the presence of AWGN can be simulated using the Monte Carlo method. Figure (2.4) shows the End to end BER performance of a PLNC system compared to the performance of a QPSK system in the presence of AWGN.

2.4.1 Amplify and Forward Scheme

Before the work of Zhang et al [6], the traditional network designers were evading interference because they were accustomed to designing single channels in which interference is a problem. Separate packets were sent in different time slots using TDMA. The new approach is to support the the mixing of the signals in the physical layer and resolve the data packets arriving to the end nodes in the network layer. The mixing is therefore occurring in the symbol level instead of the bit level and the method is called analogue network coding. The same method described earlier is used to extract the desired signal from this mixture. The end node uses its knowledge of its own sent message and subtracts it from the mix to find the desired signal in the network layer. In this technique, the relay or

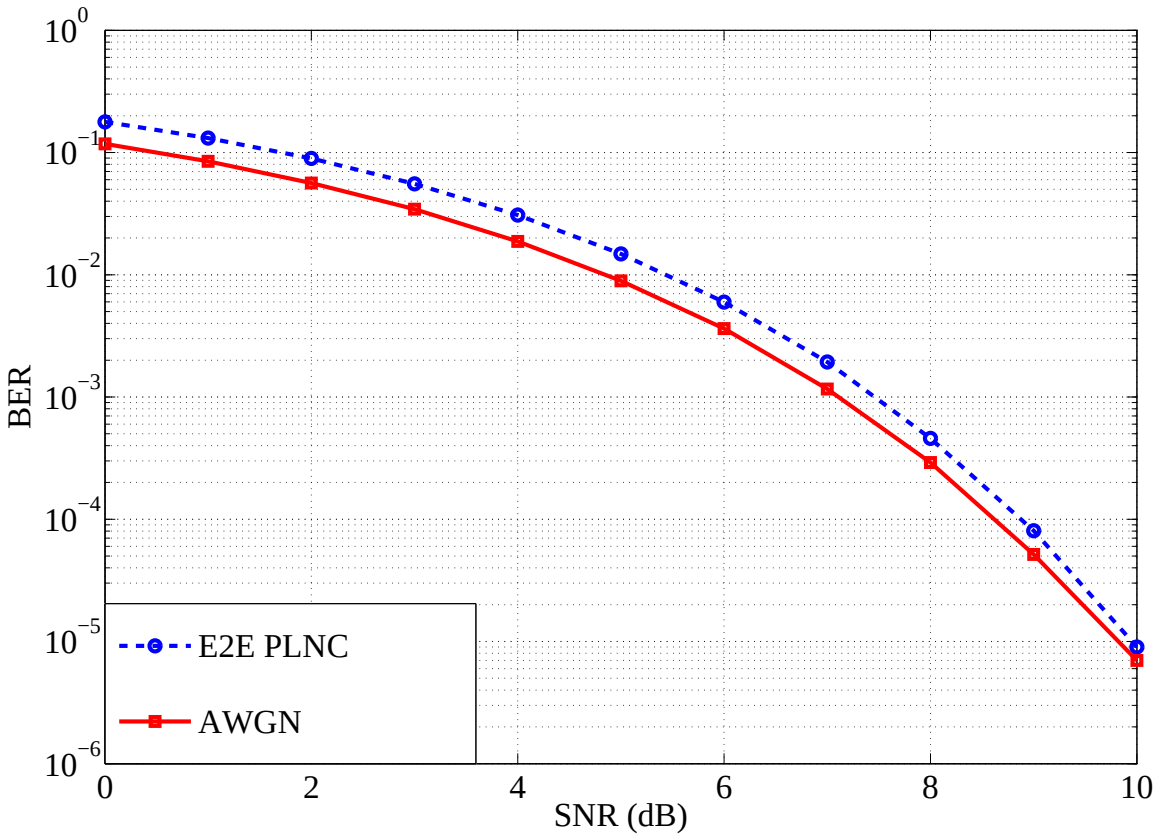

Figure 2.4: End to end BER performance of a PLNC system compared to the performance of a QPSK system both with AWGN.

router is reduced to playing the role of a booster that amplifies the received signals and forwards it back to the senders. This technique is therefore referred to as amplify and forward (AF). Synchronization issues and some practical aspects of this method are well presented in [3]. In this method, the signals at the relay are corrupted with additive noise. No attempt is made to de-noise the signal and instead it is amplified and directly broadcasted back to the end nodes. This leads to some degradation in the BER performance compared to the de-noising approach. This is always the case, yet the AF method also has its advantages. For example, the complexity of the system can be reduced especially at the relay and this is shown in the work done in this thesis. The AF method can also help improve the security of communication systems [25, 26, 27, 28, 29, 30]. For simplicity and without loss of generality let us assume that S_1 and S_2 arrive at the receiver through a unity gain flat fading channel with AWGN. Then the received signal for one symbol period can be written as

$$y = S_1 + S_2 + w_r, \tag{2.5}$$

where w_r represents the zero mean AWGN noise at that period. The broadcasted signal can then be expressed as

$$r = g_{AF}(S_1 + S_2 + w_r), \tag{2.6}$$

where g_{AF} is the amplify and forward gain at the relay. From equation (2.6) it is clear that the noise is multiplied by g_{AF}. Equation (2.6) shows that the two signal will arrive at the same level of power. These interfering signals will have nearly the same power value for unequal flat channel gains meaning that this method works for signal to interference ratio (SINR) of -3dB to 0dB [3]. If signals are to be separated using interference cancellation methods, the required SINR will be arround 6dB [31].

2.4.2 De-noise and Forward Scheme

In this technique, the basic idea is to de-map the added signals at the relay. This does not necessarily mean that the individual signals are to be separated but instead only the XOR of the signals is to be found. This is done through the mapping of the symbols to the corresponding bits as explained earlier. The actual received signal at the relay during one symbol period will be $y = S_1 + S_2 + w_r$. This can be written as

$$\begin{aligned} y &= (S_1^I + jS_1^Q) + (S_2^I + jS_2^Q) + (w_r^I + jw_r^Q) \\ &= (S_1^I + S_2^I + w_r^I) + j(S_1^Q + S_2^Q + w_r^Q). \end{aligned} \tag{2.7}$$

Considering the in-phase component of the received vector, a decision has to be made to fit the received values to the closest number in the set $\{-2, 0, 2\}$. This hard decision process can be considered as a de-noising operation. The estimate of $S_1^I + S_2^I$ is then broadcasted to the end nodes. The same holds true for the quadrature components. It has been shown that this method has a better BER performance than the traditional network coding despite the fact that it uses less bandwidth [32].

For flat fading channels with different gains, the decision is not based on the set $\{-2, 0, 2\}$. Let g_1 and g_2 be the gains of channels 1 and 2 respectively . The received signal for one symbol period can then be written as

$$\begin{aligned} y &= g_1(S_1^I + jS_1^Q) + g_2(S_2^I + jS_2^Q) + (w_r^I + jw_r^Q) \\ &= (g_1S_1^I + g_2S_2^I + w_r^I) + j(g_1S_1^Q + g_2S_2^Q + w_r^Q). \end{aligned} \tag{2.8}$$

As the relay demodulator separates the in-phase from the quadrature components, then we can consider the in-phase component only which will be

$$y^I = g_1 S_1^I + g_2 S_2^I + w_r^I. \tag{2.9}$$

If the noise in equation (2.9) is set to zero, then the set of values used by the decision device can be found by substituting all the possible values of S_1^I and S_1^I, where $S_1^I \,\&\, S_2^I \in \{-1, 1\}$. This results in the set $\{-g_1-g_2\ ,\ -g_1+g_2\ ,\ g_1-g_2\ ,\ g_1+g_2\}$ which corresponds to the ordered set $(S_1^I, S_2^I) \in \{(-1,-1)\ ,\ (-1,1)\ ,\ (1,-1)\ ,\ (1,1)\ \}$. This set can also be viewed as the constellation of the received signal.

2.5 Review of the Recent Advances in PLNC

The topic of PLNC is attracting many researchers. Scanning all the work done in this area exceeds the limits of this thesis so this section will only give some of the important work and recent advances.

In 2017, K. Ravindran et al. [33] considered a network-coded TWRN at very high SNR with the PAM and QAM constellations used for modulation. This was done for different network strategies including the ring based non-linear network mapping. This work takes into account the network strategies but does not address the issue of frequency selective channels. Derivation of the probability of error is given and the results there show that ring based strategy is better than the other methods.

P. Chen et al. [34], 2017 proposed a bit interleaved coded modulation (BIMC) to be used in PLNC systems and investigated the use of non-binary coding and low parity density check LDPC. the system is iterative and therefore more complex than what is proposed here and does not take into account frequency selective channels. Derivation is given for the achievable rates of BICM systems in higher order modulation schemes with different bits-to-symbol mappings. Higher performance was achieved through soft decision and iterative decoding at the expense of complexity. An interesting conclusion is that the behaviour of PLNC systems are different than conventional point to point communication systems.

In the same year, T. Yang et al. [35] proposed a system in which many users are sharing the same relay node in a non-frequency selective environment. Multiple antennas are used at the relay only. A cascade-computation decoding scheme is proposed to resolve the desired signals at the relay. This generalized onion peeling approach enables the system to have a performance close to and bounded by that of a single user system.

Although this is an iterative approach, yet it has the interesting similarity with our work in using multiple antennas at the relay and using the single user performance as a lower BER bound.

In 2016, F. Cao et al. [36] considered PLNC systems with both AWGN and pulse noise in a Rayleigh fading channel. The BER performance was studied and theoretical lower and upper bounds were found. Moreover, the Reed-Solomon coding was applied and the BER performance was enhanced.

X. Chen et al. [37], 2016, studied a PLNC system with asymmetric two-way relay channels. the importance of this study is that it shows that the downlink channel has more influence on the performance of the system compared to the uplink channel. This was illustrated through outage probability.

J. He and S. Liew [38], 2016, considered simple building blocks other than the simple TWRN that can be used to construct more complex networks that use PLNC. This opens the door to studying the error control problem in networks with applying the PLNC system in general. Also, the error control problem in networks constructed from various building blocks is studied. This is important because it shows that the PLNC is in most cases a part of a larger network and must be compatible to different network configurations.

An interesting work of a PLNC receiver when the channel model is a time selective Rayleigh flat-fading model was done in 2016 by X. Li and P. Ho [39]. To achieve this, a decision feedback receiver is used with pilotless orthogonal signaling. Although this considered flat fading it does touch on the issue of time selective channels.

In 2016, H. Zhang et al. [40], studied the PLNC implementation with heterogeneous modulations. This lead to enhancing the throughput and energy efficiency of the system by selecting the modulation according to the bottleneck link's channel condition in the downlink phase. The BER performance of QPSK-BPSK heterogeneous modulation PNC was analysed under AWGN and Rayleigh fading channels. This highlights the importance of PLNC systems being able to work with different types of modulation techniques as also considered in this thesis.

H. Phan et al. [41], 2016, proposed an amplify and forward PLNC system with frequency non-selective channels under the influence of co-channel interference. An antenna array is used to achieve that goal. This research clearly has some similarities to this thesis but in the simpler case of flat fading channels. The theoretical performance of the system was calculated. The work also sheds some light on the design of future PLNC systems.

In 2016, B. Nguyen et al. [42], address the issue of signal power loss due to sym-

bol misalignment. This complements the studies on the synchronization issue in PLNC systems. The researchers proposed using Gaussian pulses to achieve higher BER performance over systems using square-root raised-cosine (RRC) pulses especially when symbol misalignment occurs. This observation is verified through simulation results.

In the same year, Q. Yue et al. [43], considered the implementation of PLNC systems with FSK and MFSK modulation. Theoretical performance of the system is derived. The study shows that 2FSK provides a worse BER performance than that of BPSK. Although this is the case, the effect of asynchronous transmission on PNC systems using 2FSK is less than effect on BPSK PNC. The BER performance can be enhanced by increasing the order of modulation at the expense of bandwidth efficiency. The possibility of gaining from changing the modulation scheme emphasises the importance of this thesis which enables different types of modulation.

X. Dang et al. [44], 2016, proposed a noncoherent CPFSK multiplesymbol detector to solve the problem of unknown carrier-phase offset between the two transmitted signals in a PLNC system. Instead of observing one symbol, the technique considers a group of symbols. Through simulations, the researchers estimate that the algorithm with a five symbol interval has 6.7 dB higher performance over the system with one symbol observation interval. This clearly shows that PLNC systems can be implemented in a variety of different ways for performance improvement.

In 2015, Q. Yang et al. [45], proposed the implementation of PLNC in powerline systems in order to double the throughput of powerline networks. The researchers proposed a beacon-triggered TDMA protocol at the MAC layer. The BER performance is evaluated through simulation for different impulsive noise powers at different SNR values. This is important because it shows that the PLNC system is not restricted to wireless applications.

Following is some of the recent research in two selected areas involving the use of PLNC systems, namely, cognitive radio and MIMO systems.

2.5.1 PLNC in Cognitive Radio

In cognitive radio (CR) systems, the radio is dynamically programmed to use the best near by wireless channels. This is done when a channel becomes available and the spectrum is therefore efficiently used. This requires intelligent transceivers that can detect unused channels and are able to adjust output power and modulation. If CR is all about spectral efficiency, then it makes sense to use PLNC with such systems to further improve that

efficiency. Table (**??**) lists some of the recent advances in CR systems employing PLNC.

In 2016, S. Ustunbas and U. Aygolu [46], considered a pair of transmitting nodes communicating to a pair of receiving nodes through a single relay. In such a system the scenario of CR is studied when PLNC is used. No direct link exists between the two pairs of nodes and M-PSK modulation is used. The theoretical BER performance is derived for non-frequency selective channels. The results are also verified through simulation results. This shows the importance of higher order modulation and star networks in PLNC systems.

S. Hatamnia et al. [47], 2016, proposed a dual-hop two-way cognitive radio system with a half-duplex relay over finite GF(2). Interference from the primary users affect the relay and source nodes and Nakagami-m fading models are used. A closed-form expressions for the symbol error probability and outage probability of the intended primary user are obtained. An upper bound on the achievable rate of the secondary system is also derived.

In 2014, P. Velmurugan and S. Thiruvengadam [48], studied a half duplex Cognitive Radio Relay system with multi-source and multi-destination. Decode and Forward relay. Analytical expressions are derived for average BER of the proposed Cognitive Radio system in overlay and underlay mode and the performance of the proposed system is compared with non-PLNC based systems.

M. Hafeez and J. Elmirghani [49], 2013, considered the use of distributed beamforming. A system with dynamic spectrum leasing for cognitive radio networks is proposed. This system increases the spectral utilization up to 20 times more than conventional cognitive radio. Again we see the use of beamforming in a PLNC-like system.

In 2013, J. Liu et al. [50], propose a set of cognitive two-way relay nodes employing a PLNC scheme. This system comes with joint relay selection and power allocation. This energy-efficient method is carried out in two phases. First, optimal power allocation is performed assuming only one relay participates in the relaying. In the second phase, the relay that achieves the minimum energy efficiency is selected based on the optimal power allocation from the first phase. Numerical results show an increase in performance in both high and low SNR values.

2.5.2 MIMO PLNC Systems

Below are some of the recent advances in MIMO systems employing PLNC.

In 2016, H. Nguyen et al. [51], use spatial division multiplexing technique at the two source nodes. Each node is equipped two antennas and the relay node uses the channel quantization method to map a Gaussian integer weighted linear combination of two symbols into PLNC. The proposed scheme achieves higher throughput than conventional PLNC and spatial division multiplexing.

J. Lemos and F. Monteiro [52], 2016, propose a massive MIMO PLNC system with full-duplex. The system performance is calculated and depends on the number of antennas at the relay. The feasibility of the proposed scheme is discussed. Unlike the system proposed in this thesis, massive MIMO systems require a high number of antennas while here only 4 at the relay are enough.

In 2016, T. Chan and T. Lok [53], consider multi-hop MIMO channels consisting of 3 transmitter-receiver pairs and half-duplex systems. Decode-and-forward relays are used. Interference alignment ideas are used with PLNC MIMO systems. Simulation results show that the end-to-end performance of the proposed system is better than the zero-forcing filtering scheme in medium and high SNR. Once again, frequency selective channels are not considered in that work.

In the same year, N. Kaim Khani et al. [54], studied multiuser MIMO systems using BPSK/QPSK modulation in flat fading channels. The idea of Vertical-Bell Laboratories Layered Space-Time (V-BLAST) is used with PLNC to enhance throughput and performance.

J. Guo et al. [55], 2015, proposed a linear vector for MIMO PLNC systems using QAM modulation in Rayleigh fading channels. A solution is found for the generator matrix that minimizes the error probability at high SNR. Simulation results match the derived performance equation.

All the above work does not consider frequency selective channels.

2.6 Fading Channels

Communication signals pass through different types of channels. Some of these channels not only attenuate the signal but also distort it. Attenuation is the loss of signal power when it passes through a medium. When this attenuation is variable with time, then the signal is experiencing fading. In other words, when both the signal's envelope and phase are fluctuating then this is called fading [56]. In this section, only fading channels due to multipath are discussed. If the channel has more than one object that reflects

the transmitted signal back to the receiver, then the channel is called a multipath fading channel. The received signal will contain overlapping copies of the original signal each with different delays and attenuations.

There are several ways to model such channels. If a pulse is is sent through a multipath channel, then the receiver will pick up multiple pulses corresponding to each path in addition to the line of sight component (LOS) if it exists. This means that the received signal will be present for a longer time than the original pulse and this is referred to as the time delay spread of the multipath channel. In narrowband fading channels, the time delay spread is very small compared to the original pulse time. This means that the received pulses from constructive and destructive components are almost aligned and arrive at the same time. The most common model in this case is the Rayleigh fading model. The Rayleigh fading model is a statistical approach to model the channel as a sum of an infinite (or very large) number of received reflections coming from all angles of the receiver with equal probabilities for all angles. As a result of this assumption, the process becomes complex Gaussian. Other variations of the Rayleigh fading channel model have also been proposed, namely the Rician model and the Nakagami model. The Rician model is used when there is a dominant line of sight, meaning that the first received component (or the first few) is fixed [57, 58] while the Nakagami model is used with maximum ratio diversity combining. In wideband fading models on the other hand, the multipath time delay spread is much greater than the original pulse width. In this case, each multipath component can be resolved separately. This leads to interference between some of these components and subsequently transmitted pulses. This is called inter-symbol interference (ISI).

2.7 Modelling of Frequency Selective Slow Fading Channels

By modelling the channel we mean finding the impulse response of the multipath channel. In the case where the reflections of the sent signal can be resolved into distinct complex gain values for each path, the impulse response can be modelled by a tapped delay line. In a digital system, signals and channels are represented by vectors arising from sampling their analogue counterparts.

Let **h** represent the channel vector in which each coefficient represents the gain and

phase of the arriving signal when an impulse is sent by the transmitter. This channel is assumed to be fixed during the period of transmission.

The received signal can then be represented by the convolution between the channel vector and the sent vector x. The received signal $y(k)$ at time k can be written as

$$y(k) = \sum_{m=0}^{L_{\mathbf{h}}-1} \mathbf{h}(m)x(k-m) + w(k), \tag{2.10}$$

where L_h is the length of the channel and $w(k)$ is the instantaneous AWGN with zero mean and variance of σ_w^2.

This channel model is shown in figure (2.5).

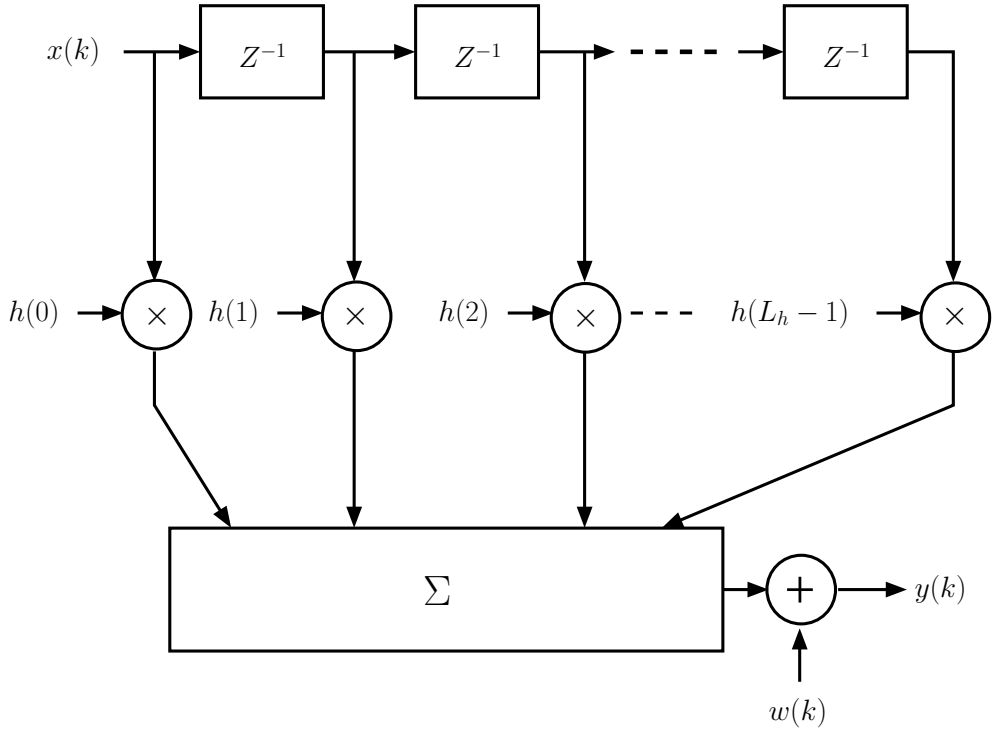

Figure 2.5: Tapped delay line model of a multipath channel.

There are different environments in which the channel profile can be represented this way including indoor office environment, outdoor to indoor and pedestrian environment and satellite environment [59].

A test channel impulse response is given in [59] for each these environments represented by a tapped delay line model. A number of taps are measured representing each path and the power of each tap is calculated relative to the power of the first tap. The multipath power-delay profile is completed with a set of delays corresponding to each tap. These delays represent the r.m.s. delay spread of each path.

2.8 Overview of Equalization Techniques

This section is dedicated to give a general understanding of the theory of equalization as channel equalizers will be used throughout this thesis. Depending on its structure, an equalizer can be either linear or non-linear. In general, non-linear equalizers outperform linear ones but are more complex so they are used in channels with more severe distortions to mitigate the effects of the channel. The basic principle of equalization is to use the channel information available at the receiver which is then used to design the equalizer in a manner that reduces or eliminates the ISI. By sending pilot symbols, the receiver side can calculate the channel taps and this process is called channel estimation.

Figure (2.6) shows some of the linear and non-linear equalization methods.

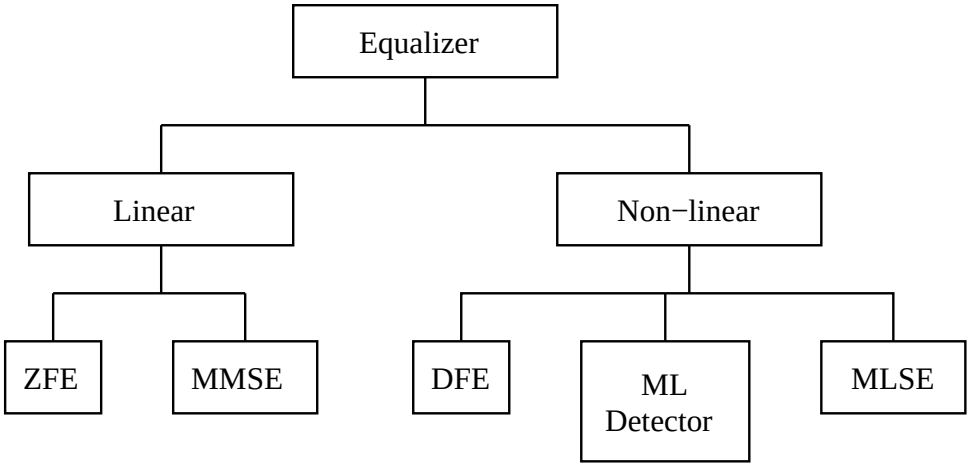

Figure 2.6: Categorization of equalization methods into linear and non-linear techniques.

Linear equalizers utilize a single FIR filter while the Decision feedback equalizer (DFE) uses two filters one of which is a feedback filter that takes its input from a decision device. Although the DFE is non-linear and outperforms the linear equalizers, yet it is considered suboptimal compared to the maximum likelihood sequence equalizer (MLSE). The MLSE calculates all the possible transmitted sequences and selects the sequence with the highest probability which will be the output of this equalizer. For a finite state discrete-time Markov process, the Viterbi algorithm can be used to solve this problem. The MLSE sacrifices complexity for better results and this depends on the channel length and the size of the used constellation. If L is the channel length and M_s is the constellation size of the sent signal, then the number of states in the Viterbi algorithm becomes M_s^L [60]. This number can become very high in some channels preventing practical implementation of this type of equalizers due to its high cost.

2.8.1 Linear Equalization

This is the simplest type of equalizers and the most cost effective and it is linear because it uses an FIR filter which is a weighted sum of the input symbols. It is not iterative and can perform block by block equalization or symbol by symbol. Besides the low performance of linear equalizers, they also introduce a small delay which is an inevitable consequence of any FIR filter. The zero forcing equalizer (ZFE) can be easy to design and can totally eliminate all the ISI. The problem is that the ZFE will also introduce a high noise amplification specially at spectral nulls or very low values and this degrades the performance of this equalizer. The tougher the channel the more severe nulls it will have and the more noise amplification will occur. The linear minimum mean square error (MMSE) equalizer does not eliminate all the ISI but instead minimizes the mean square error between the the received and transmitted signals without introducing significant noise amplification. The linear MMSE equalizer has better performance over the ZFE but for tough channels the simple linear structure is prevents acceptable BER performance and more complex non-linear equalizers are required [61].

Figure (2.7) shows the structure and building blocks of a typical linear equalizer in which $\hat{x}(k)$ is the estimation of the sent signal at instant k and $C(0)\ ,\ C(1)\ ,\ \ldots\ C(N_h{-}1)$ are the N_h coefficients of the equalizer.

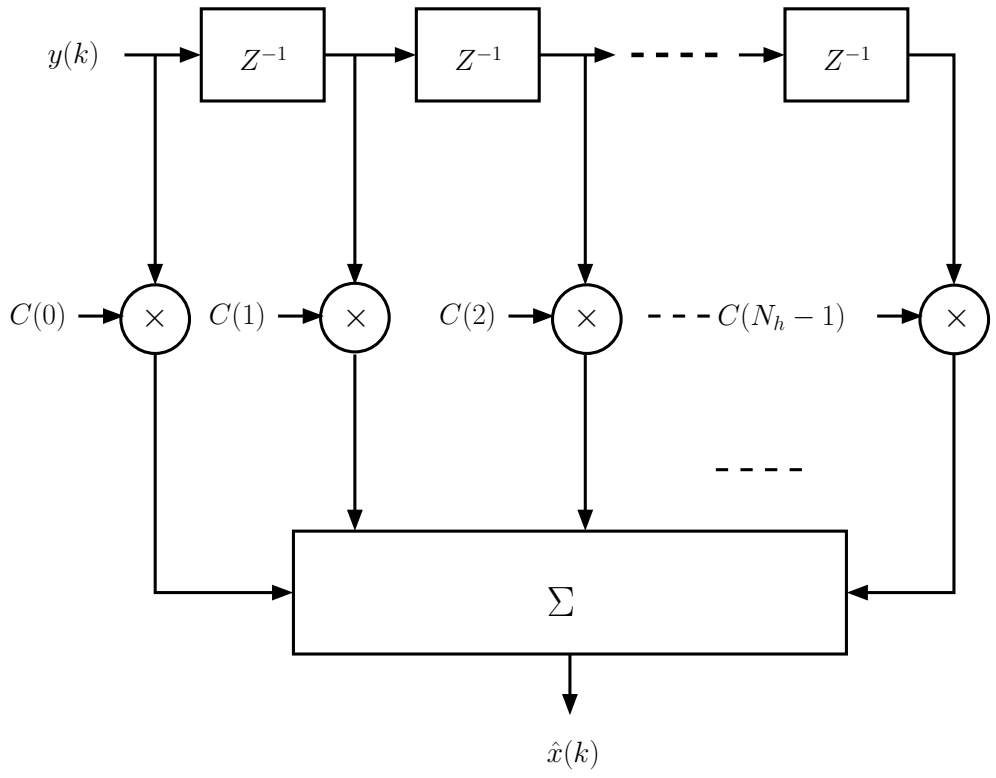

Figure 2.7: Structure of a linear equalizer.

2.8.2 DFE Equalization

The DFE is a good compromise between the low performance linear equalizers and the exponentially complex non-linear MLSE. It provides a significant performance enhancement for the addition of only one FIR feedback filter. Although the DFE consists of two linear FIR filters, yet it is considered non-linear because the input of the feedback filter comes from the non-linear decision device. Previous decisions are put into use by feeding them back and subtracting the residual trailing ISI that results from the forward filter. Once again, the channel information is used in the design and a linear derivation of the filter coefficients is made by assuming that the previous decisions are correct. For this reason, the performance of the DFE usually becomes better and better in a non-linear fashion as the SNR increases because the assumption that the previous decisions are correct becomes even more true. Ideally, the feed-forward filter has infinite length to perform as a whitening filter but practically a finite feed-forward filter is used. Minimum mean square error criteria is used to calculate the filter coefficients and the DFE is optimum in that sense. The operation of this equalizer is not iterative and is done on a symbol by symbol basis.

2.8.3 Adaptive Equalization

Adaptive filters are used here in the context of equalization. In adaptive filters, the coefficients are changing with the arrival of every new symbol [61]. Adaptive filters require more operations than in a normal filter, yet the advancement of high speed signal processing tools helps making such equalizers easier to implement. The adaptive filter first starts in the learning phase followed by the normal operation phase. The learning phase ends either when a pre-defined number of learning symbols have been processed or when the error signal reaches its minimum.

In this section, two main methods will be discussed namely, the normalized least square error (NLMS) and the recursive least square RLS. Both are considered as linear equalizers in the sense that the resulting filter is an FIR filter but with time varying filter coefficients.

2.8.3.1 NLMS

The NLMS is a method for adaptation of the equalizer filter coefficients in which the input vector is normalized in every iteration.

the following update equation is used:

$$\mathbf{C}_k = \mathbf{C}_{k-1} + \frac{\mu}{\epsilon_a + \|\mathbf{y}\|}\mathbf{y}e_r^*, \tag{2.11}$$

where $\mathbf{C}_k$ is the filter coefficient vector at instant k, $\mathbf{C}_{k-1}$ is the previous value of the filter coefficient vector, μ is the step size, $\mathbf{y}$ is the input vector, ϵ_a is a small quantity to prevent the denominator from being zero, $\|\mathbf{y}\|$ is the norm of $\mathbf{y}$, and e_r^* is the complex conjugate of the error.

2.8.3.2 RLS

In this method the previous data are taken into account with forgetting factor λ_a where

$$0 \leqslant \lambda_a \leqslant 1.$$

The method tries to approximate $\min E \mid x - \mathbf{y}\mathbf{C} \mid^2$ in a recursive way where x is the correct data symbols or bits. This is done by first starting with the initial value of the matrix $\mathbf{P}$ or $\mathbf{P}_{-1} = \Delta_a \mathbf{I}_N$, where Δ_a is a large value to insure convergence, $\mathbf{I}_N$ is the identity matrix of dimensions $(N \times N)$ and N is the equalizer length. The filter coefficients and the matrix $\mathbf{P}$ are updated using the following equations :

$$\mathbf{C}_k = \mathbf{C}_{k-1} + \mathbf{P}_k \mathbf{y}_k^* [x(k) - \mathbf{y}_k \mathbf{C}_{k-1}], \tag{2.12}$$

and

$$\mathbf{P}_k = \lambda_a^{-1} \left[\mathbf{P}_{k-1} - \frac{\lambda_a^{-1} \mathbf{P}_{k-1} \mathbf{y}_k^* \mathbf{y}_k \mathbf{P}_{k-1}}{1 + \lambda_a^{-1} \mathbf{y}_k \mathbf{P}_{k-1} \mathbf{y}_k^*} \right], \tag{2.13}$$

where k is the time index and $x(k)$ is the correct symbol in training mode.

The RLS method has a faster convergence speed and better performance compared to the NLMS scheme [62]. This comes at the expense of extra complexity. The two schemes mentioned before are linear methods and are outperformed by their non-linear counterparts. Moreover, adaptive filters in general are outperformed by optimum equalizer designs when the channel is unchanged during one frame period.

2.9 Chapter Summary

In this chapter, the development of TWRN is discussed starting from the 4 time slot relaying without network coding and finishing with the 2 time slot PLNC system. This includes the standard network coding which is presented in Section 2.3. The PLNC method in flat fading channels is described in detail in Section 2.4. The chapter also discusses the two major schemes in PLNC, namely the AF and DNF schemes. Moreover, a review of the more recent advances in the field of PLNC is provided with emphasis on its applications in cognitive radio and MIMO systems. The modelling of frequency selective slow fading channels is discussed in Section 2.7. Finally, an overview of some of the basic equalization methods is presented in Section 2.8.

Chapter 3

DFE for Frequency Selective PLNC Channels using AF

3.1 Introduction

High speed transmission of information suffers inevitably from intersymbol interference (ISI) induced by multipath propagation over frequency selective channels. ISI has been a major obstacle preventing the successful implementation of physical layer network coding (PLNC) systems in these environments. Another major obstacle is the high computational complexity of existing algorithms dealing with ISI, which is a determining factor in the design of relay nodes.

In this chapter, we propose a novel and computationally efficient decision feedback equalizer structure that is utilized at the end node and in conjunction with a simple amplify and forward (AF) technique employed at the relay. This type of system is not proposed before and allows smooth transmission in PLNC systems working with frequency selective channels. This is a major advancement in the field of PLNC as direct implementation of this system is not possible in such kind of channels. We derive the optimal equations for the decision feedback equalizer (DFE) coefficients and evaluate the end-to-end (E2E) bit error rate performance in frequency selective channels, and provide both analytical and numerical simulation results that demonstrate the feasibility of the proposed approach under realistic channel conditions. The DFE that is used instead of linear equalizers gives a great boost to the performance of such systems.

The obtained results show that E2E performance is dominated by the channel with most severe frequency selectivity.

3.2 Problem Description and Solution

The problem under examination in this chapter rests within the general goal of the thesis. This is in brief, aiming to make PLNC systems work in frequency selective environments as direct implementation of these systems in such channels is not possible. The problem with such implementation is that there will be two different ISIs from end nodes. This means that simply adding equalizers to the system also doesnt work as the data packets pass through different channels before being added up.

Moving on to the specific properties of the proposed solution. One of the most important property is that its cost effective. This arises from choosing the method of amplify and forward at the relay.

The other property in the design is the simplicity of the relay node. This is very

important in some cases like in wireless sensor networks for example, in which the relay nodes are remote. In these cases, relay nodes have limited power and computational resources. As the proposed method uses only amplify and forward at the relay, it is then more suitable for such applications.

Pre-filtering or pre-equalization has been proposed to make a PLNC system viable in frequency selective channels. The design in this chapter succeeds in avoiding this as pre-filtering designs have some extra limitations and requirements. Due to the fact that the signal passes through both of the two channels, the pre-filtering technique requires knowledge of both channels to be present at each end node. This not only adds extra overhead, but more importantly, it requires the channels to be unchanged for at least two transmission and broadcasting cycles. This need arises from the fact that the current pre-filtering operation depends on the channel estimation done in the previous cycle. The situation becomes even worse for the pre-filtering method if the relay node is shared by more than one pair of end nodes as in the star network formation for example. In the latter case, pre-filtering requires the channels to be unchanged for much more than two individual transmission cycles, while the proposed method only needs one regardless of the type and shape of the network that is used. This makes the proposed method compatible to all kinds of networks with no extra overhead for channel information exchange between end nodes.

Another advantage is that for existing PLNC systems, only simple adjustments are required and this is done at the end nodes only in order to make the system work in a frequency selective environment.

Also, the design is not restricted to BPSK modulation but can work with QPSK, 16-QAM and higher order modulation schemes.

Finally, by avoiding the use of OFDM several advantages arise. The main advantage is that we can move from the linear equalization that is used with OFDM systems to the better DFE equalizer which is non-linear. This on its own gives a lead in performance and at the same time avoids some of the problems in OFDM like peak to average power ratio PAPR and the extra cyclic prefix overhead. Although the problems of OFDM have been addressed by many researchers, yet the solutions do not come without extra complexity and cost.

3.3 Decision Feedback Equalizer

The DFE equalizer is an extension of the linear least mean square equalizer. In a linear FIR equalizer the least mean square method is used to obtain the filter coefficients. Let $\mathbf{h}$ be a one dimensional vector that represents an FIR channel. This vector is assumed to be known at the receiver side and has a length of L_h. When the data packet $\mathbf{s}$ passes through this channel, ISI is created due to the channel memory. The received signal is observed with the addition of noise $\mathbf{w}$. The vectors $\mathbf{h}$ and $\mathbf{w}$ are assumed to be independent. The observed symbol $y(k)$ can be written as

$$y(k) = \mathbf{h}(0)\mathbf{s}(k) + \sum_{m=1}^{L_h-1} \mathbf{h}(m)\mathbf{s}(k-m) + \mathbf{w}(k). \tag{3.1}$$

The second term in equation 3.1 is the ISI term and represents the effect of the previously sent symbols prior to $\mathbf{s}(\mathbf{k})$. For the equalizer to retrieve the symbol $\mathbf{s}(\mathbf{k})$, it cannot depend on the current observation $y(k)$ alone. Instead, a number of the previous measurements of y are included. This is due to the fact that these measurements contain information that is included in the ISI term of $y(k)$. The expression for $y(k-1)$ for example is

$$y(k-1) = \mathbf{h}(0)\mathbf{s}(k-1) + \sum_{m=1}^{L_h-1} \mathbf{h}(m)\mathbf{s}(k-1-m) + \mathbf{w}(k-1). \tag{3.2}$$

The ISI terms in equations 3.1 and 3.2 have many common symbols and this is why the previous measurements are useful in mitigating ISI.

3.3.1 Linear Equalizers

Discussing the linear equalizer is important for understanding the DFE equalizer. The linear equalizer is assembled as an FIR digital filter with N_F coefficients. This way the filter will deal with N_F observations at a time. These observations can be written in vector form as follows

$$\mathbf{y_k} = \begin{bmatrix} y(k) \\ y(k-1) \\ y(k-2) \\ \vdots \\ y(k-N_F+1) \end{bmatrix}. \tag{3.3}$$

The subscripts in this section are used to denote that $\mathbf{y_k}$ is a vector as opposed to $y(k)$ which refers to the scalar instantaneous value of the observation at time k. Although $\mathbf{y_k}$ is a vector, it is not fixed but rather changing depending on the time instance k.

Let the instantaneous transmitted data vector be s_k and the instantaneous noise vector be $\mathbf{w_k}$. These vectors are collected in a similar fashion to $\mathbf{y_k}$. Then the observation vector can be written as

$$\begin{bmatrix} y(k) \\ y(k-1) \\ y(k-2) \\ \vdots \\ y(k-N_F+1) \end{bmatrix} = \begin{bmatrix} h(0) & h(1) & \dots & h(L_h-1) & 0 & \dots & 0 \\ 0 & h(0) & h(1) & \dots & h(L_h-1) & \dots & 0 \\ \vdots & & & & & & \vdots \\ 0 & \dots & 0 & h(0) & h(1) & \dots & h(L_h-1) \end{bmatrix}$$

$$\times \begin{bmatrix} s(k) \\ s(k-1) \\ s(k-2) \\ \vdots \\ s(k-N_F-L_h+2) \end{bmatrix} + \begin{bmatrix} w(k) \\ w(k-1) \\ w(k-2) \\ \vdots \\ w(k-N_F+1) \end{bmatrix}, \tag{3.4}$$

or in matrix form

$$\mathbf{y} = \mathbf{H}\mathbf{s} + \mathbf{w}, \tag{3.5}$$

where $\mathbf{H}$ is the convolutional matrix of the channel with dimensions $N_F \times (N_F + L_h - 1)$.

The goal is to find an estimate of $s(k-\Delta)$ or $\hat{s}(k-\Delta)$, where Δ is a positive integer number resembling the channel induced propagation delay.

Let $\varepsilon(k-\Delta)$ be the error signal. This can be written as

$$\varepsilon(k) = s(k-\Delta) - \hat{s}(k-\Delta). \tag{3.6}$$

Define $\mathbf{fl}$ as the linear filter coefficient vector. Also, define $\mathbf{fl}_{opt}$ as the optimum value for $\mathbf{fl}$. To find $\mathbf{fl}_{opt}$, we need to minimize the cost function $E(\varepsilon\varepsilon^*)$ in a mean square error sense, where $E(.)$ is the expectation operation.

$$\min_{\mathbf{fl}} E\left|\varepsilon\right|^2. \tag{3.7}$$

Now the estimate of the transmitted symbol can be found by passing $\mathbf{y_k}$ through the equalizer filter $\mathbf{fl}_{opt}$

$$\hat{s}(k-\Delta) = \mathbf{fl}^*_{opt}\mathbf{y_k}, \tag{3.8}$$

The standard least mean square error solution is used to find $\mathbf{fl}_{opt}$ and this will be [61]

$$\mathbf{fl}_{opt} = \mathbf{R_{sy}}{\mathbf{R_y}}^{-1}, \tag{3.9}$$

where $\mathbf{R_{sy}}$ is a matrix of length $(1 \times N_F)$ and represents the cross-covariance matrix between $s(k-\Delta)$ and $\mathbf{y_k}$

$$\mathbf{R_{sy}} = E(s(k-\Delta){\mathbf{y_k}}^*), \tag{3.10}$$

and $\mathbf{R_y}$ is a matrix of length $(N_F \times N_F)$ representing the observation covariance matrix

$$\mathbf{R_y} = E(\mathbf{y_k}{\mathbf{y_k}}^*). \tag{3.11}$$

For successful implementation of the linear equalizer, equation (3.9) needs to be written in terms of the known elements in the system which are the channel matrix, the signal power σ_s^2 and the noise power σ_w^2. To do this, we must first find $\mathbf{R_{sy}}$ and $\mathbf{R_y}$. From the system equation (3.5) we can write $\mathbf{R_y}$ as

$$\mathbf{R_y} = E((\mathbf{H}s_k + \mathbf{w_k})(\mathbf{H}s_k + \mathbf{w_k})^*) = \mathbf{H}\mathbf{R_s}\mathbf{H}^* + \mathbf{R_w}, \tag{3.12}$$

where $\mathbf{R_s} = E(s_k s_k^*) = \sigma_s^2 I$ and $\mathbf{R_w} = E(\mathbf{w_k}{\mathbf{w_k}}^*) = \sigma_w^2 I$ and $\mathbf{R_y}$ will be

$$\mathbf{R_y} = \sigma_s^2\mathbf{H}\mathbf{H}^* + \sigma_w^2 I. \tag{3.13}$$

Now only $\mathbf{R_{sy}}$ is to be found and this also starts from the system equation (3.42) as follows

$$\mathbf{R_{sy}} = E(s(k-\Delta)(\mathbf{H}s(k) + w(k))^*), \tag{3.14}$$

$$\mathbf{R_{sy}} = E(s(k-\Delta)s(k)^*)\mathbf{H}^*, \tag{3.15}$$

as $E(s(k-\Delta)w(k)^*) = 0$ because the two terms are assumed to be uncorrelated.

$$\begin{aligned} E(s(k-\Delta)s(k)^*) =& s(k-\Delta)[s(k)^*\ s(k-1)^* \dots\ s(k-N_F-L_h+1)^*] \\ &= [0\ \dots\ 0\ \sigma_s^2\ 0\ \dots\ 0], \end{aligned} \tag{3.16}$$

with Δ number of zeroes before σ_s^2. This leads to

$$\mathbf{R_{sy}} = [0\ \dots\ 0\ \sigma_s^2\ 0\ \dots\ 0]\mathbf{H}^*. \tag{3.17}$$

Now substituting equations (3.13) and (3.17) in equation (3.30) leads to the desired filter design equation

$$\mathbf{fl}_{opt} = \sigma_s^2 \mathbf{e_\Delta}^* \mathbf{H}^* (\sigma_s^2 \mathbf{H}\mathbf{H}^* + \sigma_w^2 I)^{-1}, \tag{3.18}$$

where $\mathbf{e_\Delta}$ is a vector of length $(N_F + L_h - 1)$ starting with Δ number of zeroes followed by a one and succeeded by zeroes

$$\mathbf{e_\Delta} = [0\ \dots\ 0\ 1\ 0\ \dots\ 0]. \tag{3.19}$$

3.3.2 Decision Feedback Equalizer

The DFE can be considered as an extension to the linear equalizer. The channel is assumed to be FIR with L_h number of taps. The measurements include the effect of this channel with additive white Gaussian noise w. Also, w and s are uncorrelated with zero mean. Therefore equation (3.1) applies here. In the linear equalizer, current and previous measurements $\mathbf{y_k}$ are used to eliminate the effect of ISI. If the actual previous symbols were known and used, then they are more effective in achieving that goal. Although this is not the case, yet the DFE uses the previous decisions as substitutes for the previous symbols. These decisions are fed back via another filter to be used in conjunction with the feedforward or linear filter. figure (3.1) shows the block diagram of the DFE equalizer.

This equalizer estimates the delayed signal $\check{s}(k-\Delta)$, where $\mathbf{F}(z)$ is the transfer function of the feedforward filter and $B(z)$ represents the feedback filter. The decision device matches $\hat{s}(k-\Delta)$ to the nearest constellation point. If the channel $\mathbf{H}(z)$ is severe, this means it will have considerable ISI. In this case $\mathbf{H}(z)\mathbf{F}(z)$ will be a sequence instead of single impulse and it will have a significant trailing inter-symbol interference impulse

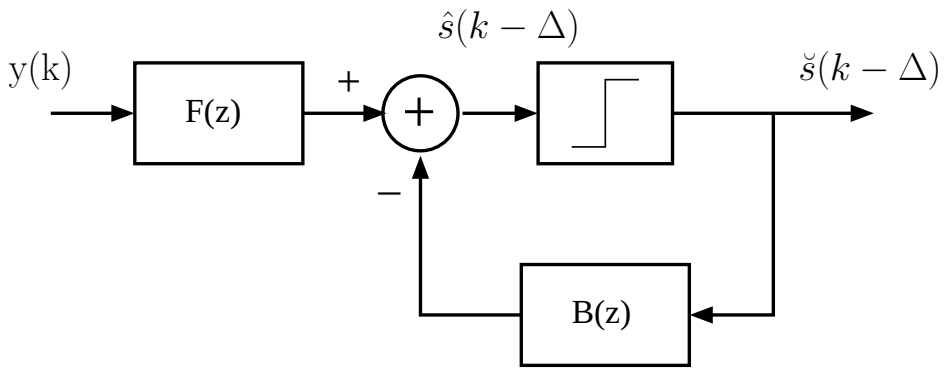

Figure 3.1: DFE equalizer block diagram.

response. This is where the feedback filter is used to reduce this trailing ISI.

Let $\mathbf{f}$ be the feed forward filter of length N_{FF} whose taps are $[\, f(0)\,,\, f(1)\,,\, \ldots\,,\, f(N_{FF}-1)\,]$ and $\mathbf{b}$ be a feedback filter of length N_{FB} whose taps are $[\, b(1)\,,\, b(2)\,,\, \ldots\,,\, b(N_{FB})\,]$. The coefficients of $\mathbf{b}$ start from $b(1)$ as the input to the feedback filter contains only the prior decisions that are being fed back. to design the equalizer, f and b need to be calculated. The optimum values $\mathbf{f}_{\text{opt}}$ and $\mathbf{b}_{\text{opt}}$ are obtained by minimizing the following cost function

$$J_k = \min_{\mathbf{f},\mathbf{b}} E\left|\varepsilon(k-\Delta)\right|^2, \tag{3.20}$$

where $\varepsilon(k-\Delta)$ is the delayed error signal and

$$\varepsilon(k-\Delta) = s(k-\Delta) - \hat{s}(k-\Delta). \tag{3.21}$$

The fact that the input of the feedback filter comes from the nonlinear decision device makes solving equation (3.20) become a nonlinear optimization problem. This also makes the DFE in general a nonlinear equalizer. To make the design problem easier, it is assumed that the decisions $\breve{s}(k-\Delta)$ are correct and therefore equal to $s(k-\Delta)$. This is not always true and when decision errors occur, they will propagate through the feedback filter causing some degradation in the performance of the DFE. In spite this degradation, the DFE outperforms the linear equalizer. Also, as the SNR increases, fewer errors occur in the output and this error propagation becomes less effective. Let

$$\mathbf{s_\Delta} = \begin{bmatrix} s(k-\Delta) \\ s(k-\Delta-1) \\ s(k-\Delta-2) \\ \vdots \\ s(k-\Delta-N_{FB}) \end{bmatrix}. \tag{3.22}$$

Define the following

$$\mathbf{R_s} = E(\mathbf{s_\Delta s_\Delta}^*), \tag{3.23}$$

$$\mathbf{R_{sy}} = E(\mathbf{s_\Delta y_k}^*), \tag{3.24}$$

$$\mathbf{R_{ys}} = E(\mathbf{y_k s_\Delta}^*), \tag{3.25}$$

and

$$\mathbf{R_y} = E(\mathbf{y_k y_k}^*), \tag{3.26}$$

where $\mathbf{R_{sy}}$, $\mathbf{R_{ys}}$, $\mathbf{R_y}$ and $\mathbf{R_s}$ are assumed to be independent of k and that $\mathbf{R_y}$ is invertible. The error signal $\varepsilon(k-\Delta)$ can be written as

$$\varepsilon(k-\Delta) = b^*\mathbf{s_\Delta} - f^*\mathbf{y_k}. \tag{3.27}$$

Equation (3.20) becomes

$$J_k = \min_{\mathbf{f},\mathbf{b}} E\left|b^*\mathbf{s_\Delta} - f^*\mathbf{y_k}\right|. \tag{3.28}$$

To solve this problem we find the solution for f assuming b is constant. Let $\alpha = b^*\mathbf{s_\Delta}$ which a scalar constant. This way the problem becomes the following linear estimation problem

$$\min_{\mathbf{f}} E\left|\alpha - \mathbf{f}^*\mathbf{y_k}\right|. \tag{3.29}$$

The linear least mean square error solution for f will be [61]

$$\mathbf{f}_{opt} = \mathbf{R}_{\alpha\mathbf{y}}{\mathbf{R_y}}^{-1} = \mathbf{b}^*\mathbf{R_{sy}}{\mathbf{R_y}}^{-1}, \tag{3.30}$$

because

$$\mathbf{R}_{\alpha\mathbf{y}} = E(\alpha\mathbf{y_k}) = E(\mathbf{b}^*\mathbf{s_\Delta}\mathbf{y_k}^*) = \mathbf{b}^*\mathbf{R_{sy}}. \tag{3.31}$$

Now that $\mathbf{f}_{opt}$ is found, the minimum mean square error becomes

$$E\left|\alpha - \mathbf{f}_{opt}^*\mathbf{y_k}\right|^2 = \mathbf{R}_\alpha - \mathbf{R}_{\alpha\mathbf{y}}\mathbf{R_y}^{-1}\mathbf{R}_{\mathbf{y}\alpha}. \tag{3.32}$$

Substituting equations (3.30) and (3.31), the minimum mean square error becomes

$$\mathbf{b}^*\mathbf{R_s}\mathbf{b} - \mathbf{b}^*\mathbf{R_{sy}}\mathbf{R_y}^{-1}\mathbf{R_{ys}}\mathbf{b}. \tag{3.33}$$

This can be written as $\mathbf{b}^* R_d \mathbf{b}$, where

$$\mathbf{R_d} = \mathbf{R_s} - \mathbf{R_{sy}}\mathbf{R_y}^{-1}\mathbf{R_{ys}}. \tag{3.34}$$

The problem is reduced to finding $\mathbf{b}_{opt}$ by solving

$$\min_{\mathbf{b}} \mathbf{b}^*\mathbf{R_d}\mathbf{b} \quad subject\ to \quad \mathbf{b}^*\mathbf{e_0} = 1, \tag{3.35}$$

where $\mathbf{e_0} = [\,1\,,\,0\,,\,\ldots\,,\,0\,]^T$ and $\mathbf{e_0}$ has a length of $N_{FB}+1$.

According to Gauss-Markov theorem, the solution will be [61]

$$\mathbf{b}_{opt} = \frac{\mathbf{e}_0\mathbf{R}_d^{-1}}{\mathbf{e}_0\mathbf{R}_d^{-1}\mathbf{e}_0}. \tag{3.36}$$

Substituting this in equation (3.30) gives

$$\mathbf{f_{opt}} = \mathbf{b}_{opt}^*\mathbf{R_{sy}}\mathbf{R_y}^{-1}. \tag{3.37}$$

The last two equations are used in tandem in the design of the DFE equalizer. Other specific aspects of the design like choosing the filter lengths and the value of Δ are discussed in a later section.

3.4 System Model

In recent years, Physical Layer Network Coding (PLNC) has attracted significant amount of research work [63] due to its ability to save transmission bandwidth, which is one of the most valuable resources in communication systems. In PLNC the goal is to exchange

information between two points or end nodes with the help of an intermediate point called the relay node (R). This process is bidirectional so that both nodes send to and receive data packets from each other. The whole exchange happens in two time slots. In the first time slot t_1 as shown in Fig. 1, both end nodes U_1 and U_2 transmit their data packets $\mathbf{a}$ and $\mathbf{b}$, respectively, to the relay. These data packets are physically added at the relay.

The lower part of Figure (3.2) shows the second time slot t_2, in which the added packets $\mathbf{a}+\mathbf{b}$ are broadcast back to the end nodes. If we consider node 1 then the desired signal $\mathbf{b}$ can be extracted from the received signal $\mathbf{a}+\mathbf{b}$ using the prior knowledge of $\mathbf{a}$. Node 2 can also extract its desired signal $\mathbf{a}$ in a similar manner and this is independent on the modulation method that is used. This is true if the channels are flat fading. Here, it is assumed that the forward and reverse channels are identical, so $\mathbf{h_1}(\tau_\iota) = h_{1\to R}(\tau_\iota) = h_{R\to 1}(\tau_\iota)$ and $\mathbf{h_2}(\tau_\iota) = h_{2\to R}(\tau_\iota) = h_{R\to 2}(\tau_\iota)$.

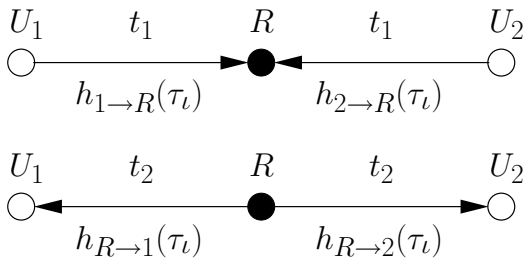

Figure 3.2: PLNC uplink and downlink phases.

3.4.1 Uplink Phase

During the uplink phase, end nodes send their packets at the same time in the first interval, t_1. The transmitted packets are distorted by the channels $\mathbf{h}_1$ and $\mathbf{h}_2$. Both channels are considered linear time-invariant and dispersive in the presence of AWGN. In this paper, we assume that the 2 channels are known at the end nodes only. Let $\mathbf{a}$ and $\mathbf{b}$ be two column vectors representing the data packets sent from nodes 1 and 2, respectively. The total received signal at the relay will be

$$y(k) = \sum_{m=0}^{L_1-1} \mathbf{h_1}(m)a(k-m) + \sum_{m=0}^{L_2-1} \mathbf{h_2}(m)b(k-m) + w_r(k), \tag{3.38}$$

where $\mathbf{w}_r$ is the uplink noise and L_1 and L_2 are the lengths of channels 1 and 2 respectively.

3.4.2 Downlink Phase

In the downlink phase, t_2, the relay broadcasts the signal in (3.38) multiplied by the AF gain, g_{AF} and no attempt is made to separate these two signals. We consider now the received signal vector $\mathbf{r}$ at node 1. The received broadcast signal at node 1 is given as

$$r(k) = g_{AF} \sum_{l=0}^{L_1-1} \mathbf{h_1}(k-l)y(l) + w_1(k), \tag{3.39}$$

where $\mathbf{w}_1$ represent AWGN at node 1. Substituting equation 3.38 in 3.39, we obtain

$$\begin{aligned} r(k) =& g_{AF} \sum_{l=0}^{L_1-1} \mathbf{h_1}(k-l)(\sum_{m=0}^{L_1-1} \mathbf{h_1}(m)a(l-m) \\ &+ \sum_{m=0}^{L_2-1} \mathbf{h_2}(m)b(l-m) + w_r(k)) + w_1(k). \end{aligned} \tag{3.40}$$

This can be expanded to

$$\begin{aligned} r(k) =& g_{AF} \sum_{l=0}^{L_1-1} \mathbf{h_1}(k-l) \sum_{m=0}^{L_1-1} \mathbf{h_1}(m)a(l-m) \\ &+ g_{AF} \sum_{l=0}^{L_1-1} \mathbf{h_1}(k-l) \sum_{m=0}^{L_2-1} \mathbf{h_2}(m)b(l-m) \\ &+ g_{AF} \sum_{l=0}^{L_1-1} \mathbf{h_1}(k-l)w_r(k) + w_1(k), \end{aligned} \tag{3.41}$$

or more compactly in matrix form

$$\mathbf{r} = g_{AF}\mathbf{H}_{11}\mathbf{a} + g_{AF}\mathbf{H}_{12}\mathbf{b} + g_{AF}\mathbf{H}_1\mathbf{w}_r + \mathbf{w}_1, \tag{3.42}$$

where $\mathbf{H}_1$ is the convolutional matrix of channel 1 such that $\mathbf{H}_1\mathbf{w}_r = \mathbf{w}_r * \mathbf{h}_1$, where $*$ denotes the convolution operation and $\mathbf{h}_1$ is a vector representing the taps of the first channel. $\mathbf{H}_{11} = \mathbf{h}_1 * \mathbf{h}_1$ and $\mathbf{H}_{12} = \mathbf{h}_1 * \mathbf{h}_2$ are constructed similarly. To illustrate this

point, $\mathbf{H}_{12}$ is given as

$$\mathbf{H}_{12} = \begin{bmatrix} h_0 & h_1 & \dots & h_L & 0 & \dots & 0 \\ 0 & h_0 & h_1 & \dots & h_L & \dots & 0 \\ \vdots & & & & & & \vdots \\ 0 & \dots & 0 & h_0 & h_1 & \dots & h_L \end{bmatrix}, \tag{3.43}$$

where $L = L_1 + L_2 - 1$.

Equation (3.42) consists of 2 signal terms followed by 2 noise terms. Assuming perfect channel estimation, the first term can be calculated at node 1 because both $\mathbf{a}$ and $\mathbf{h}_1$ are known. After calculating and subtracting the first term from $\mathbf{r}$, we are left with the second signal term, which represents the desired packet $\mathbf{b}$ convolved with the two channels plus the 2 noise signal terms.

This can be easily and efficiently handled with only one DFE filter at each end node. The design of this DFE will be discussed in the next section. The same approach can be applied at node 2 and the overall concept is illustrated in Figure 3.3.

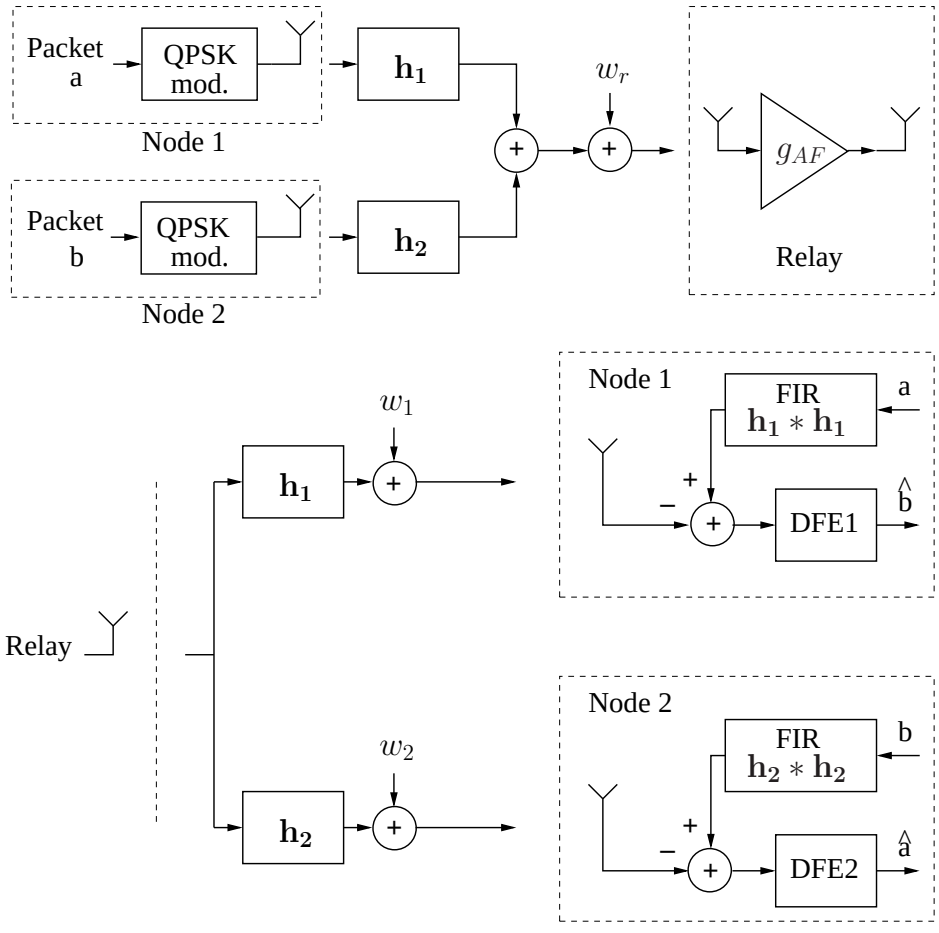

Figure 3.3: Proposed amplify and forward scheme.

It is worth highlighting that the first term in (3.42) can be pre-computed during the uplink phase, thus, putting the computational resources to optimal use. The computational complexity in the downlink time slot is hence reduced to a mere DFE computation at each end node.

3.5 Error Bound

Due to the non-linear nature of the DFE, finding the theoretical BER performance of this equalizer is not an easy task [64]. Instead, the feedback symbols are assumed to be correct and this gives the minimum achievable mean square error. If the forward filter of the DFE is assumed to have infinite length, then we arrive at the MMSE, J_{min} [64]. This error bound can be formulated as

$$J_{min} = \exp\left(\frac{T}{2\pi}\int_{-\frac{\pi}{T}}^{\frac{\pi}{T}} \ln\left(\frac{N_0}{\mathbf{H}\left(e^{j\omega t}\right)+N_0}\right)d\omega\right). \tag{3.44}$$

This error is a function of $\mathbf{H}(e^{j\omega t})$ which is the characteristics of the channel, where N_0 is the AWGN noise power for a signal sampled a rate of $\frac{1}{T}$.

For the case of a digital signal passing through a tapped delay line channel with a finite number of DFE filter coefficients, the MMSE is found to be [61].

$$\tilde{J}_{min} = \frac{1}{\mathbf{e}_0\mathbf{R}_d^{-1}\mathbf{e}_0^T}, \tag{3.45}$$

which is also depending on the channel due to the term $\mathbf{R}_d^{-1}$. To find the lower bound for the BER for frequency selective channels, we assume initially that the proposed receiver removes the ISI and only source of error is AWGN. In this case, J_{min} is given as

$$J_{min} = \frac{N_0}{1+N_0}, \tag{3.46}$$

where N_0 is the energy of the zero mean AWGN. Furthermore, J_{min} is related to the steady-state signal to interference and noise ratio, γ_∞, as [64]

$$\gamma_\infty = \frac{1-J_{min}}{J_{min}}. \tag{3.47}$$

In practice, a finite DFE can not remove all ISI, and γ_∞ will include both the remaining

ISI and AWGN. In this case, it can be empirically computed at the output of the DFE as

$$\gamma_{\infty} = \frac{E_s}{\frac{1}{N_p}\sum_{n=1}^{N_p} |\hat{a}_n - a_n|^2}, \tag{3.48}$$

where E_s is the signal power, N_p is the data packet length, a_n and $\hat{a}_n$ represent the data symbols and their estimates, respectively. It is worth pointing out that at node 2 they are replaced by b_n and $\hat{b}_n$.

3.6 Simulation Results

In this section, the performance of the proposed method is demonstrated through simulation. To insure that these simulations are fully replicable, well defined channels are used, namely ITU pedestrian channels A (Ch.102) and B (Ch.103) [59]. Also, a detailed design for the DFEs is defined. This not only includes the design equations but also how these are related to the specific choice of channels like filter lengths and Δ .

3.6.1 ITU Channels

In this section, a description of the used ITU channels is detailed. The channel profiles for channels A (Ch.102) and B (Ch.103) are shown in Table 3.1 [59].

For the simulations, the total power of each of the channel profiles has been normalized to 1 by dividing each coefficient with the factor $\sqrt{\sum_{l=0}^{L-1} 10^{P_l/10}}$. The system bandwidth is assumed to be 20 MHz and a sampling time of 44 ns was used to normalize the arrival times, which have been subsequently rounded up to the closest integer. Fig. 3.4 and 3.5 depict the magnitude of the frequency response of the two channels, which are evidently frequency selective. The 50% coherence bandwidths have been calculated approximately as 4.348 MHz and 315.8 kHz for channel A and B, respectively, using [64]

$$B_{coh} = \frac{1}{5\ \tau_{rms}}, \tag{3.49}$$

In both channels, each coefficient represents a physical obstacle. These objects reflect delayed copies of the original signal with different gains. Objects may be buildings and other surroundings in the environment used by pedestrians from which these channels

Table 3.1: ITU Channel Profiles.

ITU Pedestrian B, Ch.103						
Path l	1	2	3	4	5	6
Power P_l (dB)	0.0	-0.9	-4.9	-8.0	-7.8	-23.9
Delay τ_l (μs)	0.0	0.2	0.8	1.2	2.3	3.7
ITU Pedestrian A, Ch.102						
Path Nr.	1	2	3	4	5	6
Power P_l (dB)	0.0	-9.7	-19.2	-22.8	–	–
Delay τ_l (μs)	0.0	0.11	0.19	0.41	–	–

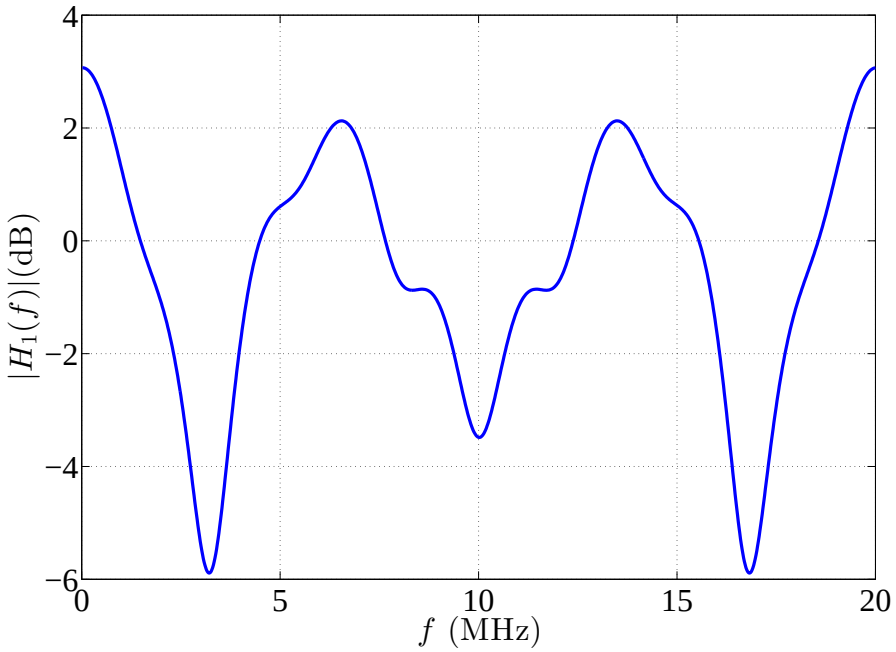

Figure 3.4: Frequency response of ITU Ped. A Ch. 102.

take their names.

As the transmitted signals of the source nodes will pass through the two frequency selective channels regardless of the communication scheme used, equalization at the end nodes is required to remove the combined ISI present in the received signals. The overall E2E performance is bounded by the BER of the end node DFE equalizer for the more severe of the two channels.

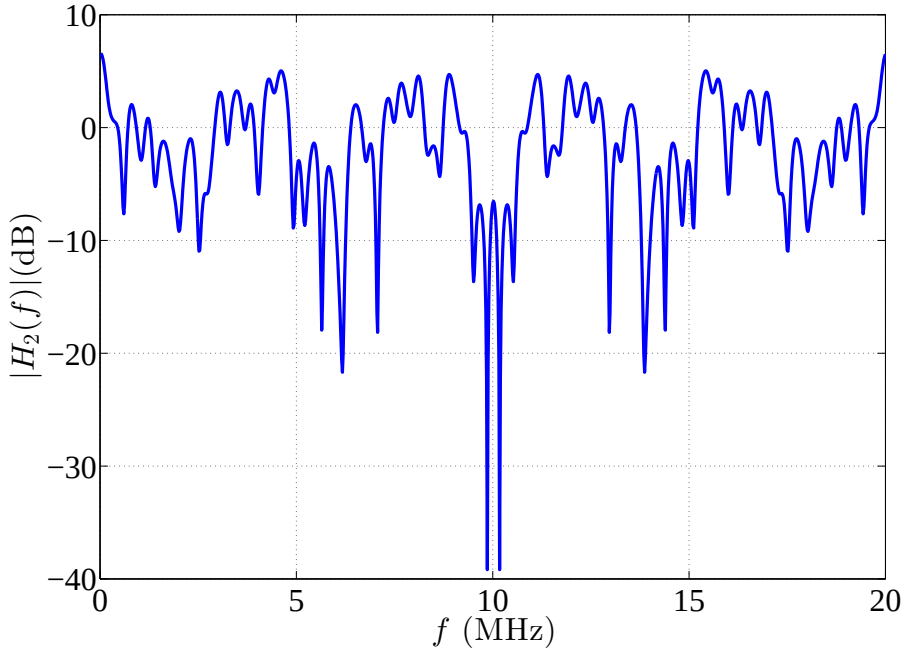

Figure 3.5: Frequency response of ITU Ped. B Ch. 103.

3.6.2 DFE Design

In this section, the design of the DFE at each end node is discussed. As the relay is working as a mere amplify and forward node, hence no equalization is required there. The equations derived in Section (3.3.2) are implemented with some changes. Let the observation vector at the receiver is $\mathbf{y}$ and the noise vector is $\mathbf{w}$ where $\mathbf{y}$ and $\mathbf{w} \in \mathbb{C}^{L_p}$ where, L_p is the data packet length. Then the observation covariance matrix $\mathbf{R_y}$ can be found as follows

$$\mathbf{R_y} = \sigma_s^2 \mathbf{H}\mathbf{H}^* + \sigma_w^2 \mathbf{I}_{L_p}, \tag{3.50}$$

where $\mathbf{H} \in \mathbb{C}^{L_p \times L_p + L_h - 1}$ is a toeplitz matrix created in a similar way as the one in equation (3.43),L_h is the channel length, σ_s^2 and σ_w^2 are the signal and noise variances respectively and $\mathbf{R_y} \in \mathbb{C}^{L_p \times L_p}$. The cross covariance matrix $\mathbf{R_{sy}} \in \mathbb{C}^{(N_{FB}+1) \times L_p}$ is defined as

$$\mathbf{R_{sy}} = \begin{bmatrix} \mathbf{0}_{(N_{FB}+1)\times\Delta} & \sigma_s^2 \mathbf{I}_{N_{FB}+1} & \mathbf{0} \end{bmatrix} \mathbf{H}^*, \tag{3.51}$$

where the appended zero matrix is chosen to make the size of the matrix between brackets become $(N_{FB}+1) \times (L_p + L_h - 1)$.

The desired feedback and feedforward filter coefficients are calculated using equations

(3.36) and (3.37) where

$$\mathbf{R}_d = \mathbf{\Phi}\left(\frac{\mathbf{I}_{L_p+L_h-1}}{\sigma_s^2} + \frac{\mathbf{H}^*\mathbf{H}}{\sigma_w^2}\right)^{-1}\mathbf{\Phi}^*, \tag{3.52}$$

$$\mathbf{\Phi} = [\mathbf{0}_{(N_{FB}+1)\times\Delta}\ \ \mathbf{I}_{N_{FB}+1}\ \ 0], \tag{3.53}$$

$\mathbf{e_0} = [1,\ 0,\ 0,\ \ldots,\ 0]$, $\mathbf{\Phi} \in \mathbb{C}^{(N_{FB}+1)\times(L_p+L_h-1)}$ and $\mathbf{R}_d \in \mathbb{C}^{(N_{FB}+1)\times(N_{FB}+1)}$.

Successful implementation of this optimum DFE requires knowledge of channel taps and noise power, which can be acquired through channel estimation. Also, matrix $\mathbf{H}$ must be replaced by $\mathbf{H}_{12}$ mentioned in equation (3.43) for both equalizers DFE1 and DFE2. This is according to the derivation in Section 3.4.2.

Now we discuss the choice of Δ and filter lengths. In general, the length of the forward filter N_{FF} must be greater than the length of the combined channels, i.e. $N_{FF} > L_t = L_1 + L_2$. For the purpose of simulation of the selected channels, $L_1 = 10$, $L_2 = 85$ and $N_{FF} = 1024$ taps were selected. The choice of Δ and N_{FB} must satisfy [61]

$$\Delta + N_{FB} \leq N_{FF} + L_t - 2. \tag{3.54}$$

This can be easily met by taking Δ in the region around $\frac{N_{FF}+L_t}{2}$ because N_{FB} has a relatively small value compared to N_{FF}. In this case, $\Delta = 768$ and $N_{FB} = 32$ taps were selected.

The two non equalizer FIR filters are constructed from the estimated coefficients $\mathbf{h_1}$ and $\mathbf{h_2}$. At node 1 this filter will have coefficients equal to the convolution between $\mathbf{h_1}$ and itself or $\mathbf{h_1} * \mathbf{h_1}$, while it will be $\mathbf{h_2} * \mathbf{h_2}$ for the second end node filter.

3.6.3 End to End Performance

After designing both equalizers, the performance of the proposed system can be obtained. The system is run in different signal to noise ratios using the Monte Carlo method. Also, point-to-point simulation of QPSK transmission through both channels A and B to the relay is demonstrated using an optimum DFE equalizer. Detection in these cases is accomplished by replacing $\mathbf{H}$ by $\mathbf{H}_1$ and $\mathbf{H}_2$ in the DFE design, where these matrices are formed using $\mathbf{h_1}$ and $\mathbf{h_2}$ instead of $\mathbf{h_1} * \mathbf{h_2}$.

Figure (3.6) shows the performance of the proposed AF method alongside point to point performance of the non-PLNC single channel performances for channels A and

B. The performance of denoise and forward based PLNC in AWGN is included as a benchmark for comparison. Finally, we focus on the E2E performance of the proposed AF scheme. Inspecting this figure shows that at a BER level of 10^{-3} the proposed method is about 3 dB away from the performance curve of channel B which is the worst of the two channels. It is logical for the overall performance to be less than the toughest of the two channels keeping in mind that this degradation is not only due to the other channel but also the use of the PLNC system instead of mere point to point transmission. This performance is affected by the choice of channels, the length of the filters and the choice of Δ.

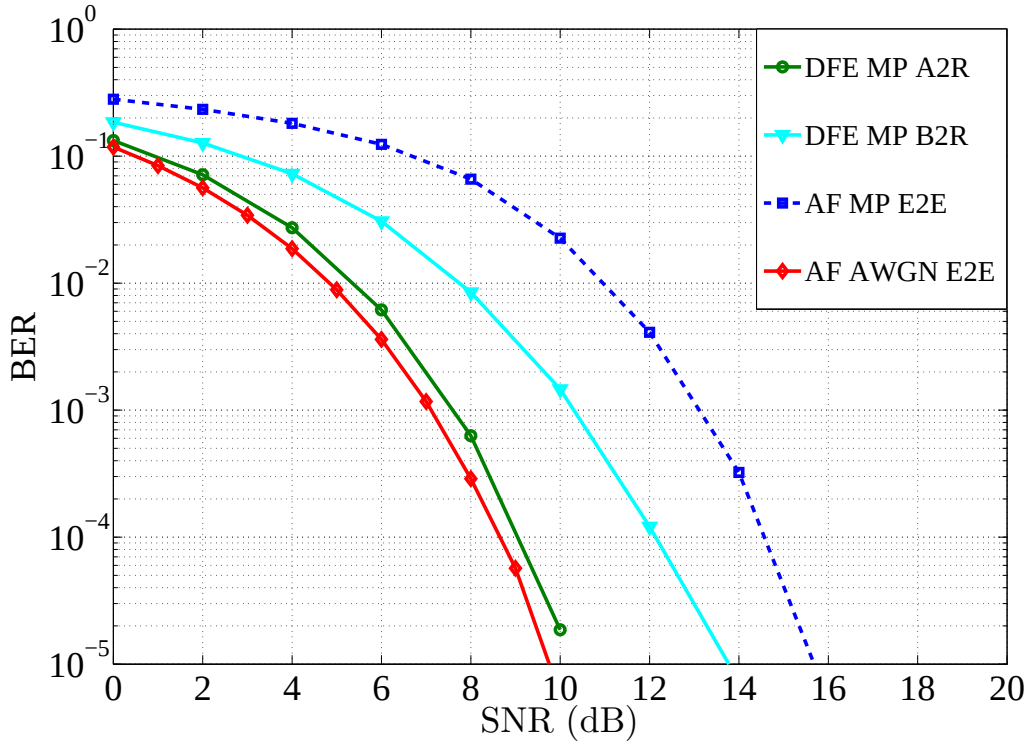

Figure 3.6: Performances of the proposed AF method, point to point DFE with channels A and B alone and AF in AWGN.

Fig. 3.7 shows the performance of the proposed system for different number of feedback taps N_{FB}. A closer look at this figure shows that $N_{FB} = 32$ taps results in the best performance. By increasing the feedback coefficients from 10 to 32, approximately 1 and 2 dB gains in SNR were observed at a BER of 10^{-3} and 10^{-5}, respectively. Additional simulations were performed for $N_{FB} > 32$ but demonstrated no further improvement in performance. This also shows that only a relatively small number of feedback taps are required to deal satisfactory with the main multipath arrivals. Fig. 3.8 shows γ_∞ calculated using (3.48) as a function of the input SNR, denoted as SNR_i. At $\mathrm{SNR}_i = 20$ dB

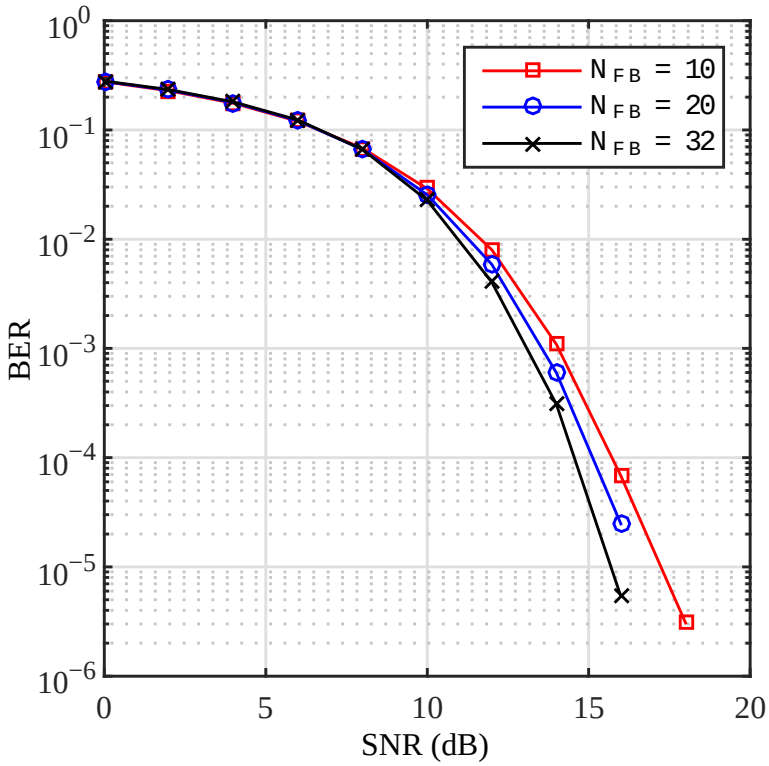

Figure 3.7: E2E BER performance of the proposed AF method for different feedback tap lengths.

for $N_{FB} = 32$ the degradation in performance due to residual ISI is 5.3 dB, while for $N_{FB} = 10$ the degradation is 6.7 dB. It is also observed that the degradation increases significantly at lower SNR levels due to error propagation in the FB filters.

Fig. 3.9 shows the constellation at the end node at the output of the DFE for an input $\mathrm{SNR}_i = 16$ dB. Inspecting this constellation shows that although the QPSK constellation is readily distinguishable, the scatter spread is wider and equivalent to 12 dB of SNR due to the residual ISI that the DFE was unable to cancel.

3.7 Pre-filtering

In this section, the pre-filtering technique is discussed for the sake of comparison. This process is also called pre-equalization or transmit filtering. The first step is to estimate the channel at the sending end or the transmitter. This can be done in several ways. For example, the receiver can have a channel estimator and the channel information can be fed back to the transmitter in the form of overhead r through a low rate backward channel.

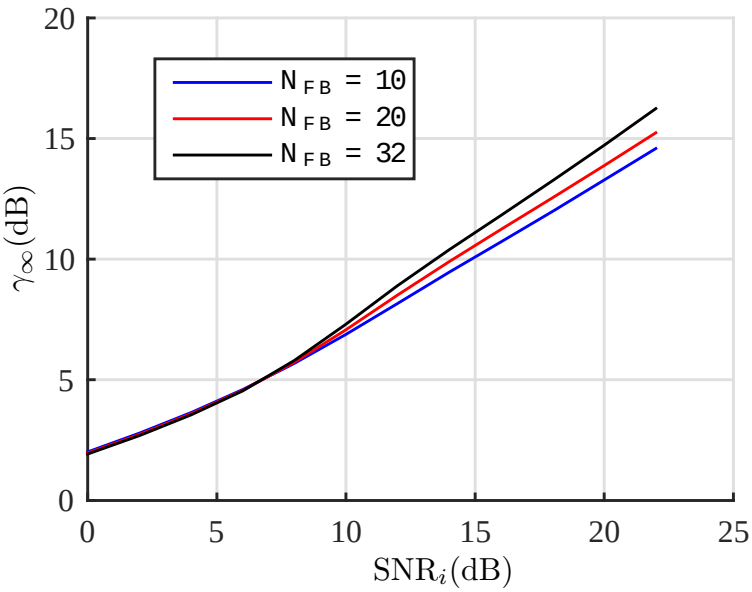

Figure 3.8: γ_∞ as a function of SNR_i and N_{FB}.

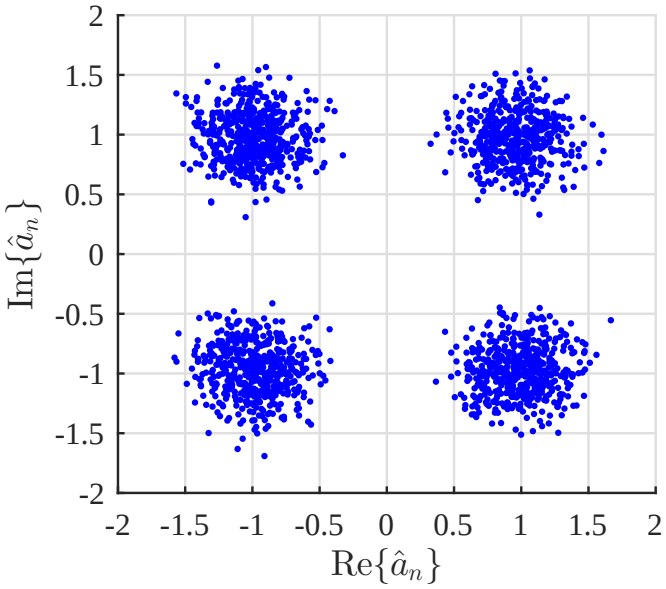

Figure 3.9: IQ constellation at 16 dB using the proposed AF method.

A necessary condition for this to work is that the channel must be either slowly varying or fixed. By this we mean slow enough that the channel is only slightly changed during one transmission receive cycle.

The second step is to use this information to filter the signal. This can be done for ex-

ample by finding the normalized inverse of this channel and then using these coefficients for the pre-filter in the transmitter. This works as an equalization process that happens at the transmitter and in this specific example it is a linear zero forcing equalizer. By doing this, we are avoiding to some extent the effect of the noise on the equalization operation.

Another way is to shift only the feedback section of the DFE to the transmitter side. As this is the section of the DFE that requires knowledge of the correct symbols, it makes sense to shift it to the sending side where these symbols have not yet experienced any channel or noise effects. This process is called the Tomlinson-Harashima precoding. Due to the non-linear nature of the DFE, this precoding is also non-linear. This process can be perceived as a way of splitting the equalization operation between the transmitter and the receiver because the receiver needs to do the forward part of the DFE. Another variation of this equalization split is seen in MIMO systems that use OFDM or discrete multi-tone (DMT) transmission. Here, a method called singular value decomposition (SVD) is performed on the channel matrix. This is done based on the eigenvectors of the channel matrix in an algorithm known as vector coding [65]. This process is linear.

Table (3.2) summarizes the equalization methods discussed so far showing where the equalization takes place being at the transmitter, receiver or split and categorizing them into linear and non-linear equalization techniques.

A more general approach in PLNC systems is to make the two signals from both end nodes experience the same overall channel response.

Table 3.2: Various Equalization and Pre-equalization techniques.

Linearity	Side	Name
Linear	Receiver	Z.F. Equalizer
	Transmitter	Z.F. Pre-equalizer
	Transmitter/Receiver	OFDM/DMT vector coding
Non-linear	Receiver	DFE
	Transmitter/Receiver	Tomlinson-Harashima precoding

This way, the two received signals at the relay are allowed to be wirelessly added and equalized at the relay with only one equalizer. To achieve this, the following equation must be satisfied [66]

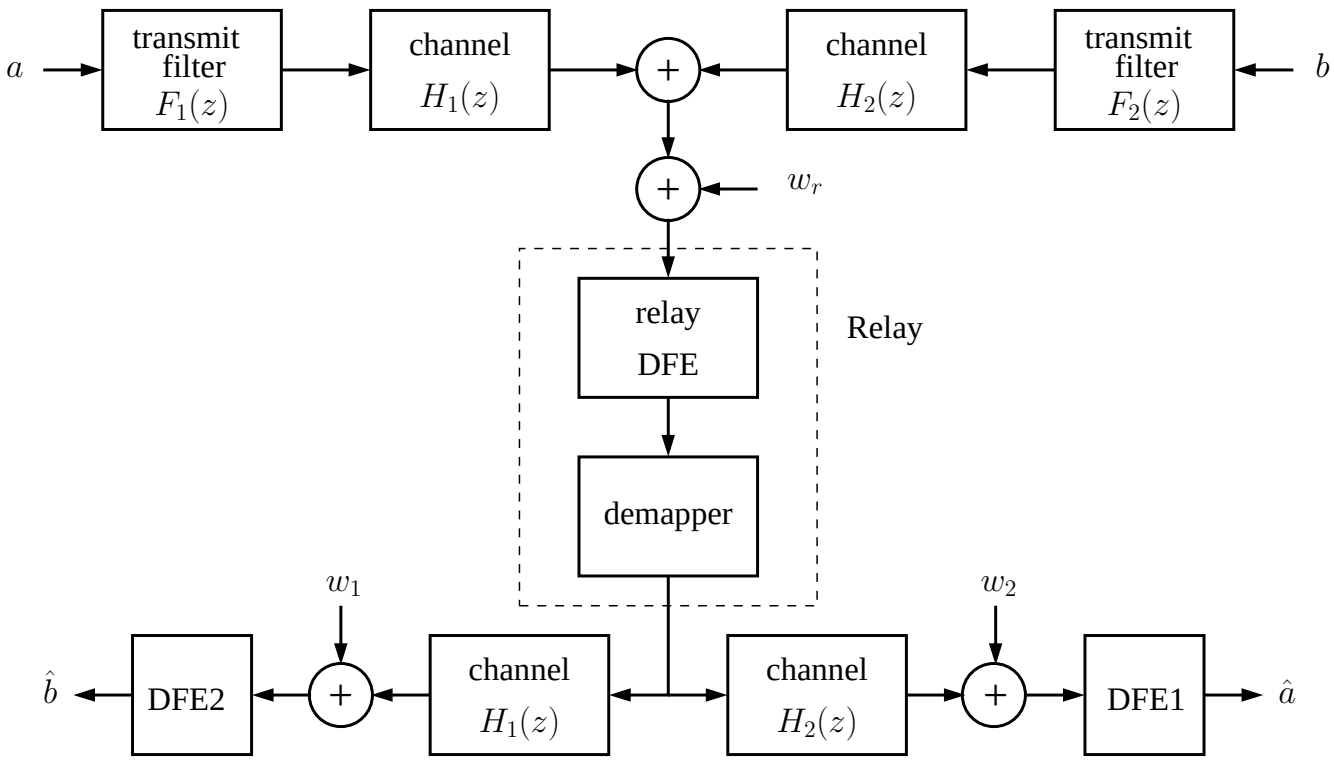

Figure 3.10: Block diagram of the Max SNR prefiltering method.

$$\mathbf{H}_1(f)\mathbf{F}_1(f) = \mathbf{H}_2(f)\mathbf{F}_2(f), \tag{3.55}$$

where $\mathbf{H}_1(f)$ and $\mathbf{H}_2(f)$ are the frequency responses for channels 1 and 2 respectively and $\mathbf{H}_1(f)$ and $\mathbf{H}_2(f)$ are the pre-filters used at nodes 1 and 2 respectively.

In [66, 67], the authors deal with the problem of PLNC systems in frequency selective channels using this technique and maximize the SNR under the constraint of limited power in both end nodes while assuming perfect channel estimation and also that full knowledge of the two channels is available at both end nodes. This is done in time domain which avoids the drawbacks of OFDM systems like frequency offset, PAPR and costly linear amplifiers.

The block diagram of this technique is shown in figure (3.10), where a and b are the data packets sent from nodes 1 and 2 respetively, w_r is the noise vector at the relay and w_1 and w_2 are the noise vectors at nodes 1 and 2 respectively.

The design of the pre-filters namely $\mathbf{F}_1(z)$ and $\mathbf{F}_2(z)$ is not only affected by the selection of the channels but also by the two end node power constraints and the solution is arrived at after some iterations. It is very important to mention that more than one transmission-broadcasting cycle is required for the channel estimation information to reach from one end node to the other. This has to be done before any proper data

exchange can happen. The channel information exchange can be done either by some extra overhead on the packets or, alternatively, a separate feedback channel is used to send the estimate of the opposing channel. In both cases, two cycles are required. This is very important as with more complex network configurations or network delay between transmission cycles the larger the channel estimation error will be unless the channel is non-varying and is unchanged.

3.8 Comparison Under Different Estimation Errors

In this section, the estimation error is interjected for both the proposed system and the pre-filtering technique. The general pre-filtering approach discussed in the previous section is selected as a representative of the pre-equalization methods. For simplicity, the pre-filtering technique is given the advantage by lifting the power constraints that normally exist at both end nodes to simplify the design. Also, both channels are normalized. Under these circumstances, the design is optimized at $\mathbf{F}_1(z) = \mathbf{H}_2(z)$ and $\mathbf{F}_2(z) = \mathbf{H}_1(z)$ and therefore no iterations are required for calculating the pre-filters.

The first comparison is between the two systems in the ideal case where no estimation error exists. Figure (3.11) shows the performances of both the proposed AF DFE system and the de-noise and forward (DNF) maximum SNR pre-filtering system.

The simulations in both cases were executed using ITU pedestrian channels A and B at end nodes 1 and 2 respectively. The end to end performance is at node 1 is influenced by channel A and therefore will be better than the performance at node 2 because channel B is a tougher channel. The channel profiles are normalized in both cases and the power constraints at the end nodes are lifted for the the pre-filtering technique. In this case, the DFE at the relay for the pre-filtering method will have the same design as the AF DFE at the end node. The delay is $\Delta = 768$, the forward filter length is $N_{FF} = 1024$ and the feedback filter length is $N_{FB} = 32$.

Equations (3.36) and (3.37) are used in the design as explained in Section (3.3.2). The downlink in the AF DFE is straightforward as no equalization is required at the relay. The signal in the pre-filtering case will suffer additional ISI when passing through the channels in the downlink phase. This requires end node equalization as shown in figure (3.10). The same design equations namely (3.36) and (3.37) are used to design the second DFE.

From figure (3.11), it is clear that the pre-filtering system has better performance than

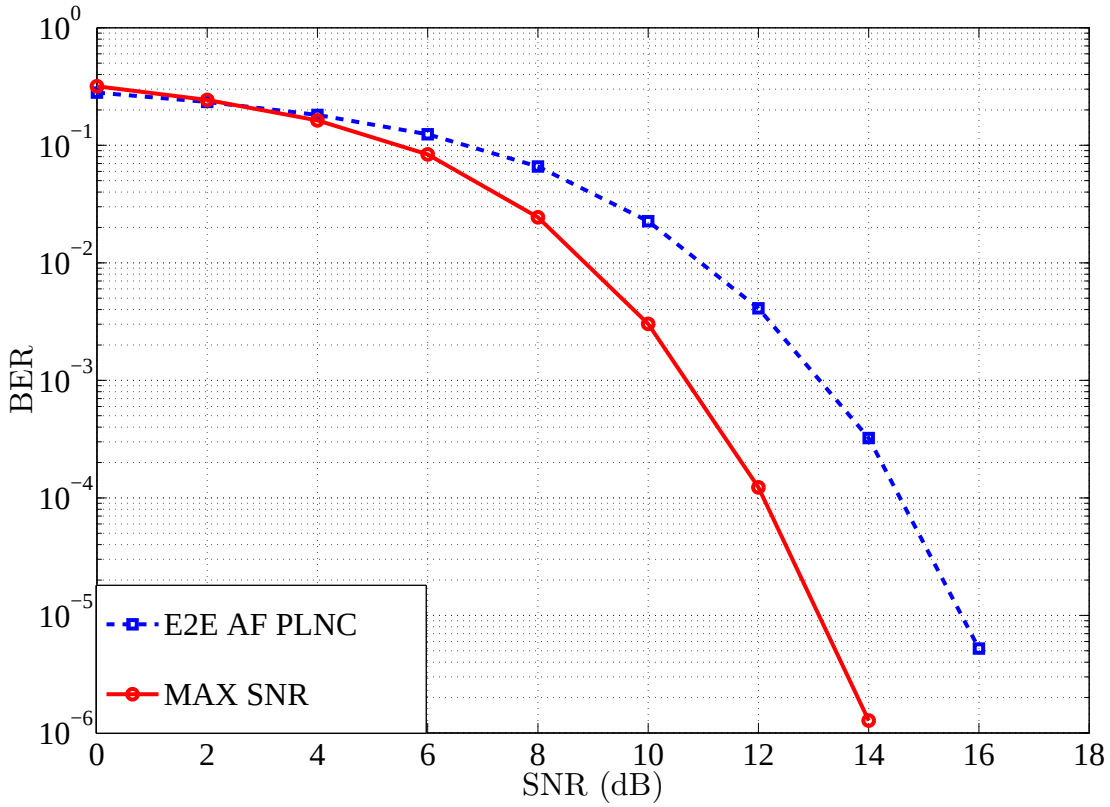

Figure 3.11: Performance of the proposed AF method vs Max SNR prefiltering.

the AF DFE system in the ideal case with no power constraints and no estimation error. This outcome is expected as it is known that DNF schemes are generally better than AF schemes in performance due to some noise amplification in the later method.

Before moving on to the next step, it is worth mentioning that even if this was the case all the time, the proposed AF DFE still holds a lot of advantages like simplicity of the relay, lower computational complexity and compatibility to all network configurations.

When the channel is slowly varying, the delay between the time when the estimation happens and the time when this information is used becomes more important.

Define r as the average percentage of estimation error that occurs in each individual channel coefficient during one time slot. A time slot is the time required for the data packet to move from one end node to the relay node or backwards. The estimation error in one coefficient is assumed to be uncorrelated with the error in the other coefficients. As r is a percentage, then the term containing it must be divided by 100. Let t_s be the number of time slots during which the channel is changed. Then the above mentioned term must be multiplied by t_s to include the effect of all the time slots. Let $\mathbf{v_r}$ be a zero mean random vector with unity variance representing the random change in the original channel vector

$\mathbf{H}$. This error due to channel changes is proportional to the original channel value at each tap k, namely $\mathbf{H}(k)$. Then the overall error affecting tap k taking all the previous variables into account will be $0.01\ r\ \mathbf{v_r}\ t_s\ \mathbf{H}(k)$. Then the channel with the estimation error $\mathbf{H}_e$ can be found in terms of r and the original channel $\mathbf{H}$ as follows

$$\mathbf{H}_e(k) = \mathbf{H}(k) + 0.01\ r\ \mathbf{v_r}\ t_s\ \mathbf{H}(k). \tag{3.56}$$

This holds for $k = 1,\ 2,\ \ldots\ L_h$, where L_h is the channel length.

In order to use this equation properly for the two systems under consideration, we need to calculate the total delay between the channel estimation and the time this estimation is used measured in time slots (t_s). As the estimation is done in one time slot, then it is convenient to assume that the estimation process captures the changes that happen during that one time slot, i.e. ideal channel estimation.

Looking at the AF DFE system from end node 1 under the previous assumption, the estimation of $\mathbf{h_1}$ via an overhead added at the relay will be perfect, while the estimation of $\mathbf{h_2}$ via an overhead added from end node 2 will reach the relay perfectly but suffers one time slot error when it reaches end node 1. Therefore $t_s = 1$ for channel B. For the pre-filtering system, it takes two cycles or 4 time slots for the estimation to reach its useful destination. As we have assumed that no error occurs in the estimation slot, then this leaves us with $t_s = 3$ for channel B estimated at node 1. This value of t_s is used in equation (3.56). The newly calculated channel coefficients with estimation errors are then used for the remaining performance comparisons under different values of error percentage per time slot (r).

Figure (3.12) shows the simulation performance of the proposed AF DFE system for $r = 10\%\ and\ 20\%$. At $r = 10\%$ the simulation performance is asymptotic to the original performance in figure (3.6), while at $r = 20\%$ which is a high value, the simulation performance drops about 3dB at BER of 10^{-3}. This shows that the proposed system is resistant to estimation error and this is mainly because of the low time delay between the estimation and its usage in the DFE that leads to $s_t = 1$.

When estimation error is interjected on the channels used the pre-filtering system, then the performance becomes more sensitive to the value of r. Figure (3.13) shows the simulation performance of the Max SNR pre-filtering method for $r = 3,\ 4,\ 6,\ and\ 10\%$. This degradation of performance is simulated assuming that the transmission is uninterrupted and that the relay node is not shared by other users. If any cause of more delay

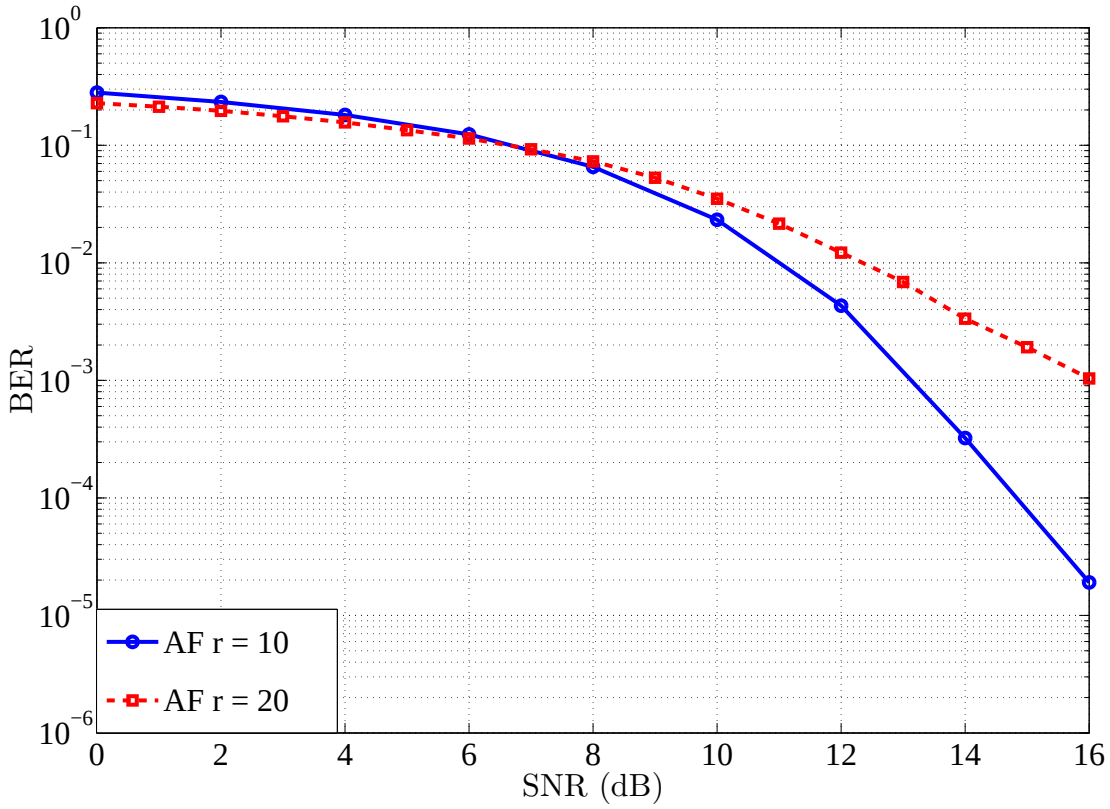

Figure 3.12: Performance of AF DFE for r = 10.

occurs then the performance of the pre-filtering becomes worse, while the proposed AF DFE system is not affected.

Figure (3.14) shows a comparison between the simulation performances of the two systems when $r = 4\%$. From this figure, it is clear that the two performances become close. Although the difference is very small, yet at this value of r, the pre-filtering is still slightly better.

Figure (3.15) shows the simulation of the performances of both systems at $r = 6\%$. At this value, the proposed AF DFE system is clearly better especially in the region where SNR is 9dB and higher. The region of the percentage of estimation error between 4% and 6% is where both methods have the same performance but the exact value of r is not fixed as it depends on the selection of the two channels and their severity. Although this is the case, yet we can safely say that the proposed AF DFE method becomes better for r greater than 6%. At $r = 10\%$, the performance of the pre-filtering system is highly degraded, while the proposed AF DFE method is hardly affected as shown in figure (3.16).

All the previous comparisons have been made in the case where channel A is the

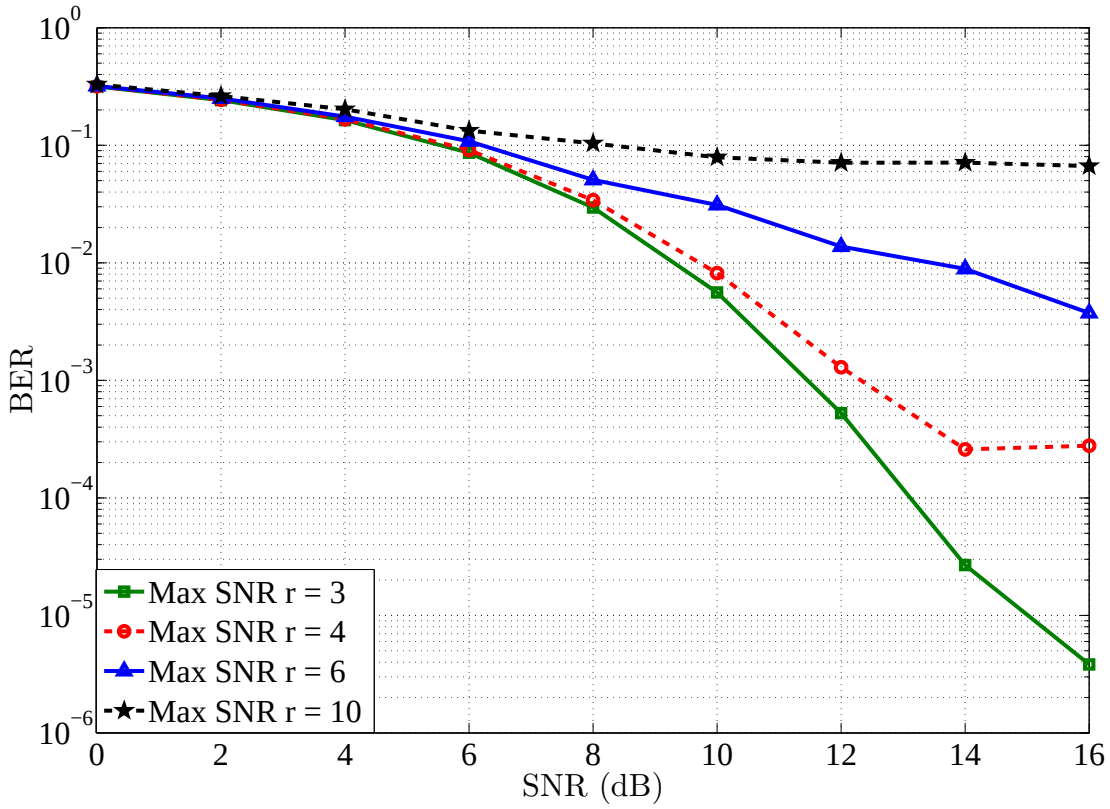

Figure 3.13: Performance of Max SNR method for r = 3, 4, 6 and 10.

downlink channel. This has no impact on the proposed system but for the pre-filtering with estimation error, the performance is affected by the downlink channel. With a tougher channel, the impact of the downlink becomes greater on the performance.

Figure (3.17) shows the effect on the performance observed from node 2 compared to node 1 at $r = 4\%$. From this figure, it is clear that the performance of the proposed system can become better that the pre-filtering system even at $r = 4\%$ instead of $r = 6\%$ if it is observed from node 2.

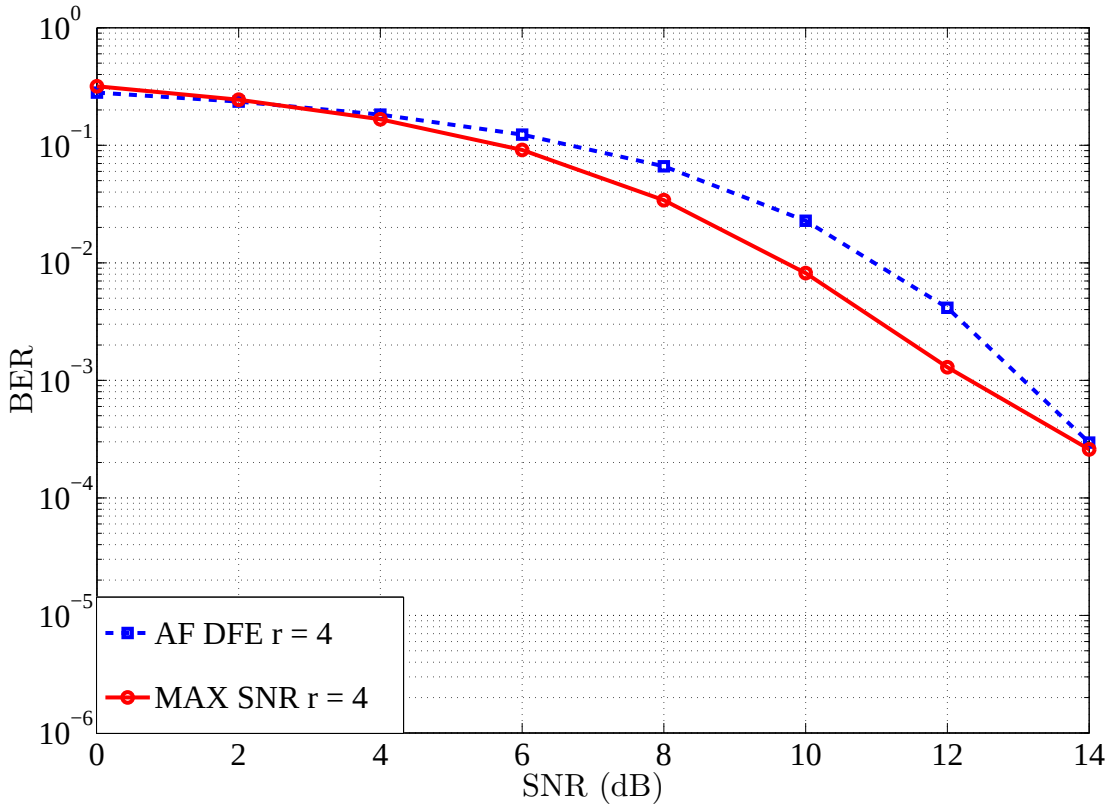

Figure 3.14: Performance of the proposed method compared to Max SNR at r = 4.

3.9 Chapter Summary

This chapter presented an overview of equalizers with a focus on the optimum DFE equalizer and the equations used in its design. Some guidelines that help in the selection of the design parameters are also presented. The chapter also discusses some of the pre-filtering methods especially where they have been used to solve the problem of frequency selective channels in PLNC systems.

A new method to solve this problem is presented and compared with the pre-filtering under the assumption of slowly varying channels for different values of percentage error per time slot. The proposed method has less computational complexity, better performance for $r > 5\%$ in general and is compatible to all network configurations. The fact that the proposed method is in the AF category makes it especially useful in wireless sensor networks because of the simplicity of the relay node.

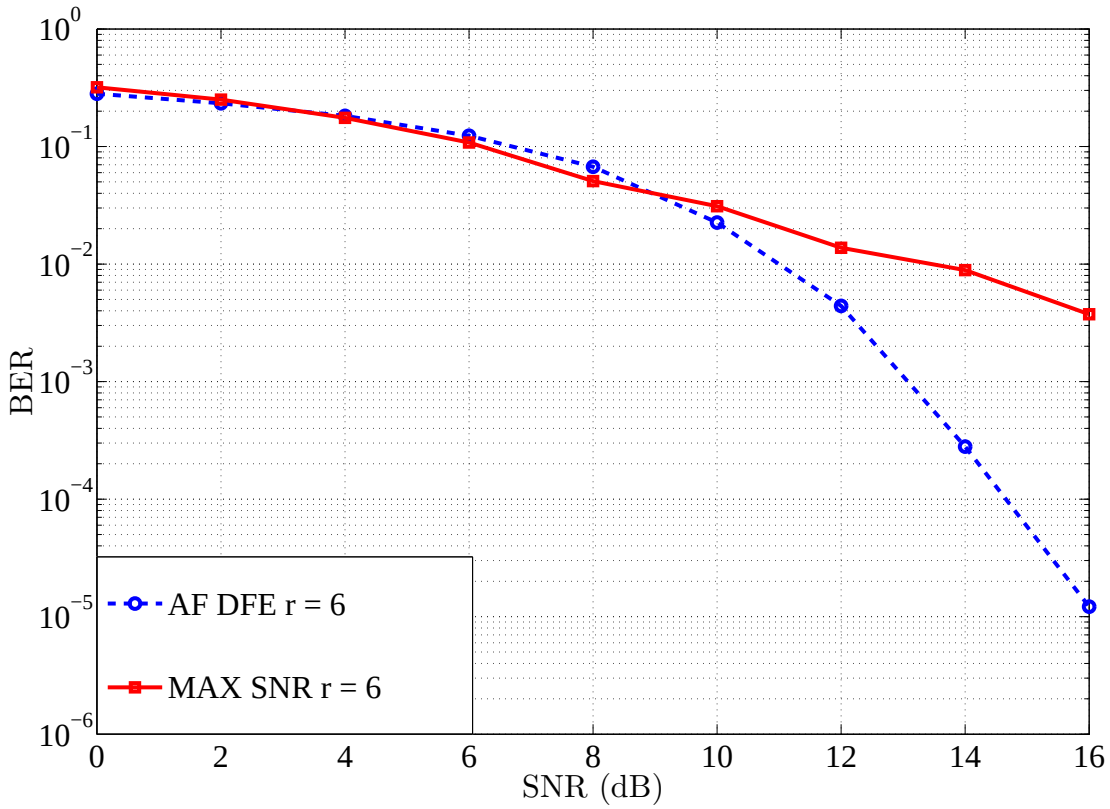

Figure 3.15: Performance of the proposed method compared to Max SNR at r = 6.

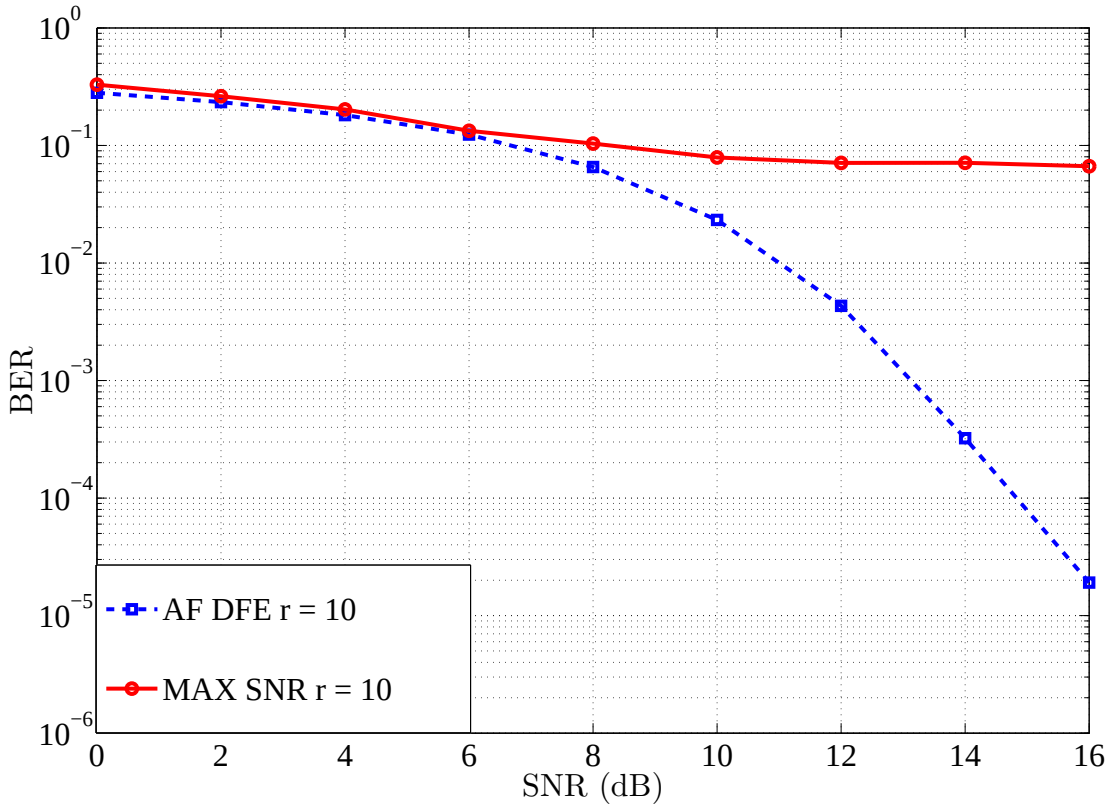

Figure 3.16: Performance of the proposed method compared to Max SNR at r = 10.

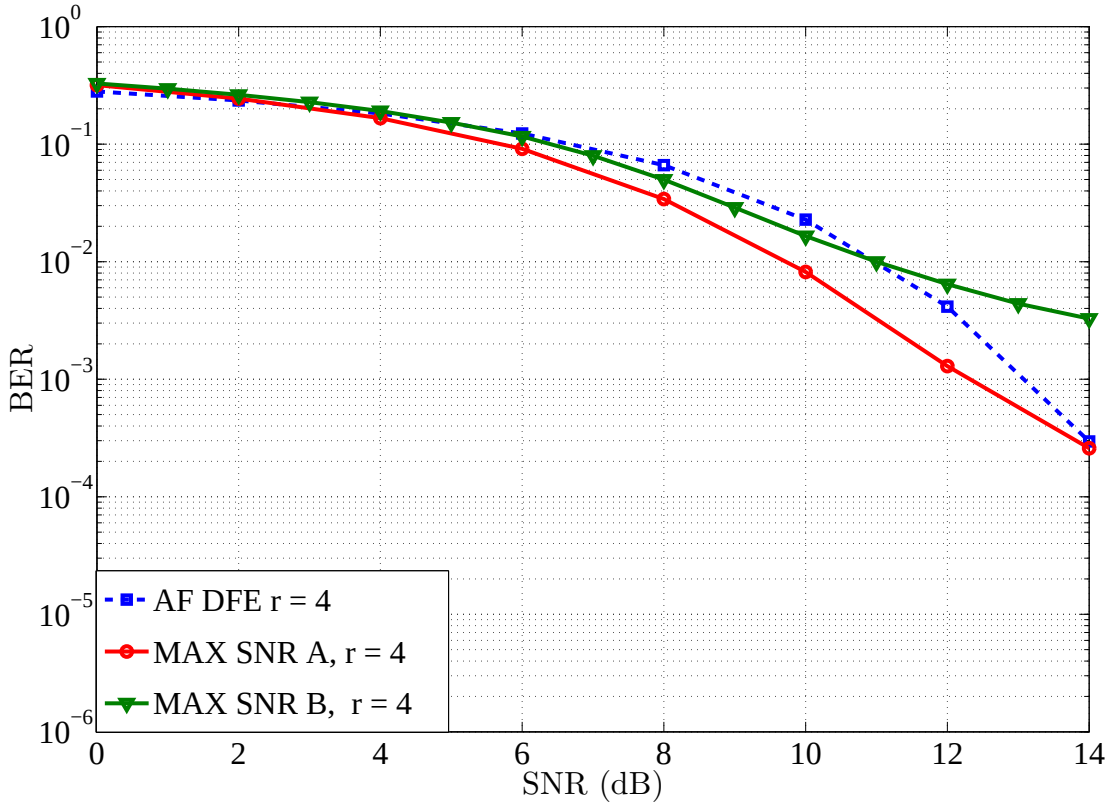

Figure 3.17: Performance of the proposed method compared to Max SNR measured from end nodes 1 and 2 at r = 4.

Chapter 4

Optimum Combining for De-noise and Forward PLNC Systems in Frequency Selective Channels

4.1 Introduction

In the case where the relay node has access to computational resources, the use the denoise and forward (DNF) approach is considered because it has a better BER performance than the AF approach in general.

In DNF systems, the received signal is decoded and mapped to give an estimate of the XOR of the transmitted bits from both end nodes. In this case, most of the additive noise from the uplink is eliminated. By doing this, we are also avoiding noise amplification that happens in the AF system and therefore we can get an improved performance.

To achieve a functional PLNC system with a DNF approach working with frequency selective channels, a linear antenna array is added at the relay.

The insertion of the antenna array not only makes the PLNC functional in frequency selective environments, but also has another advantage which makes the this novelty so important. This advantage is that by enabling the DNF scheme, the BER performance is greatly enhanced with only a small number of antennas and this is what makes this novelty so important.

The proposed system uses optimum combining (OC) and a pair of optimum DFE equalizers at the relay node. The new proposed system has similar advantages to the AF DFE system proposed in the previous chapter including computational complexity, simple design and compatibility with network configurations.

4.2 Problem Description

The main goal of this chapter is to achieve a functional PLNC system in a frequency selective environment with a DNF method that can have better BER performance and at the same time avoiding the drawbacks of some previous DNF methods. The solution has to be cost effective and one that is simple to design with lower computational complexity.

By avoiding the pre-equalization methods, the proposed design is liberated from the limitations and requirements of these methods. This way, no knowledge of the opposing channel is required before the pre-filtering and therefore the need of a feedback channel is cancelled.

The fact that the proposed solution is not iterative also contributes to the simplicity and lower computational complexity issue. The new design is also compatible to all network

configurations.

In terms of sensitivity to channel variations, the new proposed system is also better in this area as will be explained in detail in this chapter. In this respect, the proposed solution is even better than the AF DFE system and with better BER performance.

The proposed solution is time based which means that it avoids the drawbacks of the OFDM system like PAPR, linearity of the power amplifiers and the extra cyclic prefix overhead. This is not to say that some of these drawbacks have not been addressed by many researchers, but the solutions to these problems do not come without extra complexity and cost.

If all the previous reasons were not enough to justify leaving the OFDM system, then the lead in BER performance alone is enough. This performance enhancement is mainly due to the fact that OFDM PLNC systems can only use linear equalizers mostly in the frequency domain like frequency domain zero forcing or MMSE equalizers.

The solution is also not restricted to BPSK or QPSK modulation and can easily function with 16-QAM or higher order modulation schemes.

The principles of beamforming and optimum combining used in this chapter will be explained in the following subsections after introducing antenna arrays.

4.3 Antenna Arrays

The use of multiple antennas has become popular in the field of communications for some time. This can benefit the performance of communication systems in many ways like achieving diversity gain, antenna gain or multiplexing gain [68].

Multiple antenna systems are also called multiple input multiple output (MIMO) systems.

With single antenna systems, the conventional methods were aimed at achieving good performance in either the time domain or the frequency domain. With multiple antenna systems the new dimension of spatial domain enriches to the possibilities of these systems mitigating error rates or decreasing the co-channel interference especially in cellular communication systems. Good examples on spatial diversity gain techniques in systems having multiple transmit antennas are the space-time trellis codes [9] and the Alamouti system [69].

Spatial multiplexing is used in the field of multi-user communications to achieve multiplexing gain, while space time coding is aimed at achieving a diversity gain. On the other

hand, beam-forming is more of a signal processing technique aimed at manipulating the antenna gain pattern to maximize the signal to interference plus noise ratio (SINR). The last of the mentioned techniques will be utilized in this chapter.

The idea in short is to find the best linear weighting vector that gives the highest SINR by improving the antenna gain in the desired direction and reducing or possibly nullifying the gain in the interference direction while taking the noise into account.

The use of antenna arrays has quickly moved from theory to practical implementation in the third generation (3G) and fourth generation (4G) communication system standards.

For example, MIMO systems are standardized in wireless local area networks (WLAN) [70] and the Alamouti method has also been used in some practical systems [71]. This concept has also been implemented for wideband code division multiplexing (WCDMA) [72]. Surveys on this subject can be found in [73, 74, 75, 76, 77, 78, 79, 80, 81] each from a different point of view.

4.4 Classical Beam Forming

In this section, only the techniques that lead to antenna gain are considered because the aim of the antenna array in this work is not to create a MIMO system. The system is therefore kept to a reasonable complexity and the end users are using a single antenna.

The proposed antenna array at the relay consists of N_a antennas or elements aligned equally spaced in a straight line. The distance between the elements is d.

The conventional beam former collects the signals from the antenna array and then finds a linear combination of these signals to form the output signal. the weights of these elements can be collected in a vector called the weight vector. These coefficients are complex valued with unity magnitude, but are normalized by dividing them by the number of elements N_a so that the overall gain does not exceed one.

To maximize the gain in the direction of a far field source, the phases of these coefficients are changed to make the antenna array look in the direction of this source. This operation is called steering and the weighting vector is also referred to as the steering vector. The source is also assumed to be in the the plane of the antenna array with non dispersive wave propagation. Steering the antenna in this case is done electronically as opposed to mechanical beam steering.

There are many applications of antenna gain. One such application is the use of the array to determine the direction of arrival (DOA) or sometimes called the angle of arrival

(AOA).

For single transmitter systems passing through a multipath channel with distinct paths, the steering vector can be designed to have a maximum in the main line of sight direction in the transmitter. This is called transmit beam forming.

Another idea is for the transmitter or receiver beam formers to have nulls in the other non line of sight directions and therefore reducing the delay spread of the channel [68]. In this work, the antenna array is used in the context of co-channel interference suppression (CCI). In these techniques, the receive beam former is designed to have a high value in the DOA of the desired direction and a low value or a null in the direction of interference. If the method depends on nulling the interference then this is called null steering while maximizing the SINR is called optimum combining.

Considering a far field source transmitting a baseband electromagnetic signal $EM(t)$ of the form

$$EM(t) = s(t)e^{jw_c t}, \tag{4.1}$$

where $s(t)$ is the signal envelope and w_c is the carrier frequency. The assumption that the source is far from the antenna array ensures that the wave front of the arriving signals can be assumed planar to the array.

Let θ be the DOA of the received wave measured from the broadside of the antenna array. The distance between two adjacent elements in the array will be $d\ \cos(\theta)$. This distance causes the signals to arrive at these elements at different times and the time delay Δt between any two adjacent elements will be $\Delta t = \frac{d\ \cos(\theta)}{c}$ where c is the propagation speed. This speed can also be written as

$$c = \frac{w_c \lambda}{2\pi}, \tag{4.2}$$

where λ is the wavelength of the electromagnetic signal.

Then Δt can be rewritten as

$$\Delta t = \frac{2\pi d\ \cos(\theta)}{w_c \lambda}. \tag{4.3}$$

For a slowly varying signal envelope, the time difference between two elements in the array can be neglected and therefore we can say that $s(t) \approx s(t + \Delta t)$ and the delayed

electromagnetic signal can be written as

$$s(t)e^{jw_c(t+\frac{2\pi d\ \cos(\theta)}{w_c\lambda})} = s(t)e^{jw_ct}e^{j\frac{2\pi d}{\lambda}\cos(\theta)}. \tag{4.4}$$

Applying this equation to all the signals at each element of the antenna, then these values can be collected in the following vector

$$s(t)e^{jw_ct}\left[\begin{array}{cccc} 1 & e^{j\frac{2\pi d}{\lambda}\cos(\theta)} & e^{j\frac{4\pi d}{\lambda}\cos(\theta)} & \ldots \quad e^{j\frac{2\pi(N_a-1)d}{\lambda}\cos(\theta)} \end{array}\right], \tag{4.5}$$

where the first value represents the signal from the closest antenna to the transmitter which is taken as a reference point with no delay.

The receiver with the antenna array will demodulate the signals returning them back to baseband and therefore the carrier term e^{jw_ct} is cancelled from the previous vector. Also, the time index can be removed from $s(t)$ for simplicity and s will then represent the value at the current time instant. Then the signals at each antenna can be written as

$$se^{j\frac{2\pi nd}{\lambda}\cos(\theta)}, \tag{4.6}$$

for $n = 0,\ 1,\ \ldots,\ N_a - 1$.

Let $w_1,\ w_2,\ \ldots,\ w_{N_a}$ be the noise values at each antenna at a certain time, then the received vector $\mathbf{Y}$ at that time instant can be written as

$$\mathbf{Y} = s\begin{bmatrix} 1 \\ e^{j\frac{2\pi d}{\lambda}\cos(\theta)} \\ e^{j\frac{4\pi d}{\lambda}\cos(\theta)} \\ \vdots \\ e^{j\frac{2\pi(N_a-1)d}{\lambda}\cos(\theta)} \end{bmatrix} + \begin{bmatrix} w_1 \\ w_2 \\ w_3 \\ \vdots \\ w_{Na} \end{bmatrix}. \tag{4.7}$$

Define $\mathbf{V}_s$ to be the arriving column vector and collected from the vector of the first term in equation (4.7). The second term in the equation can be collected in a column $\mathbf{W}$ defined as the noise vector in a similar fashion. Then this equation can be written as

$$\mathbf{Y} = s\mathbf{V}_s + \mathbf{W}. \tag{4.8}$$

From equation (4.7), it is clear that the antenna array receives multiple copies of the

signal s with a constant phase shift between the signal arriving at any two adjacent elements in the array. This constant phase shift depends on the value of the DOA angle θ.

4.4.1 Optimum Combining

In this method, the received signals at the antenna array are weighted and then added or combined in a way that maximizes the output SINR. This is done by reducing the total effect of the channel and the interfering signals. The weights multiplied by each antenna signal can be collected in a vector called the weight vector or weighting vector.

The weight vector $\mathbf{V}$ can be written as

$$\mathbf{V} = \begin{bmatrix} v_1 \\ v_2 \\ v_3 \\ \vdots \\ v_{Na} \end{bmatrix}, \tag{4.9}$$

where $v_1 \;\; v_2 \;\; \ldots \;\; v_{Na}$ are the complex values or weights corresponding to each antenna signal.

Let $\mathbf{Y}$ be a vector representing the set of received signals. This received vector can be written as follows

$$\mathbf{Y} = \begin{bmatrix} y_1 \\ y_2 \\ y_3 \\ \vdots \\ y_{Na} \end{bmatrix}, \tag{4.10}$$

The combined output signal y_{out} is the dot product of the received vector $\mathbf{Y}$ and the weighting vector $\mathbf{V}$

$$y_{out} = \mathbf{V}^*\mathbf{Y}. \tag{4.11}$$

Figure (4.1) shows how this is related to the antenna array.

Consider the case of a co-channel interference signal arriving at the antenna array. Let this signal vector be denoted as $\mathbf{X}$. Then this vector will be physically added to the signals

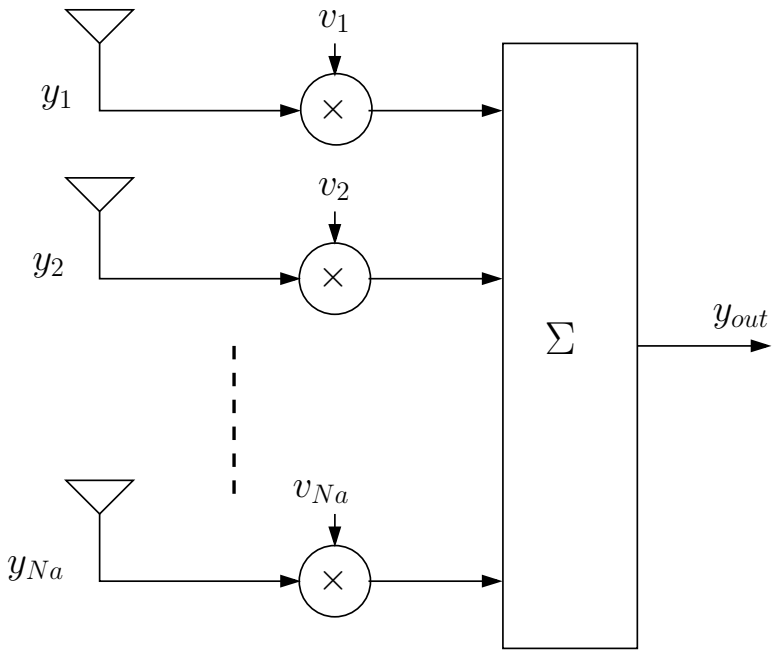

Figure 4.1: Antenna array with weighting vector.

in equation (4.7) and the received vector $\mathbf{Y}$ becomes

$$\mathbf{Y} = s\mathbf{V}_s + \mathbf{X} + \mathbf{W}. \tag{4.12}$$

For N_i number of interferers, the received vector can be written as

$$\mathbf{Y} = \mathbf{Y}_d + \mathbf{W} + \sum_{l=1}^{N_i} \mathbf{X}_l, \tag{4.13}$$

where $\mathbf{Y}_d$ and $\mathbf{X}_l$ represent the desired signal vector and the sum of N_i interfering signals $\mathbf{X}_1$, $\mathbf{X}_2$ $\ldots$ $\mathbf{X}_l$ respectively. Also, $\mathbf{Y}_d$, $\mathbf{W}$ and $\mathbf{X}_l$ are vectors of length N_a and are collected in a similar fashion to $\mathbf{Y}$.

In order to find the optimum combining vector or weighting vector $\mathbf{V}$, the received correlation matrix for the interference plus noise $\mathbf{R_{nn}}$ must be found.

Since $(\mathbf{W} + \sum_{l=1}^{N_i} \mathbf{X}_l)$ from equation (4.13) represent the interference plus noise, $\mathbf{R_{nn}}$ can be written as

$$\mathbf{R_{nn}} = E\left[(\mathbf{W} + \sum_{l=1}^{N_i} \mathbf{X}_l)\, (\mathbf{W} + \sum_{l=1}^{N_i} \mathbf{X}_l)^* \right]. \tag{4.14}$$

As $\mathbf{W}$ represents AWGN, then it is reasonable to assume that it is uncorrelated with the interfering signals. Therefore, $\mathbf{R_{nn}}$ is reduced to

$$\mathbf{R_{nn}} = \sigma_w^2 I + \sum_{l=1}^{N_i} E\left[\, \mathbf{X}_l \mathbf{X}_l^* \,\right], \tag{4.15}$$

where σ_w^2 is the noise power and I is an identity matrix of size $(N_i \times N_i)$.

In order to find the optimum combining vector $\mathbf{V}$, the solution must satisfy the condition

$$\mathbf{V}^*\mathbf{V}_s = 1. \tag{4.16}$$

This equation means that $\mathbf{V}$ is directed at the same angle as the sending side. Consider the case when only the desired signal is present without noise nor interference such the equation (4.12) becomes

$$\mathbf{Y} = s\mathbf{V}_s.$$

In this case the beamformer output y_{out} will become

$$\mathbf{V}^*\mathbf{Y} = \mathbf{V}^* s \mathbf{V}_s = s. \tag{4.17}$$

In other words, the beamformer does not distort the signal arriving in the direction of the angle θ.

In the presence of interference and noise, the beamformer is required to estimate the signal s arriving from the direction θ. This is done by by minimizing the error variance subject to the condition in equation (4.16) as follows

$$\min_{\mathbf{V}} E\left|\tilde{s}(t)\right|^2, \tag{4.18}$$

where $\tilde{s}(t) = s - \hat{s}(t)$ and $\hat{s}(t)$ is the estimate of the signal when the optimum vector $\mathbf{V}$ is used i.e. $\hat{s}(t) = \mathbf{V}^*\mathbf{Y}$.

By maximizing the SINR, the optimum combining vector $\mathbf{V}$ in terms of $\mathbf{R_{nn}}$ can be found to be [82]

$$\mathbf{V} = g_a \mathbf{R_{nn}}^{-1} \mathbf{V}_s, \tag{4.19}$$

where g_a is the antenna array gain which has no effect on the performance of the antenna array.

For all the simulations performed in this chapter, the value of $\mathbf{V}$ is normalized so that the antenna array gain and the overall effect of the weighting vector has no gain effect on the signal and the SINR as proposed in [82].

A derivation of the theoretical upper bound on the BER performance of optimum combining in Rayleigh fading channels for any number of users can be found in [83].

4.4.2 Null Steering

The second approach to linearly combining the signals arriving at an antenna array is the null steering. In this technique the weighting vector is designed in a way so that the null is steered in the direction of the interference.

In null steering techniques, there are N_a adjustable coefficients corresponding to the number of antennas. It is therefore, theoretically possible to separate the same number of signals. If one of these signals is the desired message then that leaves us with $(N_a - 1)$ adjustable nulls or suppressible interference signals [84].

Steering in this context can be achieved in many different ways. These include controlling the phase of the weighting vector [85, 86] or more recently by adjusting the amplitude of the weighting vector [87, 88].

In addition to steering the nulls in the desired directions, some techniques consider other factors or parameters like the half power beam-width, distance of the first null and the height and distance of the main sidelobe.

The four most important techniques for this are: null steering by real weight control (NSWC) [84], null steering by controlling the element positions (NSEP) [89, 90], the CLEAN technique and null steering based on direction of arrival estimation (NSDOA)[91].

The selection of the NSWC method is based on the comparative study by R. Qamar and N. Khan [92] and can be explained as follows.

For the NSEP technique, the complexity is higher than the NSWC method and the antenna structure is more expensive as it requires moving elements and a servo mechanism to change the positions of the elements in order to achieve the null steering.

Regarding the CLEAN technique, the complexity is also higher than the NSWC method as it is iterative. The main disadvantage though is that it requires a large number of antennas. The maximum number of interfering signals that can be cancelled using the CLEAN technique is one tenth of the required elements in the antenna array.

In the NSDOA technique, the complexity is higher once again. Moreover, this tech-

nique and the other previously mentioned techniques have other disadvantages like low null depth and side lobe levels.

In the following, the combiner design that uses the (NSWC) method is explained. Assuming that the transmitted signals are modulated with QPSK, then the time delays between any two adjacent elements in the array can be represented as phase shifts. This phase shift will be $e^{(j\psi)}$, where

$$\psi = \frac{2\pi}{\lambda} d\cos(\theta), \tag{4.20}$$

where λ is the wavelength [92, 84].

At the receiver, the signal from each element in the array will be multiplied by a coefficient Υ_i. These signals are added after this weighting and the arising vector is called the array factor F_a, where

$$F_a = \Upsilon_0 + \Upsilon_1 e^{j\psi} + \Upsilon_2 e^{j2\psi} + \cdots + \Upsilon_{(N-1)} e^{j(N-1)\psi}. \tag{4.21}$$

Let

$$Z = e^{(j\psi)}, \tag{4.22}$$

then equation 4.21 can be written as

$$F_a = \Upsilon_0 + \Upsilon_1 Z + \Upsilon_2 Z^2 + \cdots + \Upsilon_{(N-1)} Z^{(N-1)}. \tag{4.23}$$

The NSWC method assumes all the weights to be real valued.

The implementation of null steering in PLNC systems requires only one null to be steered. To achieve this, an array with only 3 elements is required [84].

For 3 elements, equation 4.23 becomes [84],

$$F_a = (Z - Z_1)(Z - Z_1^*) = 1 + \beta_n Z + Z^2, \tag{4.24}$$

where β_n is the real weight that steers the null in the desired direction θ_r and can be calculated as,

$$\beta_n = -(Z + Z_1^*) = -\cos(\frac{2\pi}{\lambda} d\cos(\theta) + \frac{2\pi}{\lambda} d\cos(\theta_r)). \tag{4.25}$$

To conclude the design, we go through the last few equations backwards. So first β_n is calculated using the known values of θ and θ_r from equation (4.25). Then the vector F_a

is found from equation(4.24) by substituting the values of β_n and Z.

Figure (4.2) shows this three element array for steering one null.

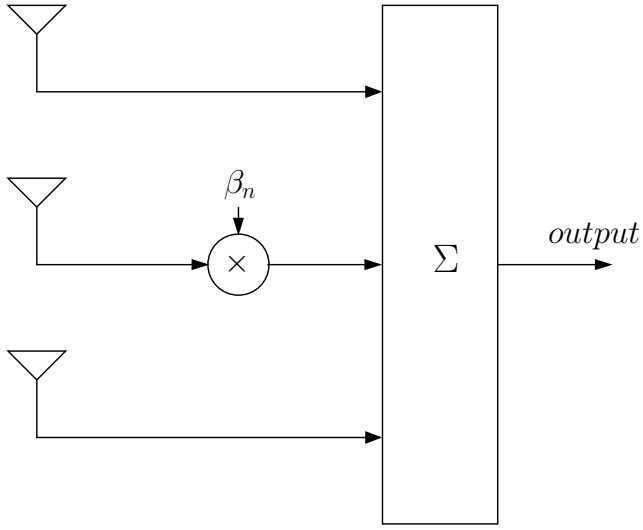

Figure 4.2: Three element array for steering one null.

This array is simple to implement due to the low number of elements and the use of only one real value, namely β_n to complete the design.

4.5 System Model

Consider a PLNC network consisting of a relay and two end nodes. The end nodes are equipped with a single antenna, while the relay has a linear antenna array. The packet exchange cycle requires two phases, the uplink phase and the downlink phase.

For both optimum combining (OC) and null steering techniques, the antenna array consists of N_a elements with a constant distance d between them. The received signals at the antenna array will arrive at different time instants depending on the angle of arrival θ which is measured between the direction of arrival and the broadside.

4.5.1 Uplink Phase

Let $\mathbf{U}_1$ and $\mathbf{U}_2$ be the signal propagation vectors from nodes 1 and 2 respectively.

The Additive White Gaussian Noise (AWGN) vector $\mathbf{W}$ is assumed to be be uncorrelated with $\mathbf{U}_1$ and $\mathbf{U}_2$.

For simplicity, the signals are assumed to have equal power. Then the signal at the relay $\mathbf{Y}(k)$ at time k will be

$$\mathbf{Y}(k) = \mathbf{U}_1 a(k) + \mathbf{U}_2 b(k) + \mathbf{W}(k), \tag{4.26}$$

where $a(k)$ and $b(k)$ are the sent signals from nodes 1 and 2 respectively.

Let $\mathbf{A}(k)$ and $\mathbf{B}(k)$ represent the data symbols received at time k from nodes 1 and 2 respectively.

$$\mathbf{A}(k) = \begin{bmatrix} a_1(k) \\ a_2(k) \\ \vdots \\ a_N(k) \end{bmatrix}, \quad \mathbf{B}(k) = \begin{bmatrix} b_1(k) \\ b_2(k) \\ \vdots \\ b_N(k) \end{bmatrix},$$

where a_i represents the symbol received at element i of the antenna array from node 1. Also, $a_{i+1} = e^{(j\psi)} a_i$ and b_i is the same as a_i for the second node. $\mathbf{A}(k)$ and $\mathbf{B}(k)$ can be expressed as

$$\mathbf{A}(k) = \mathbf{U}_1 a(k), \tag{4.27}$$

and

$$\mathbf{B}(k) = \mathbf{U}_2 b(k). \tag{4.28}$$

For unity flat fading channels, the received signal at antenna i will be $y_i(k) = a_i(k) + b_i(k) + w_i(k)$. This can be written in matrix form as $\mathbf{Y}(k) = \mathbf{A}(k) + \mathbf{B}(k) + \mathbf{W}(k)$. Let $\mathbf{h}_1$ and $\mathbf{h}_2$ represent the two tapped delay line channel vectors of length L_1 and L_2 respectively. These channels that arise from a multipath environment are assumed to be frequency selective. Then the received signal at antenna i will be

$$\begin{aligned} y_i(k) = &\sum_{m=0}^{L_1-1} \mathbf{h}_1(m) a_i(k-m) \\ &+ \sum_{m=0}^{L_2-1} \mathbf{h}_2(m) b_i(k-m) + w_i(k). \end{aligned} \tag{4.29}$$

This can also be written in matrix form as

$$\mathbf{Y}(k) = \mathbf{A}'(k) + \mathbf{B}'(k) + \mathbf{W}(k), \tag{4.30}$$

where $\mathbf{A}'(k)$ is a vector collected from the first term of equation 4.29 for all values of i in a similar fashion to $\mathbf{A}(k)$ and similarly for $\mathbf{B}'(k)$ which is the collection of the second

term. At the relay, OC is applied using vectors $\mathbf{V}_1$ and $\mathbf{V}_2$ as shown in figure 4.3.

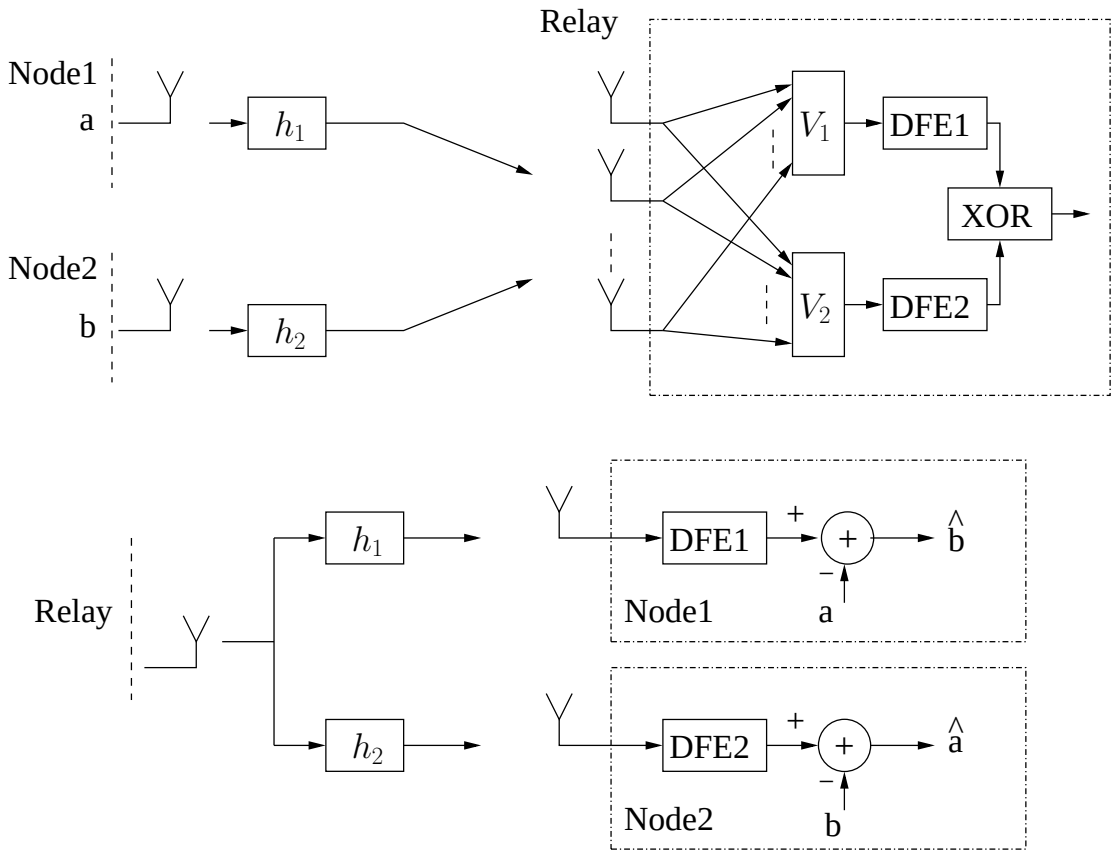

Figure 4.3: OC PLNC system with DFE equalizers.

4.5.2 Relay Operation and Downlink Phase

In this section, the operation of the relay shown in figure (4.3) is discussed. Although the proposed system utilizes OC for the design of both $\mathbf{V}_1$ and $\mathbf{V}_2$, yet the same structure can be used with null steering. In fact, the structure is used in the simulations with null steering for comparison.

When both end nodes send their packets, namely a and b, they reach the relay convolved with channels $\mathbf{h}_1$ and $\mathbf{h}_2$ respectively as formulated in equation (4.30).

4.5.2.1 Design with the OC Approach

This is the method of choice in this work. The OC approach is used twice to find an estimate of $\mathbf{A}'(k)$ and $\mathbf{B}'(k)$ at each time instant k. This is done through using vectors $\mathbf{V}_1$ and $\mathbf{V}_2$ depending on the two direction of arrival angles θ_1 and θ_2 respectively.

The next step is to remove the effect of the multipath channels from each individual signal. One of the most efficient ways to do that is by using the optimum DFE equalizer. A separate DFE is placed for each channel. Although perfect channel estimation is assumed, the estimation error is small and can be neglected.

It is worth mentioning that a separate time overhead is required for each channel estimation and this is unavoidable. The input to DFE1 at time k according to equation (4.11) will be

$$\mathbf{V}_1^* \mathbf{Y}(k).$$

Similarly, the OC vector $\mathbf{V}_2$ and DFE2 are used to find an estimate of the packet from the second node. The two estimated signals are then added and the whole uplink side is depicted in the upper-right side of figure 4.3.

It should be noted that this process entails symbol detection at each branch. This is due to the decision device included in the DFE. Each time the decision is correct, this will act as a de-noising effect and therefore the method is considered as a DNF.

To design the OC vectors $\mathbf{V}_1$ and $\mathbf{V}_2$, equation (4.12) is replaced by equation (4.26). For the first vector $\mathbf{V}_1$, $\mathbf{U}_1 a(k)$ is the desired signal and $\mathbf{U}_2 b(k)$ is the interference. Therefore, $\mathbf{R_{nn}}$ in equation (4.14), becomes

$$\mathbf{R_{nn1}} = E\left[(\mathbf{W} + \mathbf{U}_2)\,(\mathbf{W} + \mathbf{U}_2)^*\right], \tag{4.31}$$

where $\mathbf{R_{nn1}}$ is the noise plus interference covariance matrix with respect to the first signal.

According to equation (4.19) and neglecting g_a, $\mathbf{V}_1$ becomes

$$\mathbf{V}_1 = \mathbf{R_{nn1}}^{-1}\mathbf{U}_1. \tag{4.32}$$

The second OC vector $\mathbf{V}_2$ can be calculated in a similar way. This leads to

$$\mathbf{V}_2 = \mathbf{R_{nn2}}^{-1}\mathbf{U}_2, \tag{4.33}$$

where

$$\mathbf{R_{nn2}} = E\left[(\mathbf{W} + \mathbf{U}_1)\,(\mathbf{W} + \mathbf{U}_1)^*\right]. \tag{4.34}$$

Using these two vectors enables the implementation of the DFEs and the symbol mapping. This de-noising effect results in a performance increase compared to AF techniques.

4.5.2.2 Design with the Null Steering Approach

This approach is studied here for comparison. Although some applications prefer null steering over OC, yet the OC method outperforms the null steering in the case at hand as will be shown later in this chapter.

The relay structure in figure (4.3) is kept the same, while null steering is used for the design of the weighting vectors $\mathbf{V}1$ and $\mathbf{V}2$.

The most suitable of the null steering methods for PLNC is the (NSWC) for many reasons including low computational complexity, the small number of required antennas, less sensitivity to quantization error and simple implementation amongst other things. It is also the method of choice in [92] where detailed comparisons are made.

Let θ_1 and θ_2 be the two DOA angles for nodes 1 and 2 respectively. Then the weighting vector $\mathbf{V}1$ can be found by applying the design method described in Section (4.4.2) as follows.

First find the value of ψ from equation (4.20) using the angle θ_1 instead of θ. Then Z can be easily found from equation (4.22).

For a three element array, the real value β_n can be found using equation (4.25) by replacing the null angle θ_r by θ_2. Finally the calculated values of Z and β_n are used to find $\mathbf{V}1$ from equation (4.24).

Replacing the roles of θ_1 and θ_2 in the previous design procedure results in the second weighting vector $\mathbf{V}_2$.

4.5.2.3 DFE Design

In this section we will only consider the design of DFE1 as DFE2 can be designed in a similar way by replacing $\mathbf{h}_2$ instead of $\mathbf{h}_1$, where $\mathbf{h}_1$ and $\mathbf{h}_2$ represent the channel coefficient vectors for channels 1 and 2 respectively.

For unchanged channels the DFEs used in the end nodes will be the same as the ones in the relay node. If the channels change in the downlink phase then the DFE at each end node can be redesigned using the new estimated channel vector instead of $\mathbf{h}_1$.

We start by calculating the observation covariance matrix $\mathbf{R}_\mathbf{y}$ which can be found by two ways. The first way is to use the definition equation

$$\mathbf{R_y} = E(\mathbf{y_k}\mathbf{y_k}^*), \tag{4.35}$$

or simply by using the previously derived equation

$$\mathbf{R_y} = \sigma_s^2\mathbf{H}\mathbf{H}^* + \sigma_v^2\mathbf{I}_{L_p}, \tag{4.36}$$

where L_p is the data packet length, σ_s^2 and σ_v^2 are the signal and noise variances respectively and $\mathbf{R_y} \in \mathbb{C}^{L_p \times L_p}$.

The toeplitz matrix $\mathbf{H} \in \mathbb{C}^{L_p \times (L_p + L_1 - 1)}$ can be written as

$$\mathbf{H} = \begin{bmatrix} \mathbf{h}_1(1) & \mathbf{h}_1(2) & \dots & \mathbf{h}_1(L_1) & \dots & 0 \\ 0 & \mathbf{h}_1(1) & \mathbf{h}_1(2) & \dots & \mathbf{h}_1(L_1) & \dots & 0 \\ & & & \vdots & & & \\ 0 & & \dots & \mathbf{h}_1(1) & \mathbf{h}_1(2) & \dots & \mathbf{h}_1(L_1) \end{bmatrix}, \tag{4.37}$$

where L_1 is the length of the first channel.

Define the cross covariance matrix $\mathbf{R_{sy}} \in \mathbb{C}^{(N_{FB}+1) \times L_p}$ as

$$\mathbf{R_{sy}} = \begin{bmatrix} \mathbf{0}_{(N_{FB}+1)\times\Delta} & \sigma_s^2\mathbf{I}_{N_{FB}+1} & \mathbf{0} \end{bmatrix} \mathbf{H}^*. \tag{4.38}$$

The desired feedback and feedforward filter coefficients will be [61]

$$\mathbf{q}_{\text{opt}} = \frac{\mathbf{e}_0\mathbf{R}_d^{-1}}{\mathbf{e}_0\mathbf{R}_d^{-1}\mathbf{e}_0}, \tag{4.39}$$

$$\mathbf{f}_{\text{opt}} = \mathbf{q}_{\text{opt}}\mathbf{R}_{sy}\mathbf{R}_y^{-1}, \tag{4.40}$$

where

$$\mathbf{R}_d = \mathbf{\Phi}\left(\frac{\mathbf{I}_{L_p+L_1-1}}{\sigma_s^2} + \frac{\mathbf{H}^*\mathbf{H}}{\sigma_v^2}\right)^{-1}\mathbf{\Phi}^*, \tag{4.41}$$

$$\mathbf{\Phi} = [\mathbf{0}_{(N_{FB}+1)\times\Delta} \;\; \mathbf{I}_{N_{FB}+1} \;\; \mathbf{0}], \tag{4.42}$$

$\mathbf{e_0} = [1,\ 0,\ 0,\ \dots,\ 0]$, $\mathbf{\Phi} \in \mathbb{C}^{(N_{FB}+1)\times(L_p+L_1-1)}$ and $\mathbf{R}_d \in \mathbb{C}^{(N_{FB}+1)\times(N_{FB}+1)}$.

4.5.3 Downlink Phase

The downlink phase is simple and straight forward. One antenna at the relay is enough to broadcast the signal from the relay back to both end nodes. This signal will once again suffer from the effect of the frequency selective channels $\mathbf{h}_1$ and $\mathbf{h}_2$.

As no mixing of signals happens in the downlink phase, only one DFE is required at each end node. For simplicity and without loss of generality, the channels are assumed to be fixed and have the same values from the uplink phase but this is not a necessary condition for the system to work. If the channels change during the phase change, then another channel estimation is done in the downlink phase and the DFEs in both end nodes are designed accordingly.

The lower part of figure 4.3 depicts the downlink phase. QPSK modulation and demodulation are used but they are omitted from the mentioned figure for simplicity.

One of the advantages of the our proposed method is that higher order modulation such as 16-QAM can be used and this modulation is done at both end nodes in the uplink phase and also at the final step in the relay during the downlink phase. As for the demodulation, it will be done at both end nodes in the downlink phase.

It is clear that the proposed method has a low computational complexity. We will show in the coming section that a small number of elements N is required. This makes the computational cost of OC negligible and the overall complexity is approximately twice that of a single DFE at the relay. As for the end nodes, the complexity is that of one DFE which consists of two FIR filters.

4.6 Simulation Results and Discussion

This section is dedicated to showing the performance of the proposed method. ITU pedestrian channels A (Ch.102) and B (Ch.103) shown in Table 3.1 are used [59].

The channel profiles are normalized by dividing each coefficient by the factor

$$\sqrt{\sum_{l=0}^{L-1} 10^{P_l/10}}.$$

Assuming the system frequency is 20 MHz, the arrival times are normalized and rounded up to the closest integer with a sampling time of 44 ns.

With the selection of these channels, the parameter values for the DFE design can be

set starting with $L_1 = 10$ and $L_2 = 85$. The length of the forward filter must be greater than the channel memory. For the simplicity of the simulations, we will use the same values of forward, feedback and Δ for all DFEs in the uplink and downlink phases. It should be noted that using specific values for each DFE will give even better performance results. In the case at hand, $N_{FF} > L$, where $L = max(L_1, L_2)$ and $N_{FF} = 256$ taps were selected.

For selecting N_{FB} and Δ, inequality (3.54) must be satisfied. N_{FB} has a small value compared to N_{FF} and is chosen to be 19 taps. Now inequality (3.54) can be satisfied by choosing Δ around $\frac{N_{FF}+L}{2}$ or slightly higher. In this case Δ is set to 181 with some fine tuning but any other value in that range works very well. These values apply for all simulations in this work.

4.6.1 OC Pattern Diagrams

When the antenna array applies a weighting vector to its elements, the result is a variable overall gain at different angles. The plot that represents the antenna array gain for all angles is called a pattern digram. Looking at the pattern diagrams for each case can give an important insight on how the array performs.

For all the simulations, the distance between elements d is chosen to be $\frac{\lambda}{2}$ but this is not a necessary condition. Also, the horizontal axis represents the broadside of the antenna array and all the angles are measured relative to that side of the array staring from $\theta = 0$ on the right hand side of the axis.

The following figures illustrate the gain patterns at the relay when OC is used.

Part (a) of figure (4.4) shows the pattern diagram simulated for DOAs $\theta_1 = 30$ and $\theta_2 = 140$ from end nodes 1 and 2 respectively with 4 elements in the antenna array at SNR of 5dB. Part (b) of the same figure shows the pattern diagram simulated for the same values while changing the first DOA to $\theta_1 = 60$. From this figure, it is clear that the gain is just below 1 in the desired DOA and has a very small value in the direction of the second user or the interference. It would be ideal if the gain was maximum at the desired angle and zero at the interference angle but this is not the case when the SINR is maximized in the OC method. The most important thing to notice in this figure is the dramatic change in the overall pattern when the desired angle θ_1 is changed.

Part (a) of figure (4.5) shows the pattern diagram simulated for DOAs $\theta_1 = 45$ and $\theta_2 = 140$ from end nodes 1 and 2 respectively at SNR of 5dB using 4 elements in the

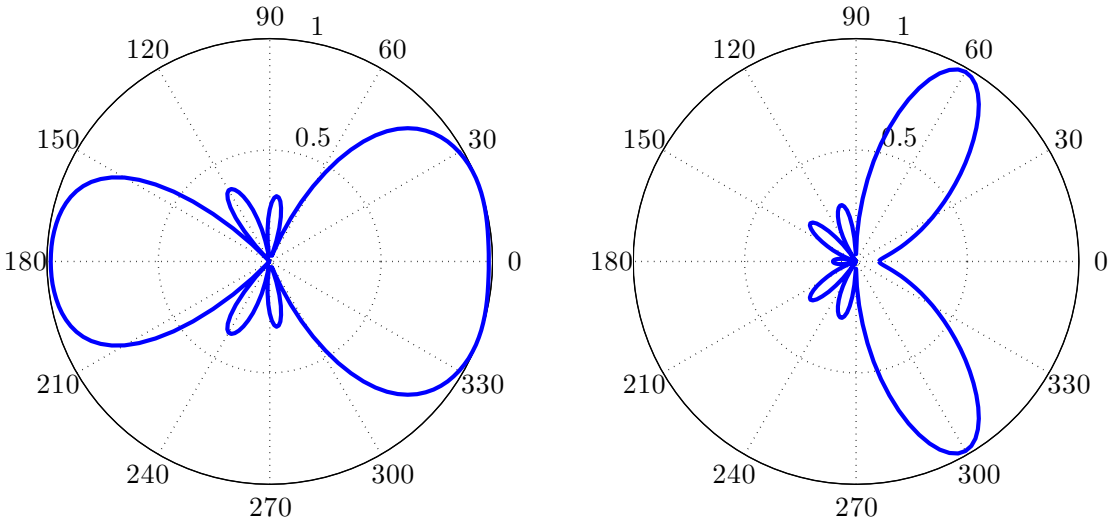

a. DOA = 30 b. DOA = 60

Figure 4.4: Pattern diagrams at the relay using OC for (a) $\theta_1 = 30, \theta_2 = 140, N_a = 4$ and SNR=5dB (b) changing θ_1 to 60.

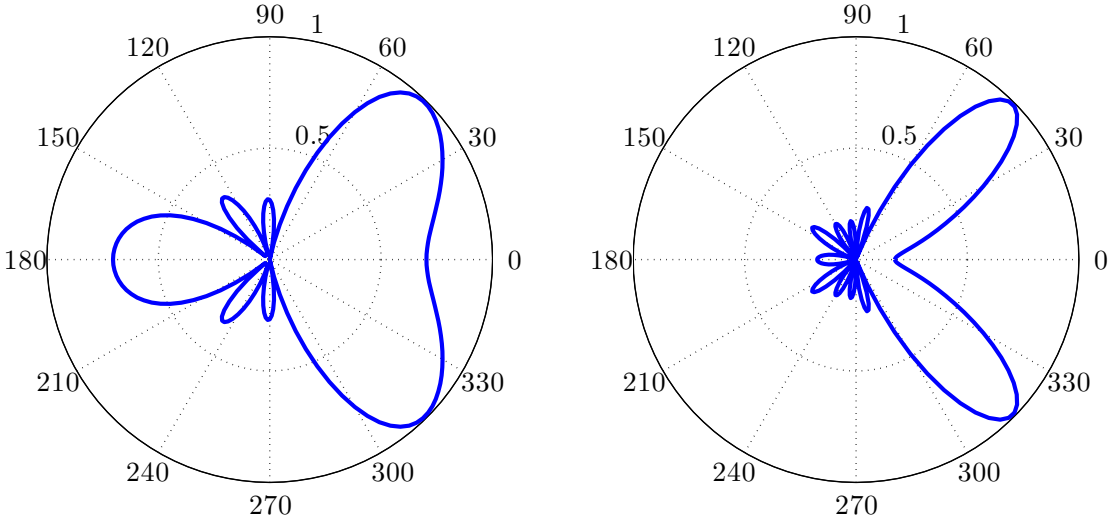

a. N_a = 4 b. N_a = 6

Figure 4.5: Pattern diagrams at the relay using OC for (a) $\theta_1 = 45, \theta_2 = 140, N_a = 4$ and SNR=5dB (b) changing N_a to 6.

antenna array. Part (b) of the same figure shows the pattern diagram simulated for the same values while changing number of elements in the antenna array to 6.

Inspecting this figure shows that the directionality is increased in the desired DOA with the increase of the number of elements from 4 to 6. Moreover, the side lobes are decreased in size in the direction of the interference but the number of lobes are increased in direct proportion with the number of the array elements.

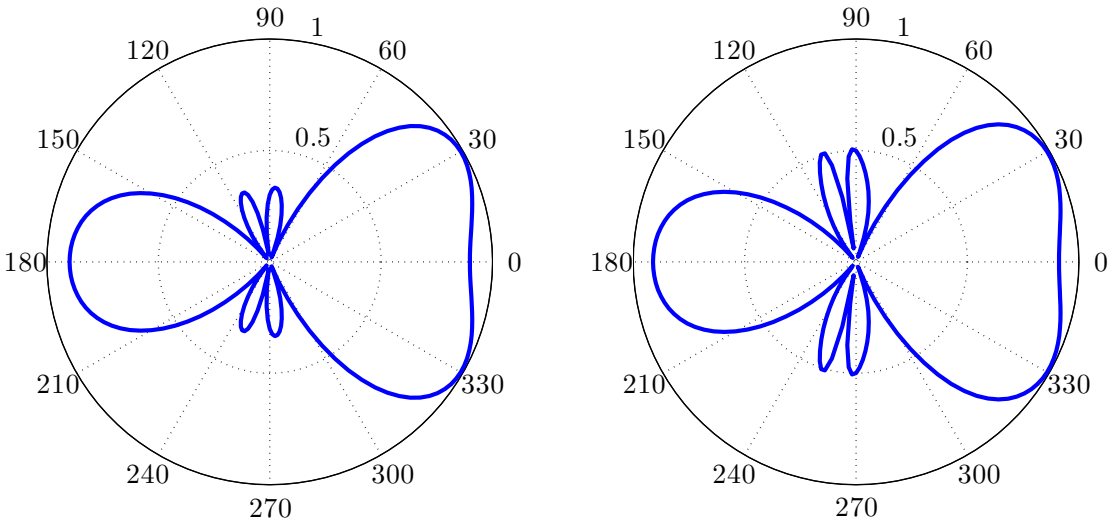

a. SNR = 5 dB

b. SNR = 12 dB

Figure 4.6: Pattern diagrams at the relay using OC for (a) $\theta_1 = 30, \theta_2 = 100, N_a = 4$ and SNR=5dB (b) changing the SNR to 12dB.

Part (a) of figure (4.6) shows the pattern diagram when OC is used at the relay node. The results are simulated for DOAs $\theta_1 = 30$ and $\theta_2 = 100$ from end nodes 1 and 2 respectively at SNR of 5dB using 4 elements in the antenna array. Part (b) of the same figure shows the pattern diagram simulated for the same values while changing the SNR to 12 dB.

It is interesting to see how the OC behaves in the case of a PLNC system with different levels of SNR. The increase of the SNR to 12 dB makes the pattern shift keeping the direction of the desired signal the same while rotating the null slightly closer to the direction of the interference $\theta_2 = 100$. This comes at the expense of increasing the levels of the side lobes which can be afforded due to the decrease of the noise level as the SNR increases.

4.6.2 BER Performance of OC PLNC

In this section, the BER performance of the proposed OC PLNC is discussed. The simulations are performed with the following parameters. Forward filter length $N_{FF} = 256$, feedback filter length $N_{FB} = 19$ and $\Delta = 181$ for all the DFEs. The desired DOAs $\theta_1 = 30$ and $\theta_2 = 140$ for the first and second end nodes respectively. Changing the DOAs does not have a big effect on the performance of the system. Moderate changes to the filter parameters also does not have a big impact on the performance.

Figure (4.7) shows the end to end (E2E) performance of the proposed OC PLNC system evaluated at channel A with number of elements $N = 2, 4$ and 6.

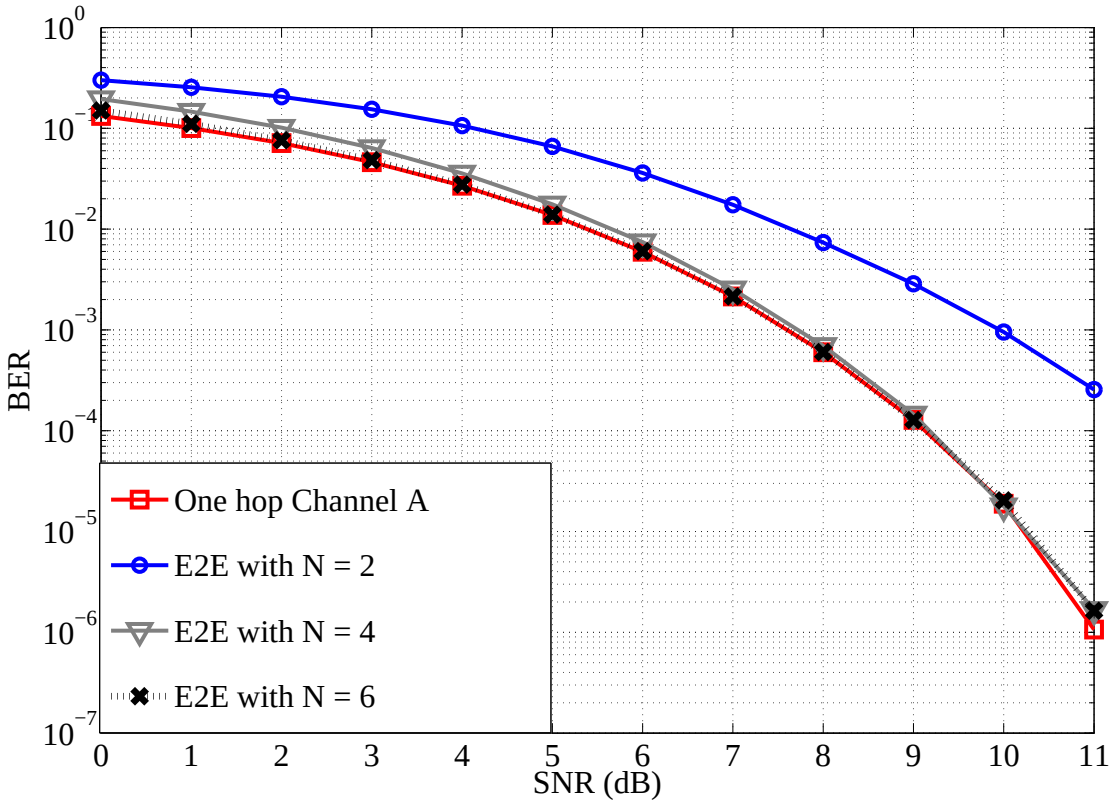

Figure 4.7: E2E Performance of OC-PLNC for $N = 2, 4$ and 6 compared to that of one hop channel A with DFE.

Clearly $N = 4$ is better than $N = 2$ but is almost identical to that of $N = 6$ or higher. Figure (4.7) also shows the performance of a one hop from relay to end node A through $\mathbf{h}_1$ with one DFE being used. This performance can be considered as the lower bound because the OC PLNC will also suffer from the same downlink channel $\mathbf{h}_1$ on the way to node A. The fact that the OC PLNC performance is asymptotic to this lower bound is evident from the mentioned figure.

Observing this figure we conclude that the OC-PLNC system with $N = 4$ is a good solution to the problem of implementing a PLNC system in a frequency selective environment. The complexity of the overall system is relatively low with a small array length of only 4 elements which gives a performance asymptotic to the case of a one hop system which is used as a lower bound.

4.6.3 Comparison with Null Steering

This section provides a comparison between the proposed OC-PLNC system with the same structure system employing null steering. The least two values for N_a in the NSWC null steering method are 3 and 7.

From the last section, we have seen that the OC-PLNC system can achieve its best performance at $N_a = 4$. Therefore, increasing the number of antennas more will only increase the system cost. This leads to choosing the least number of elements $N_a = 3$ for a fair comparison.

Through simulations, the BER is evaluated at the relay using the upper part of figure (4.3) for both the OC case and the NSWC. For this, the following values for the DOAs were used, $\theta_1 = 50$ and $\theta_2 = 140$. The resulting BER curves in figure (4.8) show that OC has a better performance of more than 2dB over NSWC. Once again the choice of the DOAs does not have a big impact on the performances in this case.

To have a deeper insight on this, the pattern diagrams at the relay of both OC and NSWC are drawn in figure (4.9) for the same values of θ_1,θ_2 and N_a. The OC part was done with SNR = 0 dB.

Inspecting figure 4.9(a) shows a high gain at θ_1 with some interference gain at θ_2. This is because the null is not exactly at the DOA of the interference. On the other hand, in figure 4.9(b) the steering of the null to match θ_2 has changed the whole pattern as mentioned before. This changing of pattern has caused a decrease in the gain at θ_1 which has an impact on the overall BER. This observation help to explain why in figure (4.8), the OC-PLNC outperforms the NSWC null steering method.

4.6.4 Comparison with Pre-filtering

Both the pre-filtering and the proposed OC-PLNC techniques are de-noise and forward methods and therefore, it is reasonable to compare their performances in terms of BER.

To do this the following parameters are chosen for the simulations. The MAX SNR

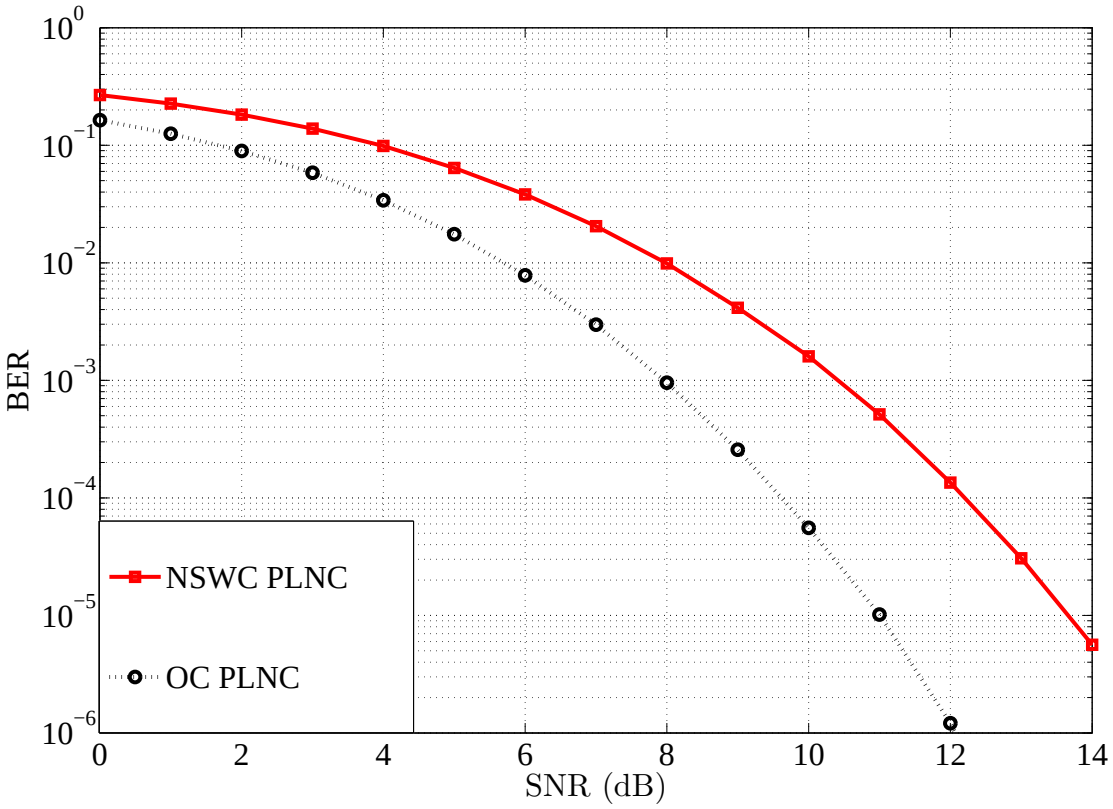

Figure 4.8: Performance of OC-PLNC and NSWC-PLNC methods at the relay.

is chosen as a representative of the pre-filtering techniques. The power constraints that normally exist at both end nodes are lifted to simplify the design. With the channels being normalized, the design is optimized at $\mathbf{F}_1(z) = \mathbf{H}_2(z)$ and $\mathbf{F}_2(z) = \mathbf{H}_1(z)$ and therefore no iterations are required for calculating the pre-filters.

As for the OC-PLNC method, the DOAs are chosen to be $\theta_1 = 30$ and $\theta_2 = 140$ and an antenna array of 4 elements is used.

ITU pedestrian channels A (Ch.102) and B (Ch.103) are used in both cases. Channels A and B are used one at a time for the downlink phase. Figure (4.10) shows the simulated BER performances for the above parameters.

It is clear from figure (4.10) that the proposed system outperforms the one with the pre-equalizer regardless of the channel used for the downlink phase. In other words, the received signal has a lower BER at both end nodes.

The proposed method uses DFEs at both the transmitter and receiver sides which requires separate channel estimations for the uplink and downlink phases. Therefore, if the channel changes in the second packet exchange then this will have no impact on the performance of the OC-PLNC system. On the other hand, the pre-filtering method is

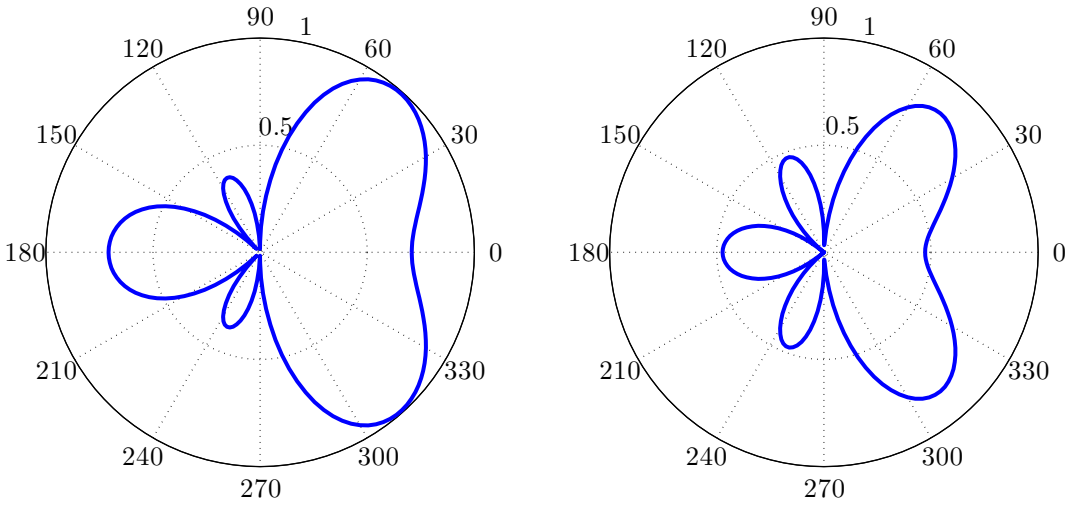

a. OC

b. Null steering

Figure 4.9: Pattern diagrams at the relay for OC-PLNC and NSWC-PLNC for $\theta_1 = 50$, $\theta_2 = 140$ and $N_a = 3$.

sensitive to variations in the channels between packet time slots. Under the assumption that the channel remains unchanged during one time slot, equation (3.56) can be used in simulating the change in BER performance for different values of average percentage of estimation error r. This is shown in figure (4.11) with the unchanged performance of the proposed method.

All of these simulations have been done assuming channel A in the downlink phase. The effect of the estimation error becomes worse for the second end node with the tougher channel B in the broadcasting phase, while the performance of the proposed method is unchanged in both cases.

4.6.5 Comparison with OFDM

In designing OFDM systems, they are assumed to be immune to the effect of the channel and this is sometimes stretched to frequency selective channels. This assumption arises from the argument that the transforming of the channel's impulse response to the frequency domain makes each frequency band flat. Although the last statement is true, yet it

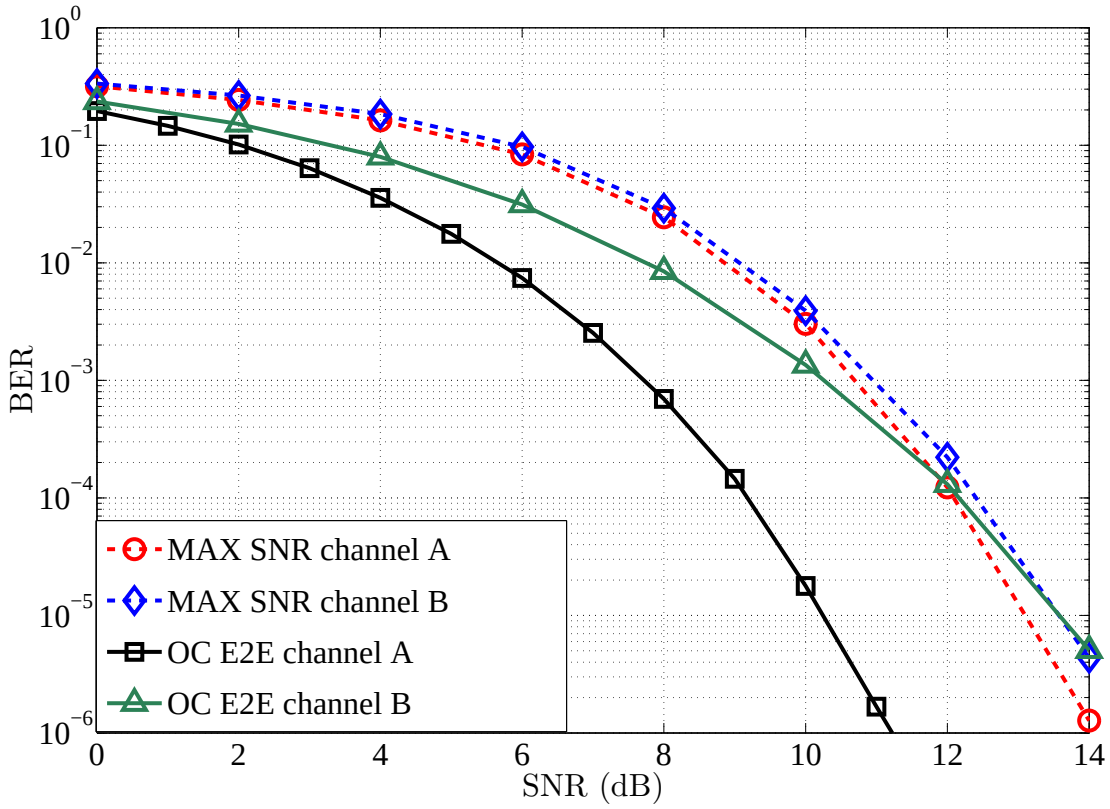

Figure 4.10: Simulated BER performances of the proposed OC-PLNC and the pre-filtering method.

fails to point out that each flat fading band is also multiplied by a different gain or attenuation. Reversing the effect of these attenuations at the receiver comes with a cost in BER performance for many reasons. One of these reasons is the imperfect channel estimation, but more importantly is the noise amplification especially at the frequency bands with high attenuation. This observation has been tested as part of the preparation for this work using simulations.

The process of directly reversing the gains at each frequency is called frequency domain equalization using a zero forcing equalizer. If the MMSE equalizer is used instead of the zero forcing equalizer, the BER performance is slightly improved but both of these techniques are considered as linear equalizers and can be greatly outperformed by non-linear equalizers such as the DFE.

As the DFE works strictly in the time domain, therefore, this equalizer cannot be used with OFDM unless the signal is transformed back to the time domain. In this case, the best option is to work in the time domain with the DFE and not having to suffer the disadvantages of the OFDM system.

To perform a successful OFDM DNF PLNC system, the relay performs a symbol by

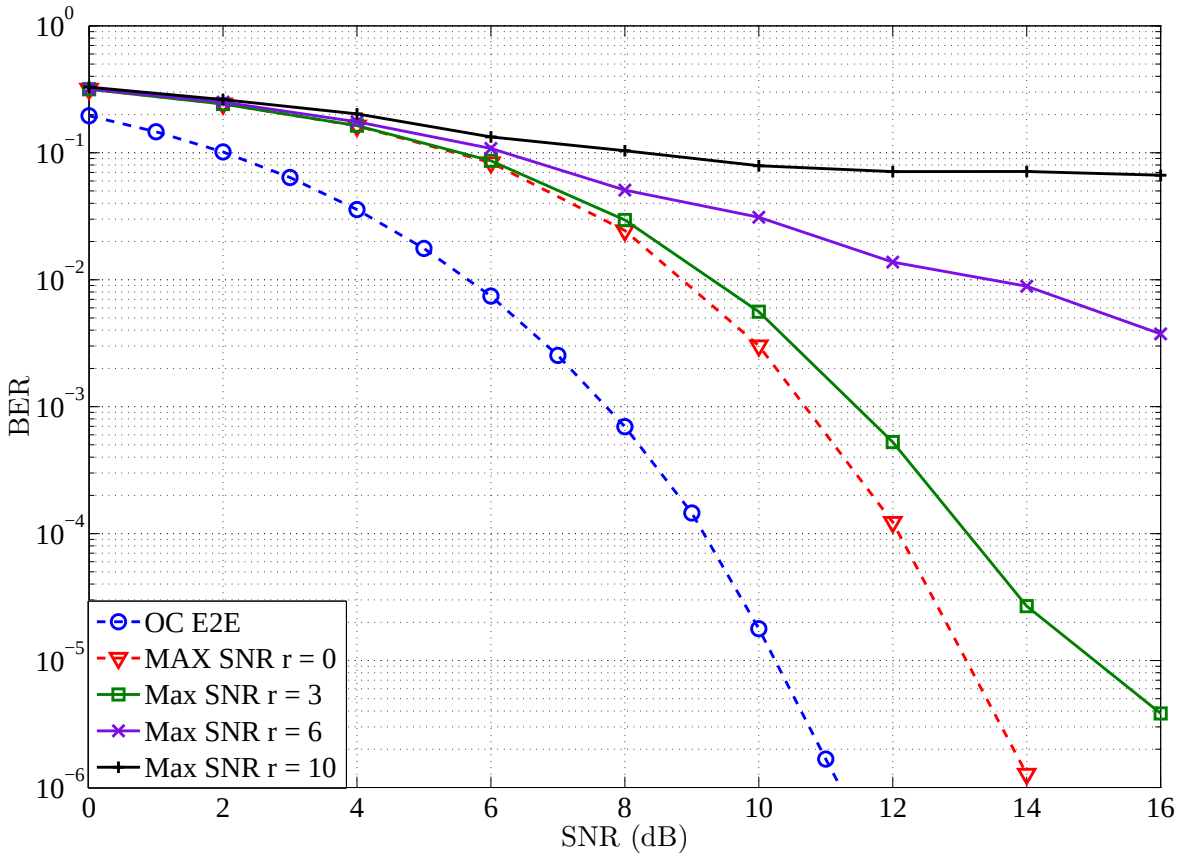

Figure 4.11: Simulated BER performances of the proposed OC-PLNC and the pre-filtering method for $r = 0$ %, 3%, 6% and 10%.

symbol maximum likelihood detection to determine the symbols. The resulting detector is called a maximum likelihood detector (MLD). Using the DNF at the relay with MLD was first proposed by T. Koike-Akino et al. [93, 94]. This approach was implemented to OFDM-PLNC systems by B.Jebur and C.Tsimenidis [95].

For the simulations of the BER performance of the OFDM syste, a packet size of 1024 is used with 25% cyclic prefix using the same frequency selective channels. Then FDE is is implemented at both end nodes using the linear MMSE method.

Figure (4.12) shows the simulated E2E BER performance for this system compared to the proposed OC-PLNC system. The performance of the PLNC in AWGN is also shown as a benchmark.

Inspecting this figure gives a clear view of the advantage of the proposed time domain OC-PLNC system in terms of performance. This comes also free of the known drawbacks of the OFDM system.

Both of the two systems under consideration are free of estimation errors if the channels are assumed to be unchanged for the duration of one packet transmission.

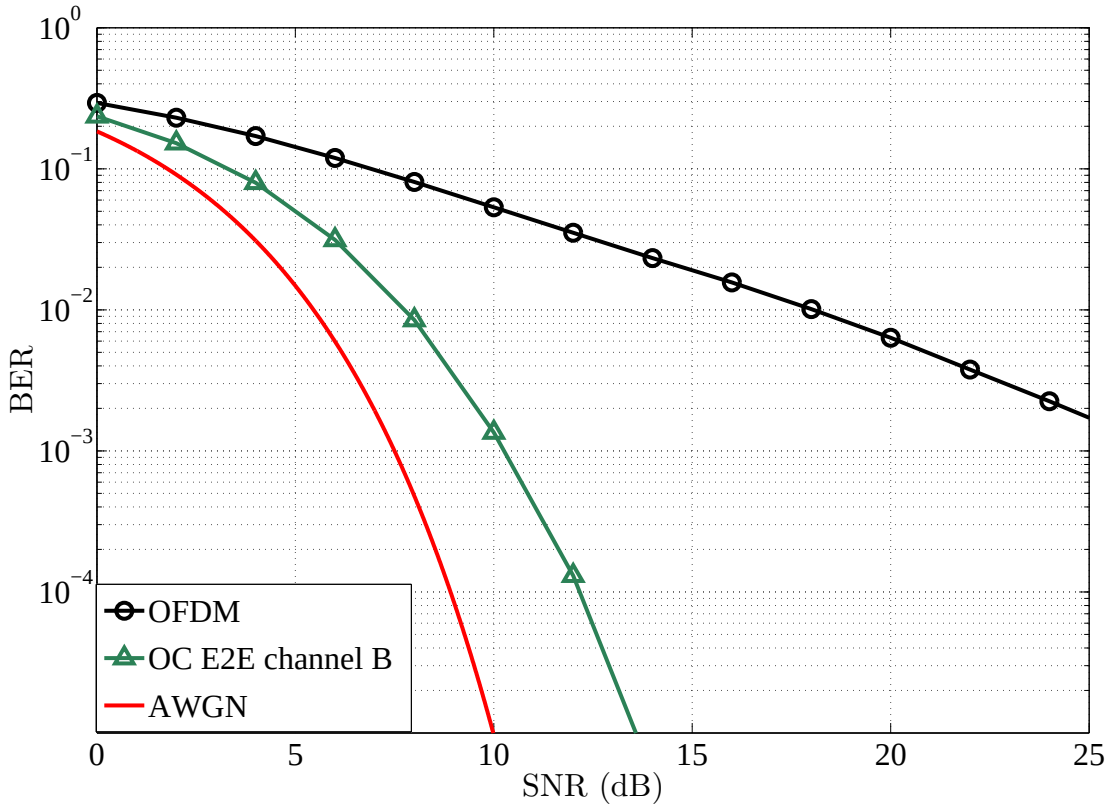

Figure 4.12: Simulated E2E BER performances of the OFDM-PLNC system, OC-PLNC system and PLNC in AWGN.

4.6.6 Comparison with AF-DFE

This section provides a comparison between the proposed OC-PLNC system and the AF-PLNC system proposed in the previous chapter.

In terms of complexity, both of the proposed methods have a low and acceptable complexity because the DFEs used in the design are not far behind the linear equalizers. The difference in the design is the placement of these DFEs. In the proposed AF PLNC, the DFEs are placed at the end nodes leaving the relay free from any calculation and this leads to efficient power consumption at the relay. On the other hand, the proposed OC DNF PLNC in this chapter has DFEs in all nodes to obtain a better BER performance. As a result of the low complexity, the cost will be also low but the OC DNF PLNC system still requires an antenna array of 4 elements.

The following parameters are used in the simulation of the OC PLNC system performance. $\theta_1 = 30$, $\theta_2 = 140$ and $N_a = 4$. Although the OC PLNC uses 4 DFEs instead of 2, yet the lengths are different than those of the AF PLNC. $N_{FF} = 256$, $\Delta = 181$ and $N_{FB} = 19$ are used with the OC PLNC system compared to $N_{FF} = 1024$, $\Delta = 768$ and

$N_{FB} = 32$ in the AF case. These numbers clearly prefer the OC PLNC system in terms of complexity of the DFE design but there is also the calculations of the OC.

Figure (4.13) shows the Simulated BER performance of the proposed OC DNF PLNC system measured at end nodes 1 and 2 with channels A and B used for the downlink respectively.

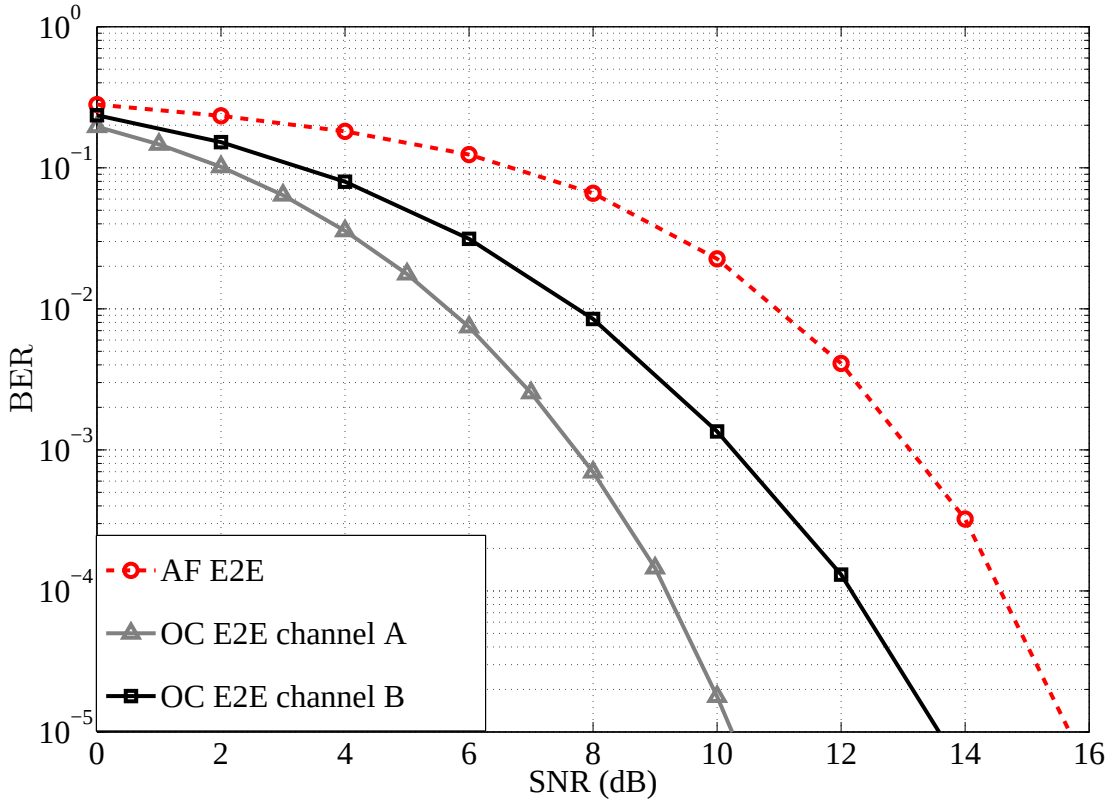

Figure 4.13: Simulated BER for AF-DFE and OC in PLNC system with channels A and B in the downlink.

From that figure, it is clear that in both cases the performance is better than that of the AF PLNC which is also shown in the same figure. The AF PLNC has the same performance at both end nodes because it uses the same DFE at those nodes and therefore only one BER curve is drawn.

As mentioned before, the performance of the OC PLNC system remains the same under the assumption that the channel is unchanged during one packet transmission. On the other hand, the AF PLNC system does suffer some degradation when the average percentage change in the channel is high. Figure (4.14) shows this degradation in performance compared to the original performances of both the systems under consideration.

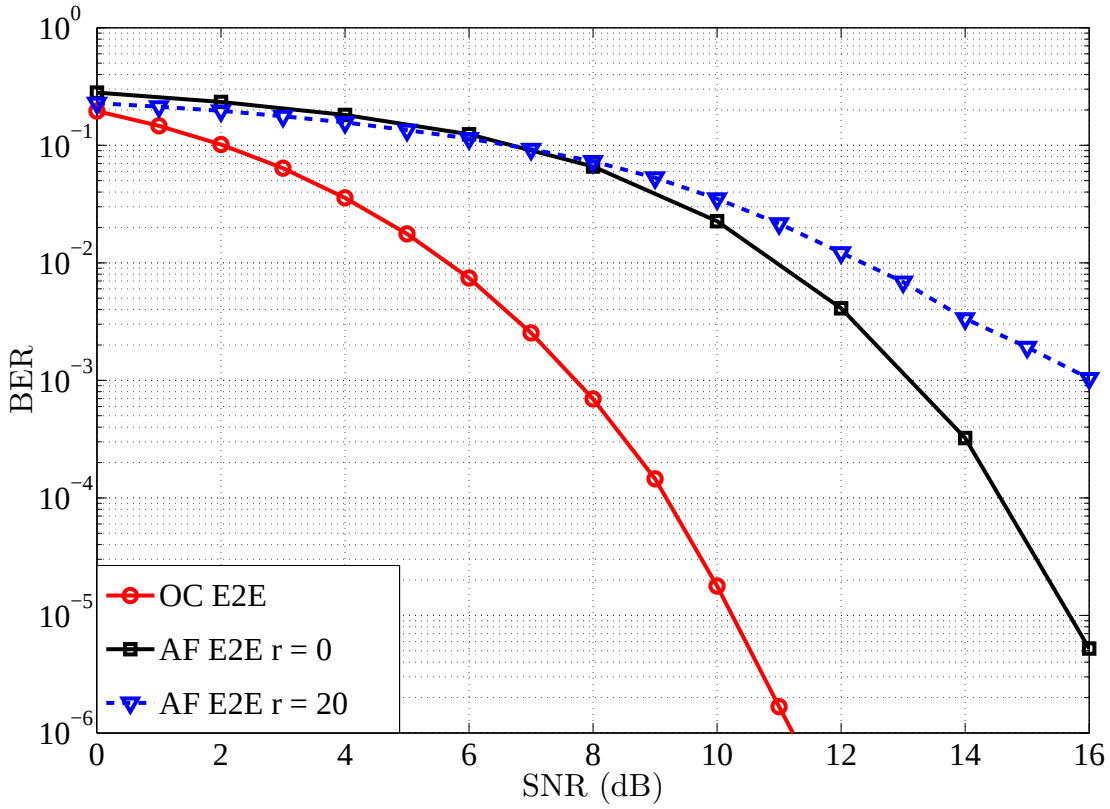

Figure 4.14: Simulated BER for OC-PLNC and AF-DFE systems with $r = 0$ and 20.

4.6.7 Application in Underwater Acoustic Communications

Underwater acoustic channels are known to be frequency selective. To successfully implement a PLNC system, the proposed method in this chapter is utilized with OC vectors at the relay and DFEs in the relay and end nodes. Two underwater channels measured in the North Sea are used in the simulations. With the selection of these channels, the parameter values for the DFE design can be set starting with $L_1 = 29$ and $L_1 = 49$. These are the lengths of the practically measured underwater channels. In this case $N_{FF} > L$, where $L = max(L_1, L_2)$. N_{FF} was selected to be 256 taps. For selecting N_{FB} and Δ, the inequality $\Delta + N_{FB} < N_{FF} + L_2$ must be satisfied. Then N_{FB} is chosen to be 22 taps and $\Delta = 170$.

Figure 4.15 shows the simulated BER performance of the underwater acoustic system compared to the BER performance of the first underwater channel alone for $\theta_1 = 45$, $\theta_2 = 135$ and $N = 4$.

Inspecting this figure shows that once again, the performance of the overall system is very close to that of a single hop performance of one of the channels alone which is the best achievable performance when DFEs are used.

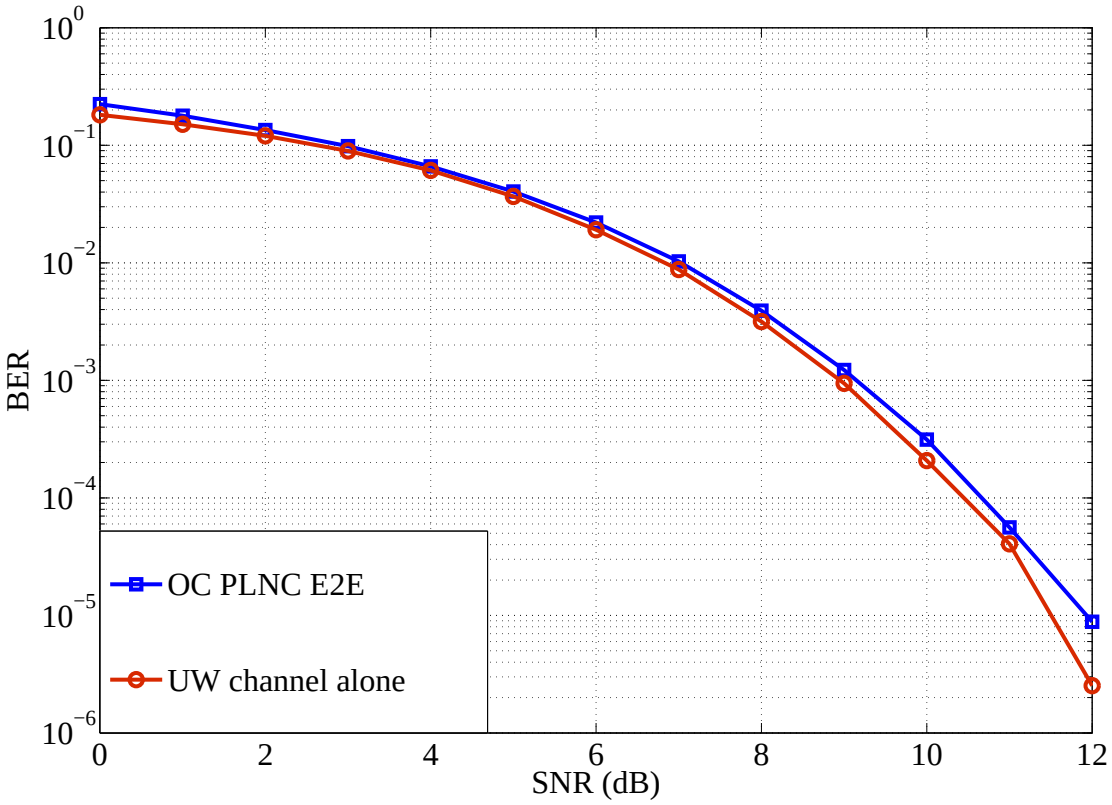

Figure 4.15: Simulated BER for OC-PLNC and single channel for underwater acoustic application.

4.7 Chapter Summary

This chapter contains a brief description of antenna arrays and the different applications of beam forming techniques. Two selected combining methods were selected for study, namely the optimum combining and null steering techniques. In both cases, a structure was proposed to enable the application of DNF PLNC systems in frequency selective environments with the use of an antenna array.

Different working conditions require different design approaches. Therefore, the proposed method in this chapter is different than the previous chapter. Here the focus is on the BER efficiency which is achieved through changing the relaying method from AF to DNF. This posed new challenges that required a new solution that included the use of an antenna array and a combining method.

Through various pattern diagrams and Monte Carlo simulations, it is concluded that the OC method is better suited for the system than null steering.

Comparing OC PLNC with the existing pre-filtering method in terms of performance reveals that the proposed method has better performance. This is achieved while relaxing

some of the conditions of the pre-filtering technique like not requiring a feedback channel to exchange channel information between end nodes.

This method is also compared to the OFDM PLNC system and shows superior BER performance while not having the well known problems the OFDM system.

The proposed method has also shown more resilience to channel changes between packets over all the other methods discussed in this chapter while maintaining better performance and low complexity at the expense of using one 4 element antenna array.

In this method, the higher order modulation can be easily used without modifying the rest of the system. Also, coding can be simply introduced using any of the existing coding methods to increase the reliability.

Chapter 5

Maximum Likelihood Decision Feedback Equalizer for Fast Implementation of PLNC Systems

5.1 Introduction

As discussed before, when frequency selective fading channels are present, the application of a PLNC system is not straight forward. Therefore, some kind of equalization is always needed.

Linear equalizers can be easily used with OFDM systems for example but with inferior BER performance to other methods. On the other hand, more complex methods like the maximum likelihood detector (MLSD) have a high computational complexity that grows exponentially with the channel length not to mention the effort needed to make these methods apply to the PLNC case.

For these reasons, the DFE was the equalizer of choice in the previous chapters. The issue of equalization doesnt end there and there is always space for improvement. For example, the design of the DFE itself can be improved. One way to do that is by using a soft decision device on the feedback filter and a hard decision for the output alongside a norm constraint on the feedback filter to reduce the effect of the backward error propagation [96].

In this chapter, the problem of implementing a functional PLNC system in frequency selective channels is addressed in a different way. The delay imposed by the other methods including linear equalization is to be eliminated. This is done while achieving a computational complexity which is lower than that of the previously proposed methods.

The combination of low complexity and zero delay makes this novel proposed approach a very powerful tool not only in PLNC systems but also in many other potential applications.

Lower complexity over DFE means not only cost effectiveness but also leads to a very fast implementation. DFEs tend to have longer FF filters for longer and more selective channels. This makes the proposed equalizer a very important novelty as it totally eliminates this filter and all the delay that comes with it. This is not only true for the DFE but also for the less effective linear equalizers which solely rely on the FF filter.

These new properties are achieved by introducing a new equalization procedure that uses a symbol by symbol maximum likelihood detector and a single feedback filter.

The derivation of the new design depends on the estimated channel coefficients and is explained in detail in this chapter. The application of this new method in an AF PLNC structure is discussed and simulated alongside the one hop DFE BER bound and compared with the previously proposed AF DFE for PLNC systems.

The new method is also applied to the DNF multi-antenna structure and adjusted to work with a single antenna for more cost reduction. The effect of error propagation is shown through simulation and the theoretical BER is derived for the case of correct feedback with no error propagation. These new configurations are compared to the OFDM PLNC system in terms of BER performance.

5.2 Problem Description

The main problem to be solved in this thesis is to implement a successful PLNC system when the channels are frequency selective. In this chapter, this is done by exploring some other equalization options that fit with the needs of the PLNC system. The solution must have the following qualities or most of them.

The solution must be cost effective and this can be achieved through a low complexity design avoiding iterative methods or computational demanding techniques like the MLSD.

The system must also be compatible with all network configurations with little effect of the channel changes on the resulting performance. As pre-filtering designs have some extra limitations and requirements, they will be avoided in this work. These limitations include that both end nodes require knowledge of the opposing end node's channel coefficients. In this chapter, all the proposed systems do not rely on the channel estimation done in the previous transmission cycle. This enables the relay node to be in the star network formation for example or for it to be shared by more than one pair of end nodes.

To have a better BER performance, the work is restricted to time domain equalization. This enables the use of non-linear techniques rather than the FDE which is restricted to linear equalization methods. By doing this, the problems of OFDM systems are also avoided and no cyclic prefix overhead is required.

Another feature of the solution is that this reduced complexity method is also applicable to higher order modulation schemes and works with both AF and DNF techniques.

Finally, the proposed methods do not introduce a delay which is inevitable in all other types of filter-based equalizers whether they are linear or non-linear.

5.3 Maximum Likelihood Detector for DNF PLNC Systems

In this section, the symbol by symbol maximum likelihood detector (MLD) is discussed because it will be an essential building block in the coming sections.

The MLD is considered optimum because it minimizes the probability of error. When the additive noise is Gaussian, the MLD calculates the Euclidean distance between the received symbol and all the possible symbol mappings then selects the minimum value.

The use of the MLD to perform DFN in a two way relay network PLNC system was first proposed in 2008 by T. Koike-Akino et al. [93, 94] where they propose a method to design and optimize the constellations to be used in PLNC systems with flat fading channels. This DNF method is time domain based and therefore it is in line with the work in this thesis. The method was further applied to OFDM systems by B. Jebur and C. Tsimenidis [95].

5.3.1 Uplink Phase

In the uplink phase, the signals are modulated and transmitted from both end nodes through two single tap flat fading channels represented by two scalar numbers, namely $\tilde{h}_1$ and $\tilde{h}_2$.

Let $\mathcal{M}$ denote the constellation mapper of a QPSK modulator. Let the transmitted signals from nodes 1 and 2 be s_1 and s_2 respectively. Then the transmitted signals from these nodes can be written as $x_1 = \mathcal{M}(s_1)$ and $x_2 = \mathcal{M}(s_2)$. These are single symbol data signals in general and contain 2 binary bits for QPSK. The mapper $\mathcal{M}$ uses Gray mapping with unity energy.

Then the received signal at the relay can be written as

$$y_r = \tilde{h}_1 s_1 + \tilde{h}_2 s_2 + w_r, \tag{5.1}$$

where w_r is the AWGN at the relay node with variance σ_w.

5.3.2 DNF at the Relay

At the relay, the received signal y_r is de-noised to a quantised version x_r by using a constellation mapper $\mathcal{M}$ and a de-noising mapper $\mathcal{C}$. This is done by using the maximum

likelihood joint detection.

For simplicity, the constellation mapper $\mathcal{M}$ is assumed to be the same constellation used for QPSK. This does not have to be the case and a more general approach to the constellation design can be found in [94].

The maximum likelihood estimates can be written as

$$(\hat{s}_1, \hat{s}_2) = \underset{(s_1,s_2)\in\mathbb{Z}_4\times\mathbb{Z}_4}{\operatorname{argmin}} \left| y_r - \left(\tilde{h}_1 \mathcal{M}(s_1) + \tilde{h}_2 \mathcal{M}(s_2) \right) \right|^2, \tag{5.2}$$

where the integer set $\mathbb{Z}_4 = \{\ 1,\ 2,\ 3,\ 4\ \}$ and $\hat{s}_1$ and $\hat{s}_2$ are the estimates of s_1 and s_2 respectively. The network coded symbol to be transmitted s_r is calculated from these estimates using the de-noising map $\mathcal{C}$. The transmitted symbol can be written as $s_r = \mathcal{C}(\hat{s}_1, \hat{s}_2)$. The de-noised symbol can then be calculated using the constellation mapper, i.e. $x_r = \mathcal{M}(s_r)$.

5.3.3 Downlink Phase

In this phase, the de-noised symbol is broadcasted to both end nodes. As both end nodes use the same procedure, we can consider only node 1.

For simplicity and without loss of generality, the single tap flat fading channel in the downlink phase $\tilde{h}_1$ is assumed to be unchanged. Then the received symbol at node 1 can be written as

$$y_1 = \tilde{h}_1 x_1 + w_1, \tag{5.3}$$

where w_1 is the AWGN at node 1.

Then, node 1 can use the knowledge of the sent symbol s_1 to estimate the desired symbol s_2 as follows

$$\hat{s}_2 = \underset{s_1\in\mathbb{Z}_4}{\operatorname{argmin}} \left| y_1 - \tilde{h}_1 \mathcal{M} \left(\mathcal{C}(s_1, s) \right) \right|^2. \tag{5.4}$$

Similarly, node 2 can use the same method to estimate the desired symbol using its knowledge of the transmitted symbol s_2.

5.4 MLDF Equalizer

In this section, the basic idea of the maximum likelihood decision feedback equalizer (MLDF) is discussed in a point to point scenario. This idea is further extended to the PLNC system with AF and DNF relaying methods.

The unwanted ISI depends on the multipath channel coefficients and the previously transmitted symbols. If the exact values of the previously transmitted symbols were known at the receiver, then they could be used to cancel the ISI assuming we have perfect channel estimation. While this is not the case, the estimation of the previous symbols can be used instead.

In the case of the DFE, the design makes use of these estimated symbols for equalization alongside the received observations. This is the core idea of the DFE which makes it different and more efficient than linear equalizers. The assumption that the estimated symbols are correct is essential to the derivation of the DFE and influences the design equations and performance. The only way to take the effect of these estimations into account is by using a feedback filter.

A similar approach is used in the proposed MLDF equalizer but in a different way. The DFE depends basically on the feed forward filter to do the job of equalization and only uses the previous estimates to fine tune the resulting signal from the feed forward filter.

In the proposed design, the feed forward filter is removed. Instead, the estimates are directly involved in attempting to eliminate the ISI.

5.4.1 Motivation and Advantages

Increasing interest in communication technology makes developing less complex systems more demanded [97]. In this context, the new proposed design has two main objectives. First, the design of the DFE is to be simplified. This does not only mean that the feed forward filter is lifted, but also the design equations are made simpler which leads to lower computational complexity and eventually a fast implementation method. The second objective is to remove the potential delay that can be caused by the conventional DFE and linear equalizers.

Every signal passing through an FIR filter will inevitably suffer from a delay which is imposed by that filter. This delay is due to the very structure of the FIR filter itself and is usually equal to half the filter length or even more. In the OFDM system for example, the

delay is more than the filter length. This is because the receiver has to wait for the whole data frame to arrive before the receiver can start to perform the FFT not to mention the added cyclic prefix.

As both the linear equalizer and the DFE have a feed forward filter, then they will only result in a delayed output signal.

Achieving low delay is important by itself in some applications like real-time speech communication system but this is not the only motive for such a requirement. An equalizer with a delay can also prevent some types of designs in the case of PLNC as will be discussed in this chapter.

5.4.2 Derivation of the MLDF Design Equations

The section provides the derivation of the design equations for a single hop MLDF equalizer. This design will be extended to the case of two users in a PLNC scenario in Section (5.6.1).

Consider a single communication channel represented by a channel vector $\mathbf{h}$. When a signal s passes through this channel, the received signal $y(k)$ at time k will be

$$y(k) = \mathbf{h}(0)s(k) + \sum_{m=1}^{L_h-1} \mathbf{h}(m)s(k-m) + w(k), \tag{5.5}$$

where w is the AWGN and L_h is the channel length.

Then at $k = 0$ there will be no ISI as $s(0)$ is the first transmitted symbol and is not preceded by other symbols and the equation becomes

$$y(0) = \mathbf{h}(0)s(0) + w(0). \tag{5.6}$$

This symbol can be estimated in a straight forward fashion using the MLD provided that the channel coefficient $\mathbf{h}(0)$ is known and the estimated symbol can be found using equation (5.4) as follows

$$\hat{s}(0) = \underset{s_0 \in \mathbb{Z}_4}{\operatorname{argmin}} \left| y(0) - \mathbf{h}(0)\mathcal{M}(s_0) \right|^2. \tag{5.7}$$

At time $k = 1$, the received signal in equation (5.5) becomes

$$y(1) = \mathbf{h}(0)s(1) + \mathbf{h}(1)s(0) + w(1). \tag{5.8}$$

In the last equation, we can substitute the known channel coefficients and replace $s(0)$ by the previously estimated value $\hat{s}(0)$. Doing this leaves us with only s_1 which can be estimated by the MLD.

Following the same method, the second estimated symbol becomes

$$\hat{s}(1) = \underset{s_0 \in \mathbb{Z}_4}{\operatorname{argmin}} \left| y(1) - \mathbf{h}(1)\hat{s}(0) - \mathbf{h}(0)\mathcal{M}(s_0) \right|^2 . \tag{5.9}$$

The same procedure can be used for all the following symbols. In general, for $k = l$ and $l < L_h$, equation (5.5) becomes

$$y(l) = \mathbf{h}(0)s(l) + \sum_{m=1}^{l-1} \mathbf{h}(m)s(l-m) + w(l). \tag{5.10}$$

For $k = l$ and $l > L_h$, the second term takes the full length of the number of channel taps excluding the first coefficient. In this case, equation (5.5) becomes

$$y(l) = \mathbf{h}(0)s(l) + \sum_{m=1}^{L_h-1} \mathbf{h}(m)s(l-m) + w(l). \tag{5.11}$$

Examining the last equation shows that only $L_h - 1$ previous symbols are involved in finding $y(l)$ no matter how many symbols have preceded it. Using the MLD to estimate $\hat{s}(l)$ in the same way as before leads to

$$\hat{s}(l) = \underset{s_0 \in \mathbb{Z}_4}{\operatorname{argmin}} \left| y(l) - \sum_{m=1}^{L_h-1} \mathbf{h}(m)\hat{s}(l-m) - \mathbf{h}(0)\mathcal{M}(s_0) \right|^2 . \tag{5.12}$$

In this equation, the unknown previous symbols have been replaced by the corresponding estimates.

To implement this idea, the ISI term in equation (5.12) has the same structure of a linear FIR filter but starting from $\mathbf{h}(1)$ instead of $\mathbf{h}(0)$.

Define H_{ML} as the FIR filter with coefficients $\{\, \mathbf{h}(1),\ \mathbf{h}(2),\ \ldots,\ \mathbf{h}(L_h - 1) \,\}$. This filter can generate the Desired ISI term ideally with the exact values of the previous symbols but instead will be replaced by the corresponding estimates. This is translated to a feedback filter with the decisions as its inputs.

According to equation (5.12), the output of the H_{ML} filter is to be subtracted from the received observations before the MLD stage. The block diagram of the resulting equalizer is shown in figure (5.1).

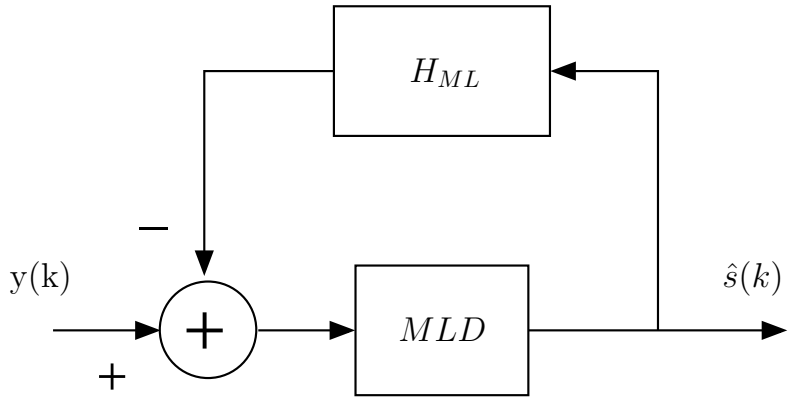

Figure 5.1: Block digram of the proposed MLDF equalizer.

As this figure shows, the equalizer is easy to implement not only because it contains a simple FIR filter but more importantly, the coefficients of this filter are taken directly from the estimated channel coefficients and plugged in excluding the first coefficient. This process removes the matrix inversions required in both the linear and DFE equalizers.

Table 5.1: Signals at different stages of the MLDF.

k	$s(k)$	$y(k)$	$\hat{s}(k)$	MLD input
0	$s(0)$	$\mathbf{h}(0)s(0)$	$\hat{s}(0)$	$y(k)$
1	$s(1)$	$\mathbf{h}(0)s(1)+\mathbf{h}(1)s(0)$	$\hat{s}(1)$	$y(k)-\mathbf{h}(1)\hat{s}(0)$
2	$s(2)$	$\mathbf{h}(0)s(2)+\mathbf{h}(1)s(1)+\mathbf{h}(2)s(0)$	$\hat{s}(2)$	$y(k)-\mathbf{h}(1)\hat{s}(1)-\mathbf{h}(2)\hat{s}(0)$
$\vdots$	$\vdots$	$\vdots$	$\vdots$	$\vdots$
l	$s(l)$	$\mathbf{h}(0)s(l)+\sum_{m=1}^{L_h-1}\mathbf{h}(m)s(l-m)$	$\hat{s}(l)$	$y(k)-\sum_{m=1}^{L_h-1}\mathbf{h}(m)\hat{s}(l-m)$

Table (5.1) further illustrates how this method works. The third column of the table represents the received signal at time k calculated using equation (5.5), while the last column is the input to the MLD. From the last column it is clear how the previous symbols from the preceding rows are being used.

The MLDF equalizer must not be confused for a regular infinite impulse response (IIR) filter. Rather, it is a non-linear device due to the existence of the non-linear MLD at the output.

The feedback signals of the MLDF are $\hat{s}(k) \in \mathcal{M}(s_0)$, where s_0 is the input to the MLD. These output symbols are bounded by definition for any constellation $\mathcal{M}$ including the QPSK under consideration.

5.5 AF System Model

The first step that comes to mind is using the MLDF equalizer in the AF relaying method. When the relay node is to be designed with minimal complexity, the best choice is the AF relaying method. This technique eliminates all computational requirements at the relay and exports them to the end nodes. This can be essential in some applications like wireless sensor networks in which the relay node has limited power and hardware resources.

When both the relay and the end nodes require very low computational complexity, then a system that uses AF relaying with MLDF equalizers can meet this requirement and still have better performance than linear equalizers.

The system model can be described as follows.

5.5.1 Uplink Phase

In the first time interval, the end nodes send the data packets represented by vectors a and b. These packets are convolved with the corresponding channels represented by vectors $\mathbf{h}_1$ and $\mathbf{h}_2$.

Assuming perfect channel estimation and fixed channel during one packet transmission, then the received signal $y(k)$ at time k can be written as

$$\begin{aligned} y(k) = &\sum_{m=0}^{L_1-1} \mathbf{h}_1(m)a(k-m) \\ &+ \sum_{m=0}^{L_2-1} \mathbf{h}_2(m)b(k-m) + w_r(k), \end{aligned} \tag{5.13}$$

where w_r is the uplink noise.

Here we are assuming that both end nodes only have access to their own channel coefficients without the need for the opposite channel information.

5.5.2 Downlink phase

In the AF scheme, the signal is multiplied by a gain g_{AF} and forwarded back to the end nodes.

Let r_1 be the received signal at node 1. This signal can be written in compact matrix form as described in chapter 3 to be

$$r_1 = g_{AF}\mathbf{H}_{11}\mathbf{a} + g_{AF}\mathbf{H}_{12}\mathbf{b} + g_{AF}\mathbf{H}_1\mathbf{w}_r + \mathbf{w}_1, \tag{5.14}$$

where $\mathbf{H}_1$ is the convolutional matrix of channel 1 such that $\mathbf{H}_1\mathbf{w}_r = \mathbf{w}_r * \mathbf{h}_1$ and $\mathbf{H}_{11} = \mathbf{h}_1 * \mathbf{h}_1$ & $\mathbf{H}_{12} = \mathbf{h}_1 * \mathbf{h}_2$ are constructed similarly.

The same approach used in chapter 3 can be used and the bolck diagram of the proposed system is shown in figure (5.2).

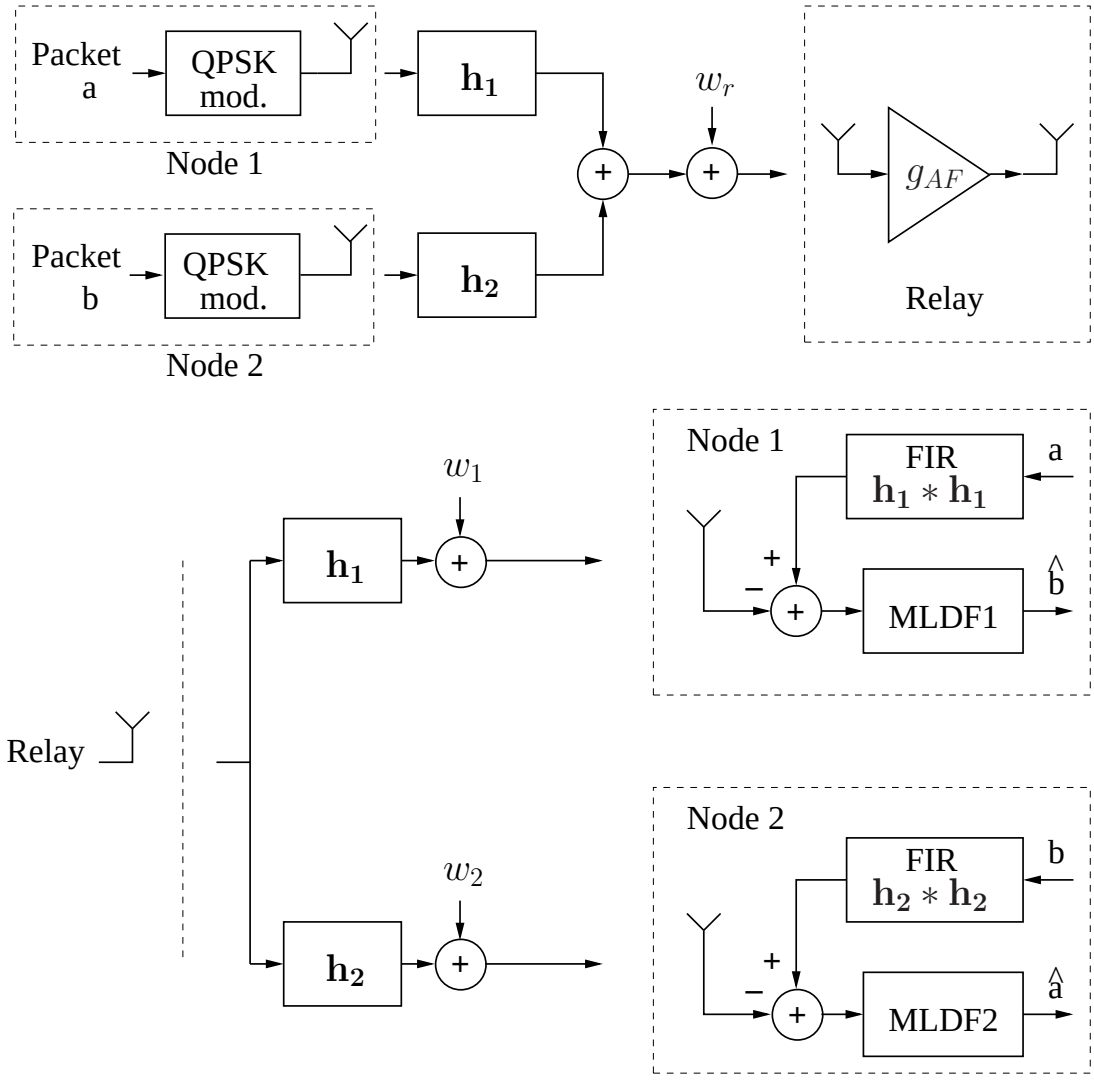

Figure 5.2: Proposed amplify and forward scheme.

The design of both MLDF1 and MLDF2 is the same as the design described in Section

(5.4) by replacing h with $\mathbf{h}_1 * \mathbf{h}_2$.

5.6 MLDF for DNF PLNC Systems

In this section, the application of the MLDF in a DNF PLNC system is discussed. This approach is an attempt to construct lower complexity systems especially at the end nodes while achieving the best possible BER performance as DNF systems in general outperform their AF counterparts.

There are basically two ways to perform this, namely single antenna systems and multi-antenna systems.

The single antenna system offers extra cost effectiveness in addition to the simplicity of the relay node as no combining method is required. Moreover, the DFE system in the previous chapter has only been applied with multi-antennas.

On the other hand, multiple antenna systems can achieve much better performance, simple design and a relatively low complexity at the expense of adding an antenna array with only 4 elements.

5.6.1 Single Antenna Systems

To take the idea of the single hop MLDF one step further, a single MLDF that is able to estimate the PLNC symbols at the relay is proposed here. This is achieved with only one antenna and therefore, the relay receives only one signal at the input.

The same notations used in this thesis will be used here. For example, $\mathbf{h}_1$ and $\mathbf{h}_2$ are used for the channel vectors with lengths L_1 and L_2, w for the noise vector and $\mathcal{M}$ for the QPSK mapping.

5.6.1.1 Uplink Phase

Consider a typical PLNC system in a frequency selective environment. As there will be no pre-processing at the start of the transmission like pre-filtering for example, then the uplink phase will be the same as discussed in previous chapters. In this phase, an overhead is added from both end nodes to perform channel estimation at the relay.

The received signal at the relay will be the same as in equation (5.13).

5.6.1.2 Relay Operation

As in the MLDF, the equalizer design is derived by looking at the received symbol values at each time k as follows.

At time $k = 0$ the symbols $a(0)$ and $b(0)$ arrive from nodes 1 and 2 respectively. These symbols are not preceded by ISI and the received signal at the relay according to equation (5.13) will be

$$y_r(0) = \mathbf{h}_1(0)a(0) + \mathbf{h}_2(0)b(0) + w_r(0). \tag{5.15}$$

At this stage, the problem can be solved by a simple maximum-likelihood joint detection (MLJD).

The ML estimates can be found as follows

$$(\hat{a}(0), \hat{b}(0)) = \underset{(s_1,s_2)\in\mathbb{Z}_4\times\mathbb{Z}_4}{\text{argmin}} \left| y_r(0) - \Big(\mathbf{h}_1(0)\mathcal{M}(s_1) + \mathbf{h}_2(0)\mathcal{M}(s_2)\Big)\right|^2, \tag{5.16}$$

where the estimates $\hat{a}(0)$ and $\hat{b}(0)$ are jointly detected.

At time $k = 1$, the received signal becomes

$$y_r(1) = \mathbf{h}_1(0)a(1) + \mathbf{h}_1(1)a(0) + \mathbf{h}_2(0)b(1) + \mathbf{h}_2(1)b(0) + w_r(1). \tag{5.17}$$

Following the same idea in this chapter, the previous values from end nodes namely, $a(0)$ and $b(0)$ are replaced by the estimates from the previous step $\hat{a}(0)$ and $\hat{b}(0)$ respectively. This leaves us with only two unknown values namely, $a(1)$ and $b(1)$. These two values can be estimated using the MLJD as before which leads to

$$\begin{aligned}(\hat{a}(1), \hat{b}(1)) = \underset{(s_1,s_2)\in\mathbb{Z}_4\times\mathbb{Z}_4}{\text{argmin}} \Big| y_r(0) - \mathbf{h}_1(1)\hat{a}(0) - \mathbf{h}_2(1)\hat{b}(0) \\ - \Big(\mathbf{h}_1(0)\mathcal{M}(s_1) + \mathbf{h}_2(0)\mathcal{M}(s_2)\Big)\Big|^2.\end{aligned} \tag{5.18}$$

The same procedure can be used for the upcoming symbols.

For $k = l$, the received symbol $y_r(l)$ becomes

$$y_r(l) = \mathbf{h}_1(0)a(l) + \mathbf{h}_2(0)b(l) + \sum_{m=1}^{L_1-1} \mathbf{h}_1(m)a(l-m) + \sum_{m=1}^{L_2-1} \mathbf{h}_2(m)b(l-m) + w_r(l). \tag{5.19}$$

Using the MLJD to estimate $\hat{a}(l)$ and $\hat{b}(l)$ in the same way as before leads to

$$(\hat{a}(1), \hat{b}(1)) = \underset{(s_1,s_2)\in\mathbb{Z}_4\times\mathbb{Z}_4}{\text{argmin}} \Big| y_r(0) - \sum_{m=1}^{L_1-1} \mathbf{h}_1(m)a(l-m) - \sum_{m=1}^{L_2-1} \mathbf{h}_2(m)b(l-m) - \Big(\mathbf{h}_1(0)\mathcal{M}(s_1) + \mathbf{h}_2(0)\mathcal{M}(s_2)\Big)\Big|^2. \tag{5.20}$$

In this equation, the unknown previous symbols have been replaced by the corresponding estimated symbols. Also, at any point in time, the summations involve only a limited number of terms corresponding to the channel lengths L_1 and L_2.

The two ISI terms can be removed in the same way as in the MLDF but this time with two FIR filters with the inputs being the two estimated symbols.

Define H_{ML1} and H_{ML2} as the FIR filters with coefficients $\{\, \mathbf{h}_1(1),\, \mathbf{h}_1(2),\, \ldots,\, \mathbf{h}_1(L_1-1) \,\}$ and $\{\, \mathbf{h}_2(1),\, \mathbf{h}_2(2),\, \ldots,\, \mathbf{h}_2(L_2-1) \,\}$ respectively.

According to equation (5.20), the outputs of these filters are to be subtracted from the received observations before the MLD stage. The block diagram of the resulting relay is shown in figure (5.3).

After performing the filtering and MLJD the rest is straight forward. The two estimated symbols are added and broadcasted back to the end nodes. By decoding the symbols with the MLJD, the relay is performing a DNF operation.

5.6.1.3 Downlink Phase

In this phase, the signals will once again suffer the effect of the channels after they are broadcasted by the relay node.

At this point, the end nodes have a wide choice of equalizers to choose from and are not restricted to the MLDF. This means that the core operation of the single antenna DNF PLNC system is performed at the relay.

For better performance, the DFE offers a reasonable complexity but the linear and

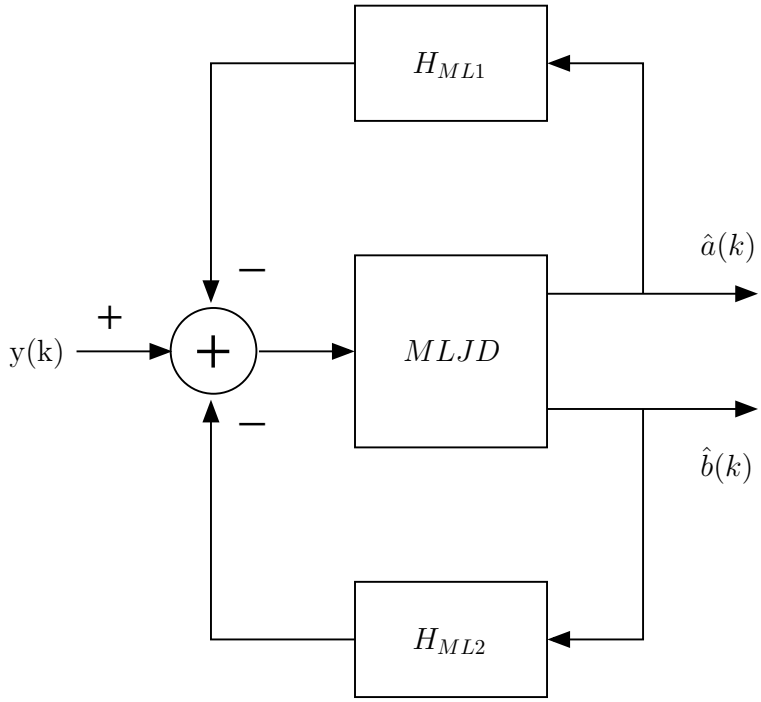

Figure 5.3: Block diagram of the relay for the single antenna MLJD-PLCN system.

MLDF equalizers are also possible.

After a simple one hop equalizer, the sent packet is subtracted to extract the desired packet similar to the normal PLNC system.

5.6.2 Theoretical BER Performance of the Single Antenna System

In this section, the theoretical BER performance of the single antenna DNF MLDF system is derived assuming correct feedback symbols.

With the existence of feedback error this formula serves as a lower bound for the BER performance.

Let s_1 and s_2 be the two sent symbols from nodes 1 and 2 respectively. Then the BER at the relay P_{relay} can be written as [98]

$$\begin{aligned} P_{relay} \;=\; & \frac{1}{2}[P(\hat{s}=1|s_1 \oplus s_2 = 0) \\ & + P(\hat{s}=0|s_1 \oplus s_2 = 1)]. \end{aligned} \tag{5.21}$$

When the symbols reach the relay, the effective channel coefficients will only be $\mathbf{h}_1(0)$ and $\mathbf{h}_2(0)$ assuming correct feedback from the two filters in the relay.

For simplicity and without loss of generality, it is assumed that $|\mathbf{h}_1(0)| > |\mathbf{h}_2(0)|$.

Then the BER at the relay can be formulated as

$$\begin{aligned} P_{relay} \;=\; \frac{1}{4}[&P(y_r \in D_{01} \cup D_{10}|(s_1, s_2) = (0, 0)) \\ &+P(y_r \in D_{00} \cup D_{11}|(s_1, s_2) = (0, 1)) \\ &+P(y_r \in D_{00} \cup D_{11}|(s_1, s_2) = (1, 0)) \\ &+P(y_r \in D_{01} \cup D_{10}|(s_1, s_2) = (1, 1))]. \end{aligned} \tag{5.22}$$

where $D_{i,j}$ is the decision region for symbols (i, j) and $i, j \in \{\ 1,\ 2\ \}$. Due to symmetry, this can be written as

$$P_{relay} = \frac{1}{2}(P_X + P_Y), \tag{5.23}$$

where

$$P_X = P[y_r \in D_{00} \cup D_{11}|(s_1, s_2) = (0, 1)], \tag{5.24}$$

and

$$P_Y = P[y_r \in D_{01} \cup D_{10}|(s_1, s_2) = (0, 0)]. \tag{5.25}$$

When the phase shift between $\mathbf{h}_1(0)$ and $\mathbf{h}_2(0)$ is zero, then this leads to [98]

$$\begin{aligned} P_X = \frac{1}{\pi}\int_0^{\frac{\pi}{2}} \exp\left[-\frac{\mathbf{h}_2(0)^2}{2\sigma_w^2 \sin^2\varphi}\right] d\varphi \\ +\frac{1}{\pi}\int_0^{\frac{\pi}{2}} \exp\left[-\frac{(2\mathbf{h}_1(0) - \mathbf{h}_2(0))^2}{2\sigma_w^2 \sin^2\varphi}\right] d\varphi, \end{aligned} \tag{5.26}$$

and

$$\begin{aligned} P_Y = \frac{1}{\pi}\int_0^{\frac{\pi}{2}} \exp\left[-\frac{\mathbf{h}_2(0)^2}{2\sigma_w^2 \sin^2\varphi}\right] d\varphi \\ -\frac{1}{\pi}\int_0^{\frac{\pi}{2}} \exp\left[-\frac{(2\mathbf{h}_1(0) - \mathbf{h}_2(0))^2}{2\sigma_w^2 \sin^2\varphi}\right] d\varphi. \end{aligned} \tag{5.27}$$

Substituting the last two equations in equation (5.23) leads to

$$P_{relay} = \frac{1}{\pi}\int_0^{\frac{\pi}{2}} \exp\left[-\frac{\mathbf{h}_2(0)^2}{2\sigma_w^2 \sin^2\varphi}\right] d\varphi. \tag{5.28}$$

This last equation can be written in terms of the Q function as

$$P_{relay} = Q(\frac{\mathbf{h}_2(0)}{\sigma_w}), \tag{5.29}$$

where

$$Q(x) \triangleq \frac{1}{\pi}\int_0^{\frac{\pi}{2}} \exp\left[-\frac{x^2}{2\sin^2\varphi}\right] d\varphi. \tag{5.30}$$

The last two equations will be verified when compared with the simulated BER performance in the results section.

5.6.3 Multi-Antenna Systems

In this section, the idea of using the MLDF is used with a multi-antenna array to increase the performance. This is done in the same fashion as with the DFE yet it is not necessary in the case of MLFD to achieve a functional system. This means that choosing a single antenna or an antenna array is up to the designer to decide depending on the cost and required BER performance.

As discussed in the previous chapter, the OC method is the method of choice with an array of only 4 elements.

For the system model, a typical two way relay network is considered with single antenna end nodes and a relay with an antenna array. The antenna array consists of N_a elements with a constant distance d between them. Therefore, the received signals at the antenna array will arrive at different time instants. This is translated to a constant phase shift between the elements and its value depends on the DOA.

The downlink phase will be the same as the DNF systems described before. Therefore only the uplink and relay operation will be discussed in the next subsections.

5.6.3.1 Uplink Phase

Consider two end nodes sending signals $a(k)$ and $b(k)$ with propagation vectors $\mathbf{U}_1$ and $\mathbf{U}_2$. At the relay, the received vector corresponding to the first and second signals will be denoted as $\mathbf{A}(k)$ and $\mathbf{B}(k)$ respectively. These vectors can be written as

$$\mathbf{A}(k) = \mathbf{U}_1 a(k), \tag{5.31}$$

and

$$\mathbf{B}(k) = \mathbf{U}_2 b(k). \tag{5.32}$$

At the relay, each element in the vector $\mathbf{A}(k)$ suffers from the effect of the multi-tap multipath channel $\mathbf{h}_1$ resulting in a convolution between the vectors a and $\mathbf{h}_1$ multiplied by the corresponding element of $\mathbf{U}_1$. This changes the value of each element in $\mathbf{A}(k)$ over time k and the resulting vector is denoted as $\mathbf{A}'(k)$. The same is true for the vector $\mathbf{B}(k)$ regarding its corresponding channel $\mathbf{h}_2$ and the resulting vector is denoted as $\mathbf{B}'(k)$.

Then the received vector becomes

$$\mathbf{Y}(k) = \mathbf{A}'(k) + \mathbf{B}'(k) + \mathbf{W}(k), \tag{5.33}$$

where $\mathbf{W}(k)$ is the independent AWGN vector.

5.6.3.2 Relay Operation

At the relay, the OC method explained in chapter 4 is used in combination with the MLDF.

The overall antenna array MLDF PLNC system is shown in figure (5.4)

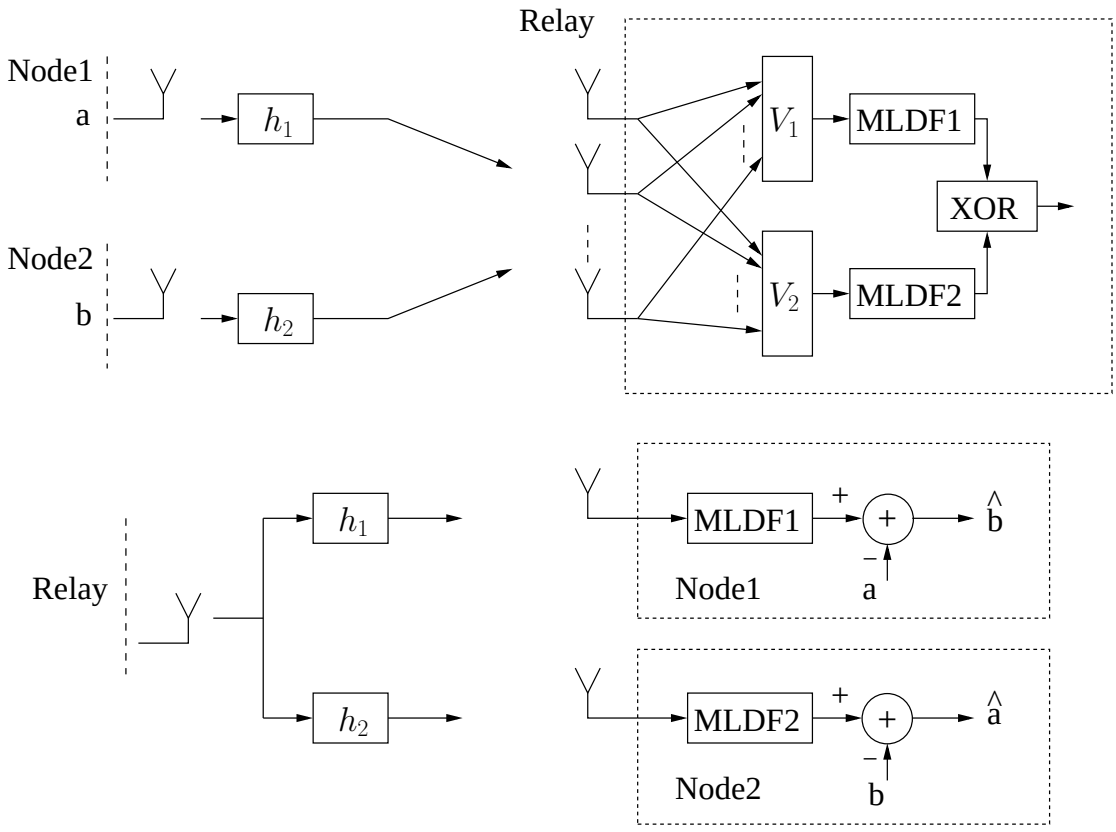

Figure 5.4: Block digram of the proposed muti-antenna MLDF PLNC system.

To find the first combining vector $\mathbf{V}_1$, the following equation derived in the previous chapter is used

$$\mathbf{V}_1 = {\mathbf{R}_{\mathbf{nn1}}}^{-1}\mathbf{U}_1, \tag{5.34}$$

where

$$\mathbf{R_{nn1}} = E\left[(\mathbf{W} + \mathbf{U}_2)\,(\mathbf{W} + \mathbf{U}_2)^*\right]. \tag{5.35}$$

Similarly, $\mathbf{V}_2$ can be calculated using the following equation

$$\mathbf{V}_2 = \mathbf{R_{nn2}}^{-1}\mathbf{U}_2, \tag{5.36}$$

where

$$\mathbf{R_{nn2}} = E\left[(\mathbf{W} + \mathbf{U}_1)\,(\mathbf{W} + \mathbf{U}_1)^*\right]. \tag{5.37}$$

Because the antenna array has only 4 elements, the equations for finding $\mathbf{V}_1$ and $\mathbf{V}_2$ involve only a small matrix inversion of the same size.

At this point, the only thing left is to remove the ISI from each separate channel using the MLDF described in Section (5.4).

The two estimates are then added and broadcasted to both end nodes as shown in figure (5.4).

5.7 OFDM with ML in PLNC Systems

In this section, the OFDM applied to DNF PLNC systems is discussed for comparison. The OFDM is used as a solution to the problem of frequency selective channels. This is due to the fact that the each sub-band in the frequency domain becomes flat. The method of equalization is called frequency domain equalization. This method is limited to linear equalization and therefore, has limited BER performance compared to the more complex time domain methods.

Figure (5.5) shows the block diagram of a basic point to point OFDM system.

This system requires the addition of a cyclic prefix overhead to the transmitted packet. Also, other blocks that may be added for CFO correction or PAPR reduction are not shown in the figure for simplicity.

For a PLNC system, the OFDM signals from both end nodes are physically added at the relay node. Although these two signals pass through different channels, yet the problem is transformed in the frequency domain into the problem of two single symbols multiplied by two single taps or values for each frequency band. Therefore, the MLD can

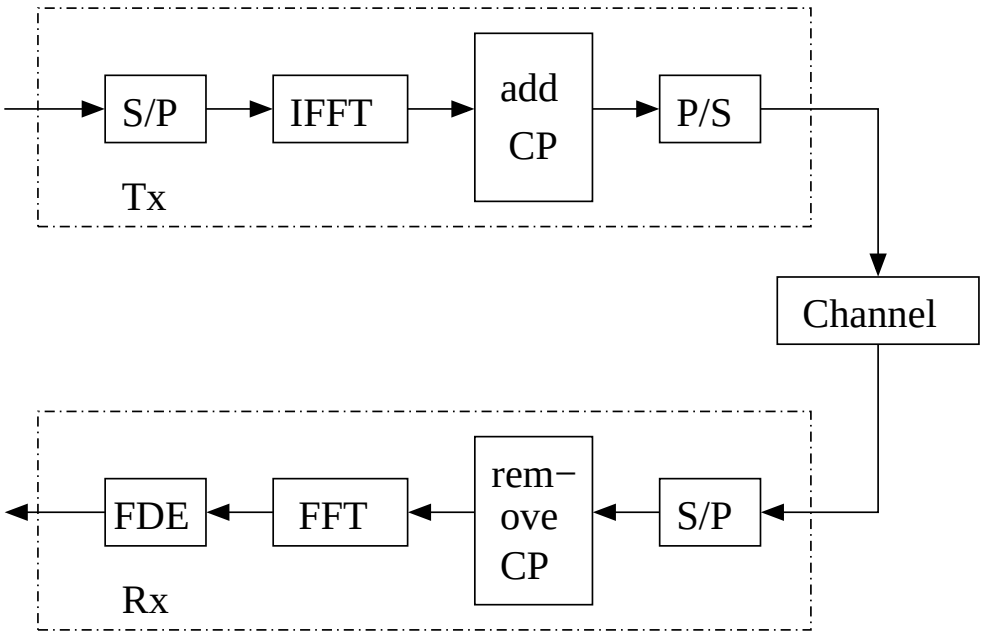

Figure 5.5: Block digram of the point to point OFDM system.

be directly applied at the relay to each frequency band. This can be done after performing the FFT in the previous figure by replacing the FDE block with a MLD.

5.8 Simulation Results

In this section, the simulation results are illustrated for the various proposed systems, comparisons are made and these results are discussed. ITU pedestrian channel A (Ch.102) is used plus the extended pedestrian channel A proposed by leading communication industries [99].

Table 3.1 shows the channel profile for the extended pedestrian channel A.

Assuming the system frequency is 20 MHz, the arrival times are normalized and rounded up to the closest integer with a sampling time of 44 ns.

The BER performance is chosen as the metric for comparison and the simulations are performed for the different PLNC systems using the Monte Carlo method.

The section provides a verification of the performance of the proposed single hop MLDF equalizer. The performance of the proposed AF MLDF system is also shown and both of these cases are compared to the corresponding DFE system.

The theoretical performance of the joint single antenna DNF MLDF is drawn and compared with the simulated BER performance when the correct symbols are fed back. Moreover, the actual BER performance of this system is simulated and compared with the DNF OFDM system.

Table 5.2: Extended pedestrian channel A Profile.

Extended pedestrian channel A		
Path l	Power P_l (dB)	Delay τ_l (μs)
1	0.0	0.0
2	-1	0.03
3	-2	0.07
4	-3	0.09
5	-8	0.11
6	-17.2	0.19
7	-20.8	0.41

Finally, the performance of the multi-antenna DNF MLDF for the PLNC scenario is shown and compared to both the AF MLDF and the DNF DFE systems.

5.8.1 BER Performance of the MLDF vs DFE

The simulation results are started with the simple case of a single hop transmission. Figure (5.6) shows the performances of the proposed MLDF equalizer compared to the efficient DFE when channels A and EPA are used.

For these simulations, the following values were used. $L_1 = 10$ and $L_2 = 10$ for the MLDF. For the DFE, the parameters were $N_{FF} = 64$, $N_{FB} = 4$ and $\Delta = 40$.

From this figure, it is clear that the DFE has better performance. The amount of degradation in the BER depends on the selection of the channels and this is clear from the figure as the difference between the two equalizers increased when the channel was changed from ITU A to channel EPA.

The difference between the MLDF and the DFE can be thought of as the difference between the zero forcing and the linear MMSE equalizers. This is in a sense that the MMSE takes into account the noise level. While this is done to avoid the noise amplification in the MMSE, both the DFE and the MLDF suffer from the error feedback. As the DFE depends on the FF filter, its FB filter can be shorter and therefore is less sensitive to this effect.

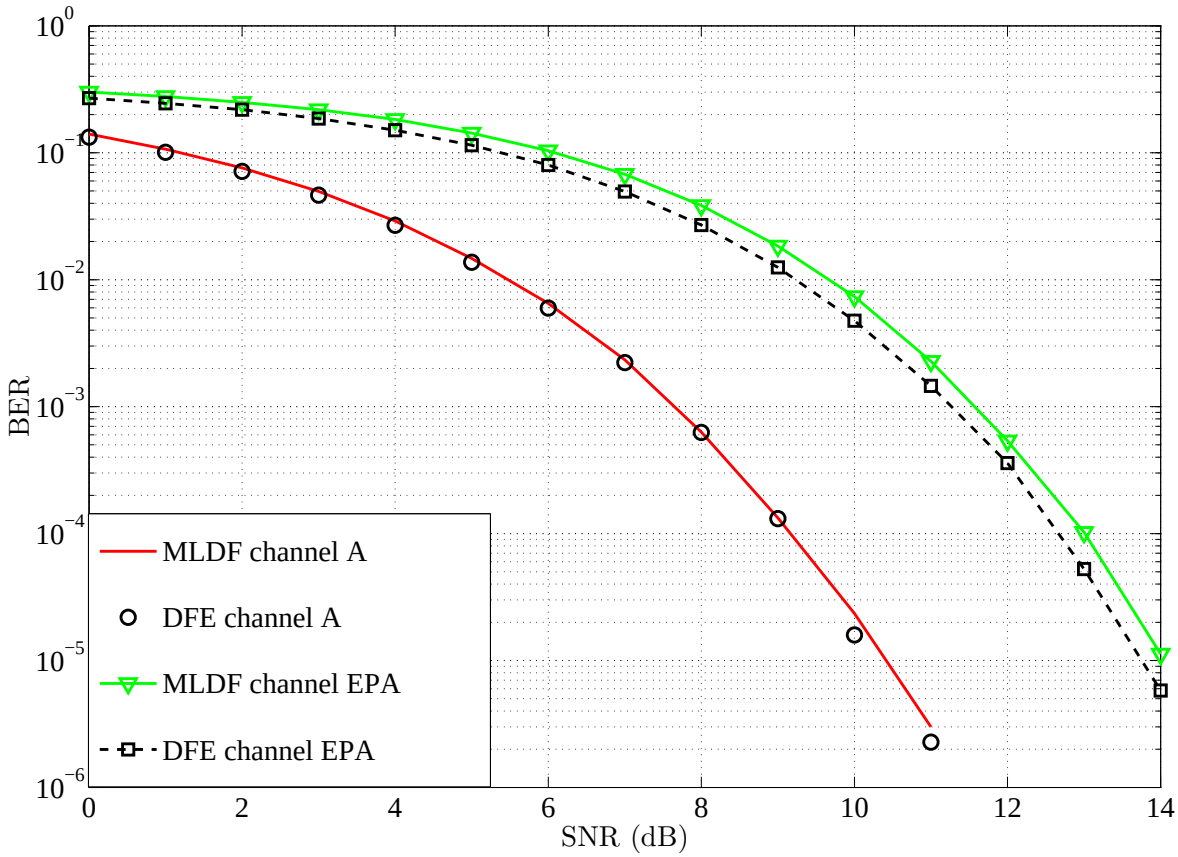

Figure 5.6: BER Performances of the single hop MLDF and DFE equalizers.

5.8.2 BER Performance of the Proposed AF MLDF System

To simulate the performance of the AF MLDF system, the filter size at the end node is set to 18 taps corresponding to the convolution of the two channels and excluding the first as described earlier.

Figure (5.7) shows the simulated E2E BER of a PLNC system using the AF MLDF method alongside the hop MLDF as a benchmark. The figure shows a degradation of about 4 dB at BER = 10^{-3}.

This result is sensitive to the choice of channels. The figure also indicates that the system's performance is greatly enhanced for higher SNR and is similar to a typical non-linear DFE equalizer.

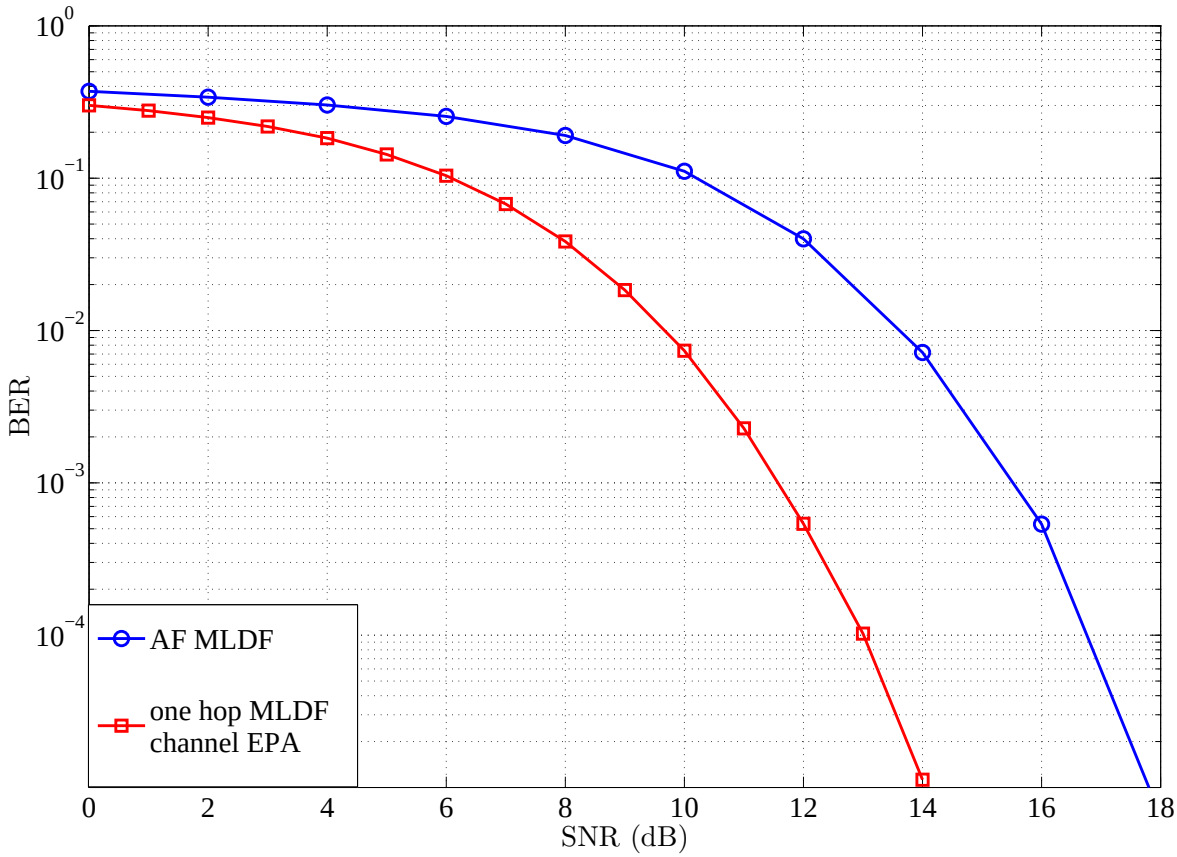

Figure 5.7: Performances of the AF MLDF and one hop MLDF systems.

5.8.3 Comparison of E2E Performances of the AF MLDF and AF DFE Systems

To perform the simulation for the AF DFE, the length of the forward filter is increase to 128 taps as opposed to 64 in the single hop for better results. Also, the feedback filter has 4 taps and $\Delta = 80$, while the end node MLDF has only 18 taps.

For both AF PLNC systems using the DFE and the MLDF, the ITU channel A is used for the downlink phase and the resulting performances are shown in figure (5.8).

From the previous figure, it is clear that only a small degradation has occurred for replacing the equalization scheme. In return, the new system uses a single and much smaller filter at the end node. Moreover, the design of this filter is found directly from the channel estimation of the channels and no complicated matrix inversion is required.

Also both these AF schemes do not perform any calculations at the relay node.

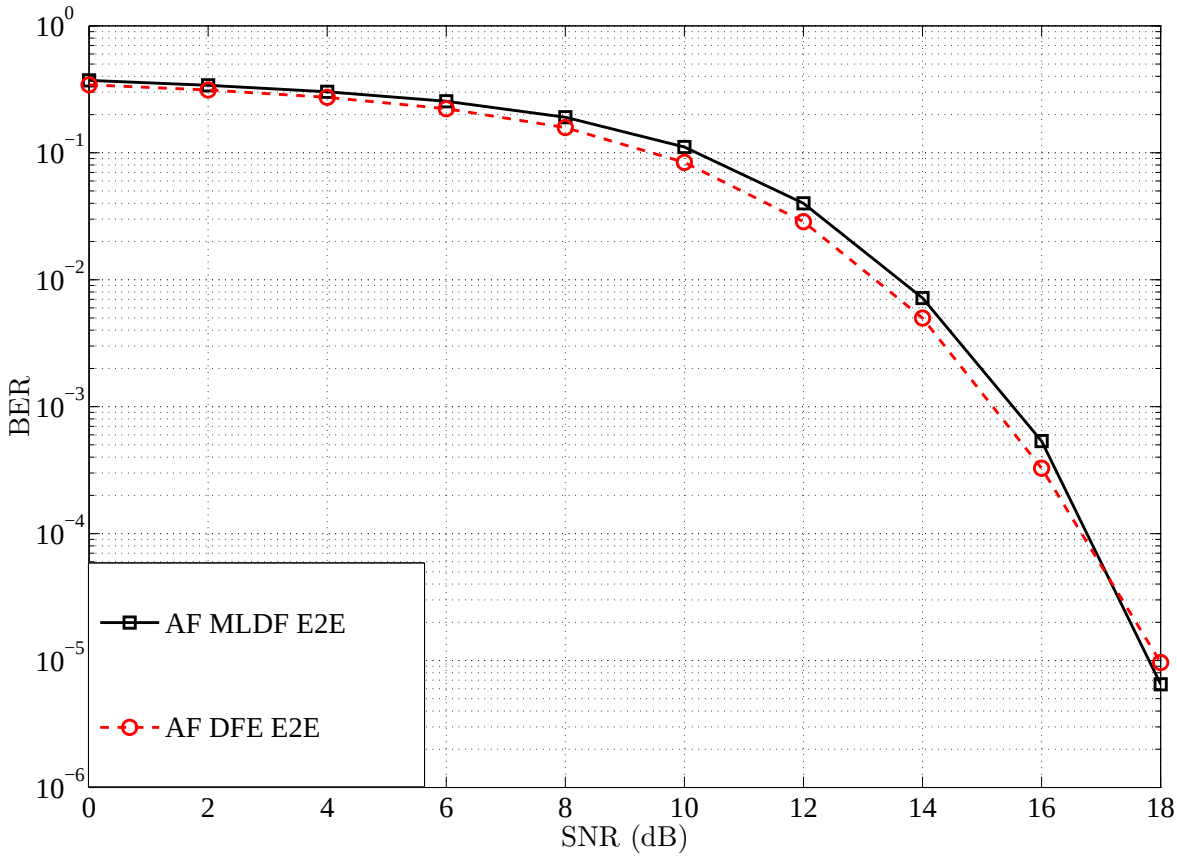

Figure 5.8: E2E performances of the AF MLDF and AF DFE systems.

5.8.4 Performance of Single Antenna DNF MLDF with and without Correct Feedback

Here, the simulated performance of the single antenna DNF MLDF is presented. Both filters used in the relay are small in size and easy to design.

Figure (5.9) shows the performance of a PLNC system at the relay when this method is applied first with the correct symbols being fed back and then with the actual decisions.

The figure shows how sensitive this method is to the feedback error as there is a big difference between the two curves. This is because there are two feedback filters instead of one. This also means that there is room for improving this technique. For example, if coding is used to reduce this feedback error, then the overall effect of coding is expected to be further enhanced.

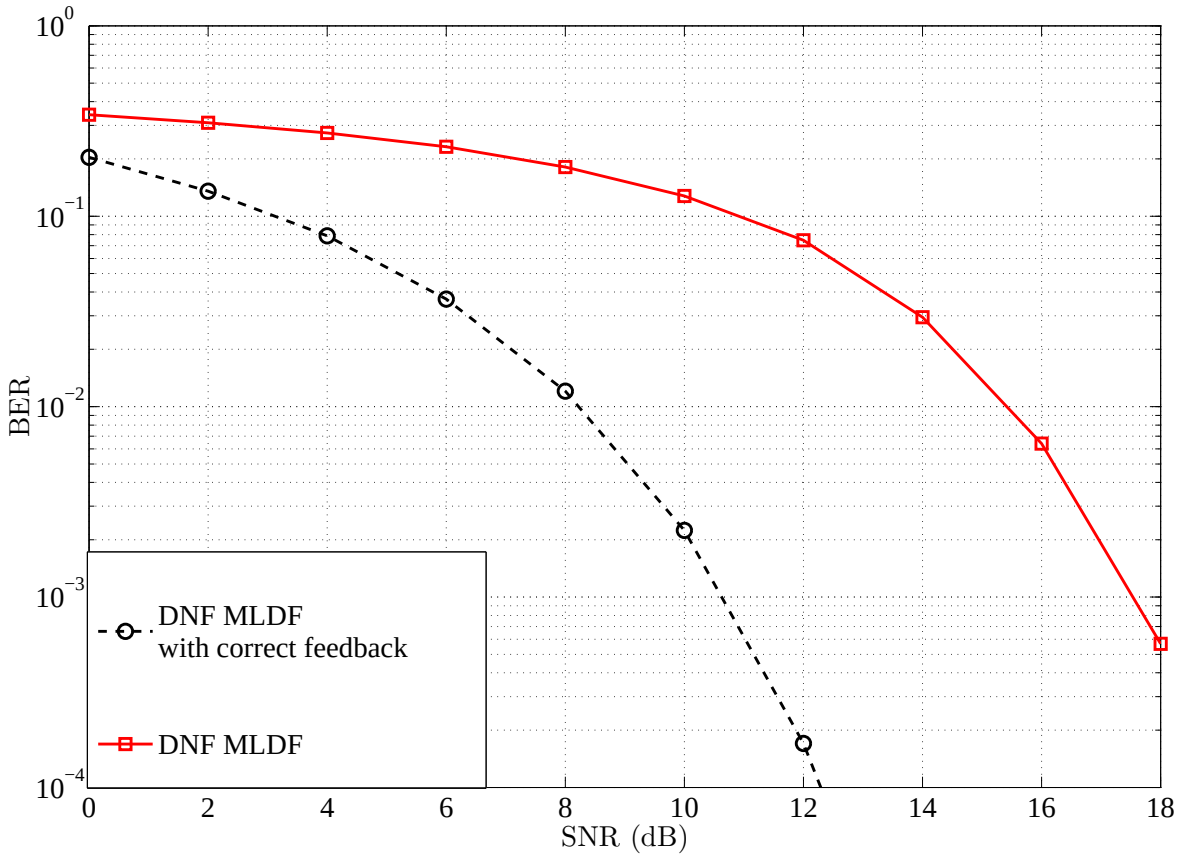

Figure 5.9: Performance of single antenna DNF MLDF with and without correct feedback.

5.8.5 Theoretical Performance of Single Antenna DNF MLDF

For a PLNC system using a single antenna at the relay and applying the DNF MLDF method, the main problem is the feedback error. Without this error, the system theoretically matches that of the single tap flat fading channel system.

Figure (5.10) illustrates how this match is achieved by simulating the DNF MLDF with correct symbol feedback and comparing the performance to the theoretical BER derived in Section (5.6.2) at the relay using the values of the first tap of both channels $\mathbf{h}_1(0) = 0.9431$ and $\mathbf{h}_2(0) = 0.6348$.

The figure shows that the simulated performance closely matches the theoretical BER.

5.8.6 Performance of the Single Antenna MLDF vs OFDM

In this section, the single antenna MLDF is compared with the OFDM PLNC system through simulation. The same design is kept for the MLDF. For the OFDM system, a packet size of 1024 is used with 25% cyclic prefix and the same frequency selective

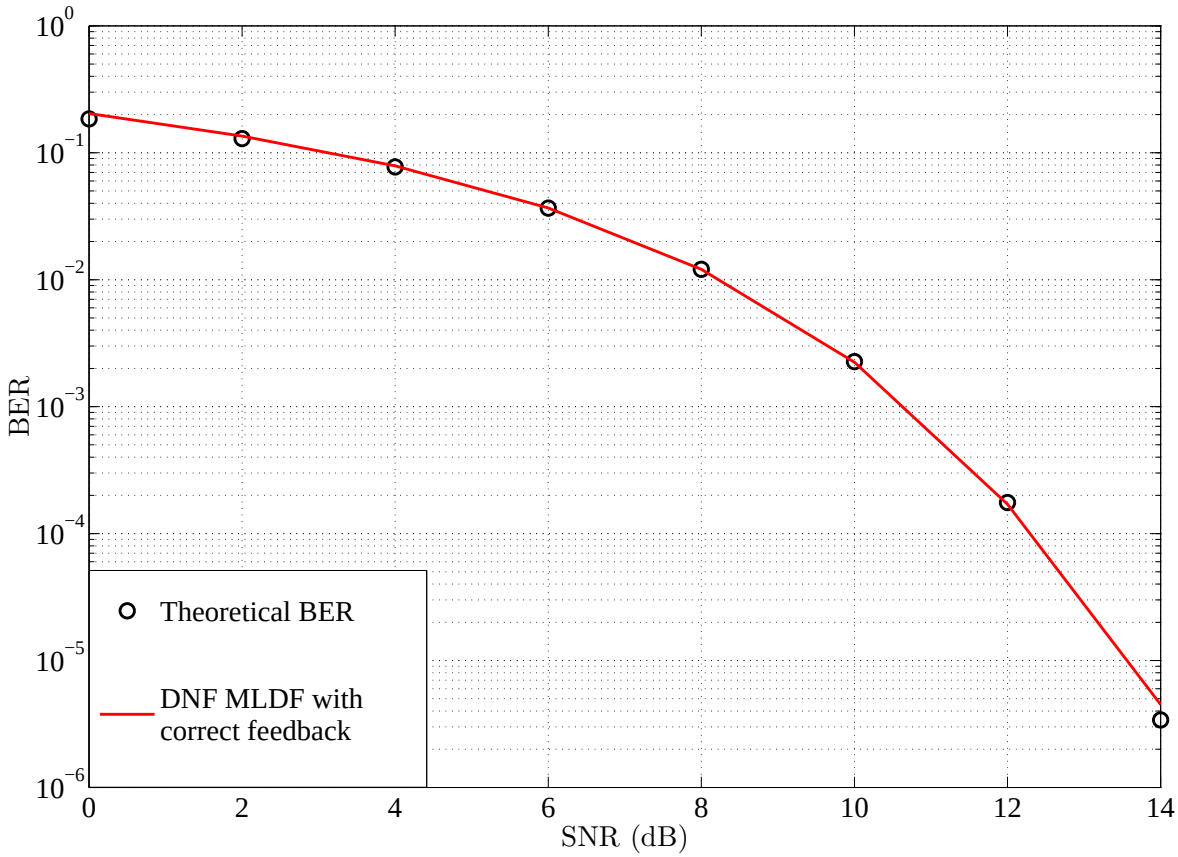

Figure 5.10: Theoretical performances of single antenna DNF MLDF and correct FB MLDF at the relay.

channels used before are used here for both systems.

Figure (5.11) shows the E2E performances of both these systems. From this figure it is clear that both systems have close performances with the MLDF doing better when the SNR is higher than 15 dB.

The DNF MLDF is highly simple compared to other methods, uses only one antenna and cost effective while maintaining better performance than other techniques that use linear equalization especially for high SNR.

5.8.7 Performance of Multi-Antenna DNF MLDF Compared to the DNF DFE System

The DNF MLDF is considered with an antenna array of 4 elements. Both the MLDF and the DFE PLNC systems are simulated with DOAs of $\theta_1 = 50$ and $\theta_2 = 160$. As discussed before, the OC method is used for the combining channel A is selected for the downlink phase in both cases.

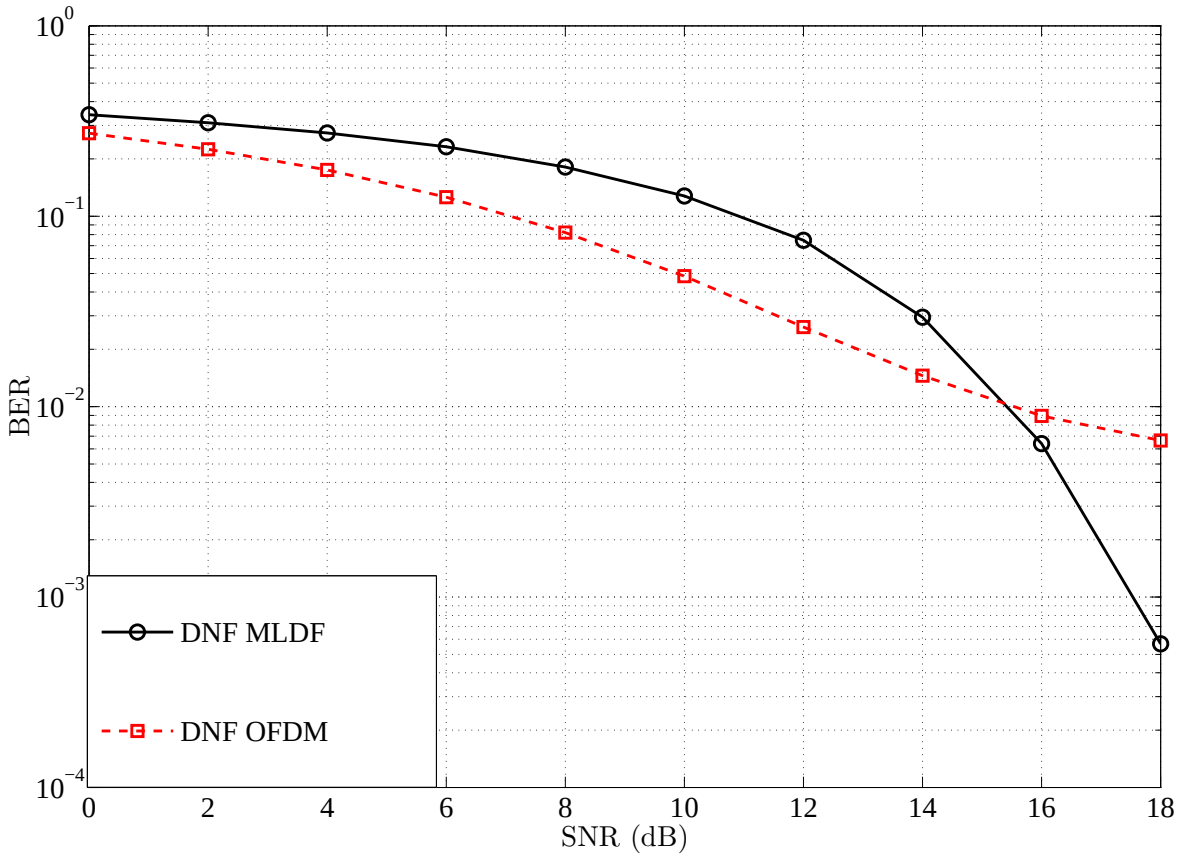

Figure 5.11: Performances of the single antenna MLDF and the OFDM systems.

Figure (5.12) illustrates the performances of these systems.

From this figure it is clear that the two systems have tightly close performances and therefore, the use of the proposed MLDF is highly justified because of its low computational complexity.

5.8.8 Performance of Multi-Antenna DNF MLDF Compared to the AF MLDF System

For the sake of comparison, both the AF and DNF systems using MLDF are shown in figure (5.13).

From this figure it is clear that the DNF outperforms the AF method and therefore, using the multi-antenna DNF is highly recommended in this case.

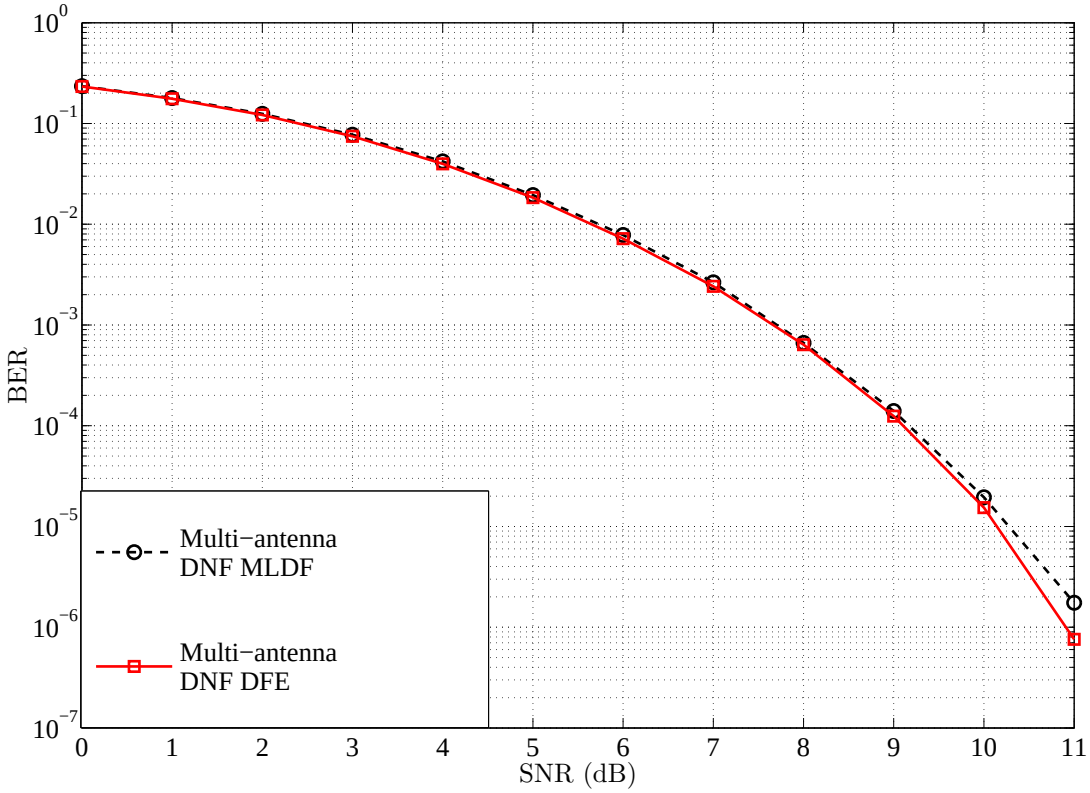

Figure 5.12: Performances of the multi-antenna DNF MLDF and the DNF DFE systems.

5.9 Chapter Summary

This chapter presented an overview of various PLNC systems using the ML technique in frequency selective channels.

First a one hop equalizer with one feedback filter was proposed. This MLDF is then used in both AF and multi-antenna DNF scenarios. Also a more simple single antenna DNF system was proposed. These systems were compared to their DFE counterparts except for the single antenna DNF system which was compared with the OFDM system.

In all of these cases except for the single antenna DNF system, the performance was only slightly degraded. On the other hand these methods offer a fast implementation due to the reduced complexity which in tern makes them cost effective. Moreover, all of the proposed systems do not introduce a time delay which is inevitable in both linear and DFE equalizers.

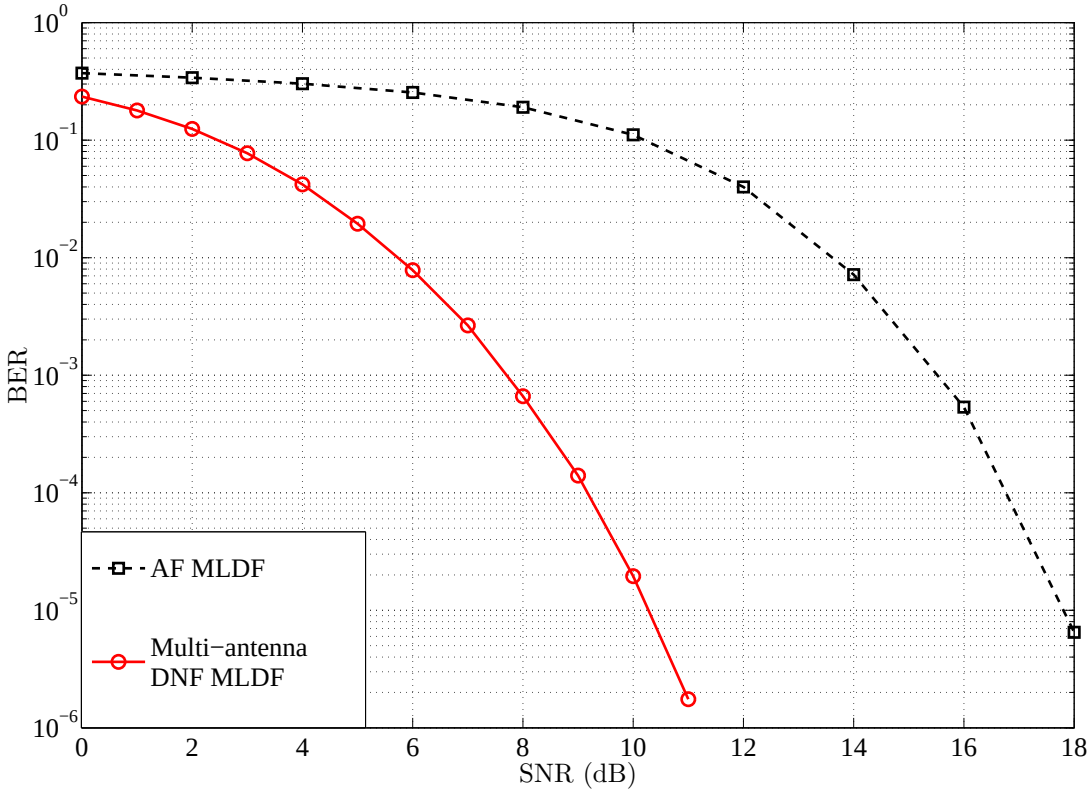

Figure 5.13: Performances of the multi-antenna DNF MLDF and the AF MLDF systems.

Chapter 6

Conclusion and Future Work

6.1 Conclusion

Before the discovery of the PLNC system, it would take 3 time slots to transfer data between two end nodes via a relay node. These systems did not have to worry about co-channel interference as they were using time division multiplexing. To achieve better spectral efficiency, the PLNC system was previously proposed, studied and implemented in flat fading channels. With this type of channel, the signals are allowed to overlap because the expression of the resulting signal is a simple linear combination of the two signals.

Not all channels are flat fading and therefore, the implementation of the PLNC system in a multi-tap multipath channels was previously studied.

There are two solutions proposed in the past for this problem. The first solution is the use of pre-filtering. This approach can be a good solution if the channels are fixed and do not change from packet to another in a simple TWRN. For more complex network configurations, the number of time slots in which the channels have to stay constant is increased. In this case, the system becomes more sensitive to channel variations even for slowly changing channels. Moreover, these types of systems require a feedback channel in order to pass the channel information from one end node to the other.

The second solution is the use of an MLD at the relay with OFDM transmission. This system requires CFO correction and PAPR reduction in addition to cyclic prefix overhead. Moreover, OFDM systems are restricted to FDE which are linear and therefore have lower performance than systems that use TDE methods like the non-linear DFE.

For these reasons, the work is motivated by the lack of a functioning PLNC in a frequency selective environment with less sensitivity to channel changes and better BER performance.

A system with reduced complexity and cost is also one of the aims in this thesis while maintaining as much performance as possible.

In all the proposed systems, great care was taken to keep these systems as simple as possible. This not only helps to reduce the cost, but is also useful in some cases like the importance of the simplicity of the relay node for wireless sensor networks where this node has limited access to power and computational resources.

In this study, some practical aspects are discussed and properly dealt with. For example, the compatibility of the system to different network configurations. Another issue of that kind is that the solutions have to take into account the implementation with higher

order modulation schemes rather than the simple QPSK modulation. The systems must also allow for a simple insertion of coding if needed to increase the BER performance to the desired level.

In chapter 3, the simple AF PLNC system is proposed. This system uses time domain equalization and this enables the utilization of the non-linear DFE. Simple insertion of a DFE into the system does not solve the problem and therefore a modified design was proposed by redesigning the DFE and adding a special FIR filter at the end nodes. The designs of the DFE and the added FIR are analytically derived.

This design has many advantages. For an existing PLNC system, only simple adjustments to the end nodes are required to upgrade the system and enable it to work in frequency selective channels. This is not true for the previous solutions. The proposed system also avoids the problems of FDE and has an enhanced performance through using the optimal non-linear DFE over the linear equalizers used in OFDM systems. Simulations show that the E2E performance of this system is about 2dB away from the performance of a single hop DFE performance for the worst of the two channels, namely channel B at SNR of 10^{-5}. Also, the relay design has minimal complexity because only amplification is required in this case which makes this design attractive for some applications. This work also shows that the proposed system will have better performance compared to the pre-filtering method for an average percentage channel error $r > 5\%$. This is very important because in some network configurations with time delay, the value of r can become high and therefore, pre-filtering will have inferior performance. The system also does not require the feedback channel required in pre-filtering methods.

In chapter 4, a DNF PLNC system is proposed. The main purpose for this is to enhance the BER performance. In DNF systems, the received signal is decoded and mapped to give an estimate of the XOR of the transmitted bits from both end nodes. This acts as a denoising process and therefore, increases the performance of the system compared to AF methods. To achieve this, a linear antenna array is added at the relay. The proposed system uses the OC method for combining the signals and a pair of optimum DFE equalizers at the relay node. In the downlink phase, only a single DFE is used for the one hop equalization at each end node.

The proposed system has the following advantages in addition to the enhanced performance. The proposed system is not sensitive to channel changes that happen after the first packet transmission. Therefore, it is compatible to network configurations with time delays. The method is not iterative and therefore, has a reduced computational complex-

ity and cost compared to trellis based methods for example. This is true not only due to the iterative nature of the trellis based equalization, but also the complexity increases when higher order modulation is used while this does not have an effect on the proposed method.

Simulation results show that the proposed method outperforms both the pre-filtering and the OFDM PLNC with or without channel changes. A comparative study was also done to choose the best combining method and the required number of antenna elements.

Chapter 5 presents several new techniques that solve the problem of PLNC systems in frequency selective channels with an emphasis on reducing the system complexity. The proposed systems maintain most of the previous advantages like compatibility, non-linearity and working with higher modulation schemes. This is done by introducing the novel MLDF equalizer which is not only less complex but also does not impose a delay like the DFE and linear equalizers. These properties facilitate a fast implementation of the PLNC system.

The single hop MLDF equalizer is proposed for fast implementation and delay cancellation. The MLDF design is derived and the simulation results show that it is only a fraction of a dB behind the powerful DFE when channel EPA is used.

The new MLDF is then used in an AF PLNC configuration similar to the previously proposed AF DFE system. Simulation results show that the new system is also close to the performance of the DFE system but with a big reduction in complexity and with no delay. This method maintains the advantages of the AF DFE system like the simplicity of the relay node, non-iterative scheme, TDE and it does not require a feedback channel.

The next step was proposing the single antenna DNF PLNC using the MLJD method. This is the simplest and less complex of all the proposed systems yet there is still room for improving its BER performance. The theoretical performance of the system is derived for correct feedback signals and the simulation results verify the derived performance equation.

Finally, a multi-antenna DNF PLNC system was proposed using the OC method for combining and MLDF for equalization. This system is also provides a fast implementation and one without delay. The performance of this system almost matches that of the DFE implementation.

6.2 Future work

In this work, There were a number of suggestions to implement a PLNC system in a frequency selective environment. Nevertheless, several aspects need more study and can provide a good opportunity for further research.

All the proposed systems were inclined to non-iterative methods. If a higher BER performance is required, then a reasonable complexity iterative procedure can be investigated to achieve that goal.

The proposed MLDF method compared to the DFE can be viewed as the relationship between the linear ZFE and the MMSE equalizer in a sense that it does not take into account the effect of the noise. This means that a more advanced MLDF design can be possible in which the noise level is considered while keeping the low complexity and zero delay of the MLDF.

Another approach to potentially refine the MLDF design is to study the case of soft feedback or other similar approaches that have been successfully applied to the DFE in order to enhance the performance.

The studied scenarios only cover the AF and DNF schemes. A more recent compute and forward scheme can be used to enable the implementation of a PLNC system in frequency selective channels in a different and possibly a more efficient way.

Throughout this work, the performance was evaluated for the systems without coding. Therefore, more research is required to evaluate the proposed systems with coding and to determine the best suitable method to achieve this.

Regarding the single antenna with MLJD, the derived theoretical performance indicates that if the feedback is correct, then the BER performance can match that of a flat fading PLNC system. This limit represents the best case scenario for a system with multi-tap channels. This observation can open a range of possibilities for future work. For example, the feedback signals can be corrected with coding and therefore can double the benefit of coding on the system.

Another approach would be to take the idea of the MLJD to the next level by making use of the estimated symbol at the relay for one user and then use it to help the other user in achieving a better estimate. This idea is not feasible with other equalization methods because of the delay between the arrival of the received signal and the time it takes the equalizer to generate an estimate.

In this work, the systems were assumed to have perfect synchronization. As future

work, the study of the effect of imperfect synchronization on the proposed methods is needed and the existing research of synchronization on the conventional PLNC serve as a starting point.

Finally, a study is needed on the effect of using other channel models. For example, in the MLDF case, the method is sensitive to the value of the first tap or the line of sight compared to the rest of the channel taps. This means that the study of the system in Rician fading channels is relevant.

References

[1] S. Younis, “Synchronization algorithms and architectures for wireless ofdm systems,” Ph.D. dissertation, Newcastle University, 3 2012.

[2] S. Zhang, S. C. Liew, and P. P. Lam, “On the synchronization of physical-layer network coding,” in *2006 IEEE Information Theory Workshop - ITW ’06 Chengdu*, Oct 2006, pp. 404–408.

[3] S. Katti, S. Gollakota, and D. Katabi, “Embracing wireless interference: Analog network coding,” *SIGCOMM Comput. Commun. Rev.*, vol. 37, no. 4, pp. 397–408, Aug. 2007.

[4] J. Elson, L. Girod, and D. Estrin, “Fine-grained network time synchronization using reference broadcasts,” *SIGOPS Oper. Syst. Rev.*, vol. 36, no. SI, pp. 147–163, Dec. 2002. [Online]. Available: http://doi.acm.org/10.1145/844128.844143

[5] M. Morelli, “Timing and frequency synchronization for the uplink of an ofdma system,” *IEEE Transactions on Communications*, vol. 52, no. 2, pp. 296–306, Feb 2004.

[6] S. Zhang, S. C. Liew, and P. P. Lam, “Hot topic: Physical-layer network coding,” in *Proceedings of the 12th Annual International Conference on Mobile Computing and Networking*, ser. MobiCom ’06. New York, NY, USA: ACM, 2006, pp. 358–365.

[7] L. Lu and S. C. Liew, “Asynchronous physical-layer network coding,” *IEEE Transactions on Wireless Communications*, vol. 11, no. 2, pp. 819–831, February 2012.

[8] Y. Li and F. C. Zheng, “A simple physical-layer network coding with fractional delay,” in *2013 IEEE/CIC International Conference on Communications in China (ICCC)*, Aug 2013, pp. 543–547.

[9] V. Tarokh, N. Seshadri, and A. R. Calderbank, "Space-time codes for high data rate wireless communication: performance criterion and code construction," *IEEE Transactions on Information Theory*, vol. 44, no. 2, pp. 744–765, Mar 1998.

[10] R. Ahlswede, N. Cai, S.-Y. Li, and R. Yeung, "Network information flow," *IEEE Trans. Inf. Theory*, vol. 46, no. 4, pp. 1204–1216, Jul 2000.

[11] R. Koetter and M. Medard, "An algebraic approach to network coding," *IEEE/ACM Transactions on Networking*, vol. 11, no. 5, pp. 782–795, Oct 2003.

[12] S. Jaggi, P. Sanders, P. A. Chou, M. Effros, S. Egner, K. Jain, and L. M. G. M. Tolhuizen, "Polynomial time algorithms for multicast network code construction," *IEEE Transactions on Information Theory*, vol. 51, no. 6, pp. 1973–1982, June 2005.

[13] S. Y. R. Li, R. W. Yeung, and N. Cai, "Linear network coding," *IEEE Transactions on Information Theory*, vol. 49, no. 2, pp. 371–381, Feb 2003.

[14] S. Katti, H. Rahul, W. Hu, D. Katabi, M. Médard, and J. Crowcroft, "Xors in the air: Practical wireless network coding," *SIGCOMM Comput. Commun. Rev.*, vol. 36, no. 4, pp. 243–254, Aug. 2006. [Online]. Available: http://doi.acm.org/10.1145/1151659.1159942

[15] J. s. Park, M. Gerla, D. S. Lun, Y. Yi, and M. Medard, "Codecast: a network-coding-based ad hoc multicast protocol," *IEEE Wireless Communications*, vol. 13, no. 5, pp. 76–81, October 2006.

[16] L. You, S. C. Liew, and L. Lu, "Reliable physical-layer network coding supporting real applications," *IEEE Transactions on Mobile Computing*, vol. PP, no. 99, pp. 1–1, 2016.

[17] S. Zong and S. Gao, "Analysis of physical-layer network coding over asymmetric two-way relay channel with carrier frequency offset," in *2015 IEEE/CIC International Conference on Communications in China (ICCC)*, Nov 2015, pp. 1–5.

[18] Q. Y. Yu, D. Y. Zhang, H. H. Chen, and W. X. Meng, "Physical-layer network coding systems with mfsk modulation," *IEEE Transactions on Vehicular Technology*, vol. 65, no. 1, pp. 204–213, Jan 2016.

[19] B. Nguyen, D. Haley, Y. Chen, and T. Chan, "Approach to frame-misalignment in physical-layer network coding," in *2015 IEEE International Conference on Acoustics, Speech and Signal Processing (ICASSP)*, April 2015, pp. 3123–3127.

[20] X. Wang and Q. Zhao, "Synchronization analysis of physical-layer network coding in lte system," in *2014 IEEE 25th Annual International Symposium on Personal, Indoor, and Mobile Radio Communication (PIMRC)*, Sept 2014, pp. 247–252.

[21] Y. Huang, S. Wang, Q. Song, L. Guo, and A. Jamalipour, "Synchronous physical-layer network coding: A feasibility study," *IEEE Transactions on Wireless Communications*, vol. 12, no. 8, pp. 4048–4057, August 2013.

[22] R. Liu, G. Wang, and B. Li, "The effect of pulse shaping on the performance of physical-layer network coding with time synchronization errors," in *2013 9th International Conference on Information, Communications Signal Processing*, Dec 2013, pp. 1–5.

[23] Y. Huang, Q. Song, S. Wang, and A. Jamalipour, "Phase-level synchronization for physical-layer network coding," in *2012 IEEE Global Communications Conference (GLOBECOM)*, Dec 2012, pp. 4423–4428.

[24] Z. Liu, M. Li, L. Lu, C. K. Chan, S. C. Liew, and L. K. Chen, "Optical physical-layer network coding," *IEEE Photonics Technology Letters*, vol. 24, no. 16, pp. 1424–1427, Aug 2012.

[25] A. H. A. El-Malek and S. A. Zummo, "Cooperative cognitive radio model for enhancing physical layer security in two-path amplify-and-forward relaying networks," in *2015 IEEE Global Communications Conference (GLOBECOM)*, Dec 2015, pp. 1–6.

[26] T. Divya, K. K. Gurrala, and S. Das, "Performance analysis of hybrid decode-amplify-forward (hdaf) relaying for improving security in cooperative wireless network," in *2015 Global Conference on Communication Technologies (GCCT)*, April 2015, pp. 682–687.

[27] H. Lei, L. Guo, and J. Zhang, "Cooperative jamming and beamforming in amplify-and-forward relay systems for physical-layer security," in *2015 11th International Conference on Heterogeneous Networking for Quality, Reliability, Security and Robustness (QSHINE)*, Aug 2015, pp. 99–103.

[28] J. Yang, B. Champagne, Y. Zou, and L. Hanzo, "Mimo af relaying security: Robust transceiver design in the presence of multiple eavesdroppers," in *2015 IEEE International Conference on Communications (ICC)*, June 2015, pp. 4937–4942.

[29] L. Fan, X. Lei, N. Yang, T. Q. Duong, and G. K. Karagiannidis, "Secure multiple amplify-and-forward relaying with cochannel interference," *IEEE Journal of Selected Topics in Signal Processing*, vol. 10, no. 8, pp. 1494–1505, Dec 2016.

[30] A. A. El-Malek, A. Salhab, and S. A. Zummo, "New bandwidth efficient relaying schemes in cooperative cognitive two-way relay networks with physical layer security," *IEEE Transactions on Vehicular Technology*, vol. PP, no. 99, pp. 1–1, 2016.

[31] J. Hamkins, "An analytic technique to separate cochannel fm signals," *IEEE Transactions on Communications*, vol. 48, no. 4, pp. 543–546, Apr 2000.

[32] S. C. Liew, S. Zhang, and L. Lu, "Physical-layer network coding: Tutorial, survey, and beyond," *Physical Communication*, vol. 6, pp. 4 – 42, 2013, network Coding and its Applications to Wireless Communications. [Online]. Available: //www.sciencedirect.com/science/article/pii/S1874490712000419

[33] K. Ravindran, A. Thangaraj, and S. Bhashyam, "High snr error analysis for bidirectional relaying with physical layer network coding," *IEEE Transactions on Communications*, vol. PP, no. 99, pp. 1–1, 2017.

[34] P. Chen, S. C. Liew, and L. Shi, "Bandwidth-efficient coded modulation schemes for physical-layer network coding with high-order modulations," *IEEE Transactions on Communications*, vol. 65, no. 1, pp. 147–160, Jan 2017.

[35] T. Yang, L. Yang, Y. Guo, and J. Yuan, "A non-orthogonal multiple-access scheme using reliable physical-layer network coding and cascade-computation decoding," *IEEE Transactions on Wireless Communications*, vol. PP, no. 99, pp. 1–1, 2017.

[36] F. F. Cao, Q. Y. Yu, W. Xiang, and W. X. Meng, "Ber analysis of physical-layer network coding in the awgn channel with burst pulses," *IEEE Access*, vol. PP, no. 99, pp. 1–1, 2016.

[37] X. Chen, H. Wang, W. Yang, G. Wang, and Z. Yan, "An optimal power allocation for two-way relay channel using physical-layer network coding," in *2016 Sixth Interna-*

tional Conference on Instrumentation Measurement, Computer, Communication and Control (IMCCC), July 2016, pp. 486–491.

[38] J. He and S. C. Liew, "Arq for physical-layer network coding," *IEEE Transactions on Mobile Computing*, vol. 15, no. 7, pp. 1614–1631, July 2016.

[39] X. Li and P. Ho, "A random channel sounding decision feedback receiver for two-way relay communication with pilotless orthogonal signaling and physical-layer network coding," *IEEE Transactions on Vehicular Technology*, vol. 65, no. 5, pp. 3086–3099, May 2016.

[40] H. Zhang, L. Zheng, and L. Cai, "Design and analysis of heterogeneous physical layer network coding," *IEEE Transactions on Wireless Communications*, vol. 15, no. 4, pp. 2484–2497, April 2016.

[41] H. Phan, F. C. Zheng, and T. M. C. Chu, "Physical-layer network coding with multi-antenna transceivers in interference limited environments," *IET Communications*, vol. 10, no. 4, pp. 363–371, 2016.

[42] B. Nguyen, T. Chan, D. Haley, and R. McKilliam, "Using gaussian pulses in physical-layer network coding with symbol misalignment," in *2016 Australian Communications Theory Workshop (AusCTW)*, Jan 2016, pp. 77–82.

[43] Q. Y. Yu, D. Y. Zhang, H. H. Chen, and W. X. Meng, "Physical-layer network coding systems with mfsk modulation," *IEEE Transactions on Vehicular Technology*, vol. 65, no. 1, pp. 204–213, Jan 2016.

[44] X. Dang, Z. Liu, B. Li, and X. Yu, "Noncoherent multiple-symbol detector of binary cpfsk in physical-layer network coding," *IEEE Communications Letters*, vol. 20, no. 1, pp. 81–84, Jan 2016.

[45] Q. Yang, H. Wang, T. Wang, L. You, L. Lu, and S. C. Liew, "Powerline-pnc: Boosting throughput of powerline networks with physical-layer network coding," in *2015 IEEE International Conference on Smart Grid Communications (SmartGridComm)*, Nov 2015, pp. 103–108.

[46] S. Ustunbas and U. Aygolu, "Ber analysis of physical-layer coding in cognitive radio cross network," in *2016 Advances in Wireless and Optical Communications (RTUWO)*, Nov 2016, pp. 173–176.

[47] S. Hatamnia, S. Vahidian, S. Aissa, B. Champagne, and M. Ahmadian-Attari, "Network-coded two-way relaying in spectrum sharing systems with quality-of-service requirements," *IEEE Transactions on Vehicular Technology*, vol. PP, no. 99, pp. 1–1, 2016.

[48] P. G. S. Velmurugan and S. J. Thiruvengadam, "Bit error rate analysis of plnc based cognitive radio relay systems in multi-source multi-destination scenario," in *2014 Annual IEEE India Conference (INDICON)*, Dec 2014, pp. 1–6.

[49] M. Hafeez and J. M. H. Elmirghani, "Dynamic spectrum leasing for beamforming cognitive radio networks using network coding," in *2013 IEEE International Conference on Communications (ICC)*, June 2013, pp. 2840–2845.

[50] J. Liu, G. Kang, Y. Zhu, Y. Zhao, and J. Mao, "Optimal energy-efficient relay selection and power allocation for cognitive two-way relay network using physical-layer network coding," in *2013 IEEE 78th Vehicular Technology Conference (VTC Fall)*, Sept 2013, pp. 1–5.

[51] H. M. Nguyen, V. B. Pham, X. N. Tran, and T. N. Tran, "Channel quantization based physical-layer network coding for mimo two-way relay networks," in *2016 International Conference on Advanced Technologies for Communications (ATC)*, Oct 2016, pp. 197–203.

[52] J. S. Lemos and F. A. Monteiro, "Full-duplex massive mimo with physical layer network coding for the two-way relay channel," in *2016 IEEE Sensor Array and Multichannel Signal Processing Workshop (SAM)*, July 2016, pp. 1–5.

[53] T. T. Chan and T. M. Lok, "Interference alignment with physical-layer network coding in mimo relay channels," in *2016 IEEE International Conference on Communications (ICC)*, May 2016, pp. 1–6.

[54] N. A. K. Khani, Z. Chen, and F. Yin, "Mimo v-blast scheme based on physical-layer network coding for data reliability in emerging wireless networks," *Canadian Journal of Electrical and Computer Engineering*, vol. 39, no. 2, pp. 103–111, Spring 2016.

[55] J. Guo, T. Yang, J. Yuan, and J. A. Zhang, "Linear vector physical-layer network coding for mimo two-way relay channels: Design and performance analysis," *IEEE Transactions on Communications*, vol. 63, no. 7, pp. 2591–2604, July 2015.

[56] M. Simon and M. Alouini, *Digital Communication over Fading Channels*, ser. Wiley Series in Telecommunications and Signal Processing. Wiley, 2005.

[57] T. Rappaport, *Wireless Communications: Principles and Practice*, ser. Prentice Hall communications engineering and emerging technologies series. Prentice Hall PTR, 2002. [Online]. Available: https://books.google.co.uk/books?id=TbgQAQAAMAAJ

[58] A. Goldsmith, *Wireless Communications:*. Cambridge: Cambridge University Press, 008 2005. [Online]. Available: https://www.cambridge.org/core/books/wireless-communications/800BA8A8211FBECB133A7BB77CD2E2BD

[59] ITU-RM.1225, "Guidlines for evaluations of radio transmission technologies for imt 2000," 1997.

[60] F. Xiong, A. Zerik, and E. Shwedyk, "Sequential sequence estimation for channels with intersymbol interference of finite or infinite length," *IEEE Transactions on Communications*, vol. 38, no. 6, pp. 795–804, Jun 1990.

[61] A. H. Sayed, *Adaptive Filters*. Wiley-IEEE Press, 2008.

[62] S. Haykin, *Adaptive Filter Theory (3rd Ed.)*. Upper Saddle River, NJ, USA: Prentice-Hall, Inc., 1996.

[63] Q. Ahmed, K.-H. Park, M.-S. Alouini, and S. Aissa, "Linear transceiver design for nonorthogonal amplify-and-forward protocol using a bit error rate criterion," *IEEE Trans. Wireless Commun.*, vol. 13, no. 4, pp. 1844–1853, April 2014.

[64] J. Proakis and M. Salehi, *Digital Communications*, ser. McGraw-Hill International Edition. McGraw-Hill, 2008.

[65] S. Kasturia, J. T. Aslanis, and J. M. Cioffi, "Vector coding for partial response channels," *IEEE Transactions on Information Theory*, vol. 36, no. 4, pp. 741–762, Jul 1990.

[66] A. Schmidt, W. Gerstacker, and R. Schober, "Maximum snr transmit filtering for linear equalization in physical layer network coding," in *2012 IEEE Globecom Workshops*, Dec 2012, pp. 80–84.

[67] ——, “Maximum snr transmit filtering for decision-feedback equalization in physical layer network coding,” in *SCC 2013; 9th International ITG Conference on Systems, Communication and Coding*, Jan 2013, pp. 1–5.

[68] J. Mietzner, R. Schober, L. Lampe, W. H. Gerstacker, and P. A. Hoeher, “Multiple-antenna techniques for wireless communications - a comprehensive literature survey,” *IEEE Communications Surveys Tutorials*, vol. 11, no. 2, pp. 87–105, Second 2009.

[69] S. M. Alamouti, “A simple transmit diversity technique for wireless communications,” *IEEE Journal on Selected Areas in Communications*, vol. 16, no. 8, pp. 1451–1458, Oct 1998.

[70] Y. Xiao, “Ieee 802.11n: enhancements for higher throughput in wireless lans,” *IEEE Wireless Communications*, vol. 12, no. 6, pp. 82–91, Dec 2005.

[71] R. T. Derryberry, S. D. Gray, D. M. Ionescu, G. Mandyam, and B. Raghothaman, “Transmit diversity in 3g cdma systems,” *IEEE Communications Magazine*, vol. 40, no. 4, pp. 68–75, Apr 2002.

[72] H. Ekstrom, A. Furuskar, J. Karlsson, M. Meyer, S. Parkvall, J. Torsner, and M. Wahlqvist, “Technical solutions for the 3g long-term evolution,” *IEEE Communications Magazine*, vol. 44, no. 3, pp. 38–45, March 2006.

[73] L. C. Godara, “Applications of antenna arrays to mobile communications. i. performance improvement, feasibility, and system considerations,” *Proceedings of the IEEE*, vol. 85, no. 7, pp. 1031–1060, Jul 1997.

[74] ——, “Application of antenna arrays to mobile communications. ii. beam-forming and direction-of-arrival considerations,” *Proceedings of the IEEE*, vol. 85, no. 8, pp. 1195–1245, Aug 1997.

[75] A. J. Paulraj and C. B. Papadias, “Space-time processing for wireless communications,” *IEEE Signal Processing Magazine*, vol. 14, no. 6, pp. 49–83, Nov 1997.

[76] A. F. Naguib, N. Seshadri, and A. R. Calderbank, “Increasing data rate over wireless channels,” *IEEE Signal Processing Magazine*, vol. 17, no. 3, pp. 76–92, May 2000.

[77] T. H. Liew and L. Hanzo, "Space-time codes and concatenated channel codes for wireless communications," *Proceedings of the IEEE*, vol. 90, no. 2, pp. 187–219, Feb 2002.

[78] D. Gesbert, M. Shafi, D. shan Shiu, P. J. Smith, and A. Naguib, "From theory to practice: an overview of mimo space-time coded wireless systems," *IEEE Journal on Selected Areas in Communications*, vol. 21, no. 3, pp. 281–302, Apr 2003.

[79] A. J. PAULRAJ, D. A. GORE, R. U. NABAR, and H. BOLCSKEI, "An overview of mimo communications - a key to gigabit wireless," *Proceedings of the IEEE*, vol. 92, no. 2, pp. 198–218, Feb 2004.

[80] S. N. DIGGAVI, N. AL-DHAHIR, A. STAMOULIS, and A. R. CALDERBANK, "Great expectations: the value of spatial diversity in wireless networks," *Proceedings of the IEEE*, vol. 92, no. 2, pp. 219–270, Feb 2004.

[81] J. Mietzner and P. A. Hoeher, "Boosting the performance of wireless communication systems: theory and practice of multiple-antenna techniques," *IEEE Communications Magazine*, vol. 42, no. 10, pp. 40–47, Oct 2004.

[82] J. Winters, "Optimum combining in digital mobile radio with cochannel interference," *Selected Areas in Communications, IEEE Journal on*, vol. 2, no. 4, pp. 528–539, July 1984.

[83] J. H. Winters and J. Salz, "Upper bounds on the bit-error rate of optimum combining in wireless systems," *IEEE Transactions on Communications*, vol. 46, no. 12, pp. 1619–1624, Dec 1998.

[84] H. Ibrahim, "Null steering by real-weight control-a method of decoupling the weights," *Antennas and Propagation, IEEE Transactions on*, vol. 39, no. 11, pp. 1648–1650, Nov 1991.

[85] D. Davies, "Independent angular steering of each zero of the directional pattern for a linear array," *IEEE Transactions on Antennas and Propagation*, vol. 15, no. 2, pp. 296–298, March 1967.

[86] R. Giusto and P. D. Vincenti, "Phase-only optimization for the generation of wide deterministic nulls in the radiation pattern of phased arrays," *IEEE Transactions on Antennas and Propagation*, vol. 31, no. 5, pp. 814–817, Sep 1983.

[87] T. B. Vu, "Method of null steering without using phase shifters," *Microwaves, Optics and Antennas, IEE Proceedings H*, vol. 131, no. 4, pp. 242–245, August 1984.

[88] T. Vu, "Simultaneous nulling in sum and difference patterns by amplitude control," *IEEE Transactions on Antennas and Propagation*, vol. 34, no. 2, pp. 214–218, Feb 1986.

[89] T. H. Ismail and M. M. Dawoud, "Null steering in phased arrays by controlling the element positions," *IEEE Transactions on Antennas and Propagation*, vol. 39, no. 11, pp. 1561–1566, Nov 1991.

[90] J. A. Hejres, "Null steering in phased arrays by controlling the positions of selected elements," *IEEE Transactions on Antennas and Propagation*, vol. 52, no. 11, pp. 2891–2895, Nov 2004.

[91] B. Friedlander and B. Porat, "Performance analysis of a null-steering algorithm based on direction-of-arrival estimation," *IEEE Transactions on Acoustics, Speech, and Signal Processing*, vol. 37, no. 4, pp. 461–466, April 1989.

[92] R. Qamar and N. Khan, "Null steering, a comparative analysis," in *Multitopic Conference, 2009. INMIC 2009. IEEE 13th International*, Dec 2009, pp. 1–5.

[93] T. Koike-Akino, P. Popovski, and V. Tarokh, "Denoising maps and constellations for wireless network coding in two-way relaying systems," in *IEEE GLOBECOM 2008 - 2008 IEEE Global Telecommunications Conference*, Nov 2008, pp. 1–5.

[94] ——, "Optimized constellations for two-way wireless relaying with physical network coding," *IEEE Journal on Selected Areas in Communications*, vol. 27, no. 5, pp. 773–787, June 2009.

[95] B. A. Jebur and C. C. Tsimenidis, "Performance analysis of ofdm-based denoise-and-forward full-duplex plnc with imperfect csi," in *2015 IEEE International Conference on Communication Workshop (ICCW)*, June 2015, pp. 997–1002.

[96] M. Reuter, J. C. Allen, J. R. Zeidler, and R. C. North, "Mitigating error propagation effects in a decision feedback equalizer," *IEEE Transactions on Communications*, vol. 49, no. 11, pp. 2028–2041, Nov 2001.

[97] R. Merched and N. R. Yousef, "Fast techniques for computing finite-length mmse decision feedback equalizers," in *2004 IEEE International Conference on Acoustics, Speech, and Signal Processing*, vol. 4, May 2004, pp. iv–1005–8 vol.4.

[98] M. Park, I. Choi, and I. Lee, "Exact ber analysis of physical layer network coding for two-way relay channels," in *2011 IEEE 73rd Vehicular Technology Conference (VTC Spring)*, May 2011, pp. 1–5.

[99] M. R. . S. Ericsson, Nokia, "Proposal for lte channel models," http://www.3gpp.org, 2007.